2010

Interleukin-7 Differentially Regulates The Activation, Proliferation, And Homing Of T-cells: Implications For Immunotherapy

Christina Kittipatarin
University of Central Florida

INTERLEUKIN-7 DIFFERENTIALLY REGULATES THE ACTIVATION, PROLIFERATION, AND HOMING OF T-CELLS: IMPLICATIONS FOR IMMUNOTHERAPY

by

CHRISTINA KITTIPATARIN
B.S. Emory University, 1999
M.S. University of Central Florida, 2003

A dissertation submitted in partial fulfillment of the requirements
for the degree of Doctor of Philosophy
in the Burnett School of Biomedical Sciences
in the College of Medicine
at the University of Central Florida
Orlando, Florida

Summer Term
2010

Major Professor: Annette R. Khaled

ABSTRACT

Interleukin-7 (IL-7) is an essential lymphocyte growth factor required for the survival and proliferation of mature T-cells. As a therapeutic agent, IL-7 has the potential to restore T-cell numbers following immune depletion and to promote immunity against cancers. While the survival function of IL-7 is well established, less is known about how it supports T-cell expansion, a critical feature of the immune response. To study the biological effects of IL-7 on T-cell growth, we developed an *in vitro* culture technique to expand T-cells *ex vivo*. A significant finding from our studies is that IL-7 did not induce the expansion of all T-cells, indicating that there are inherent differences in the response of individual T-cell subsets to IL-7. Culture with high doses of IL-7 (>150 ng/ml) preferentially expanded CD8 T-cells, but lead to the dramatic loss of CD4 T-cells which favored growth in lower dosages of IL-7 (<10 ng/ml). This effect was due to the regulation of LCK, a kinase predominantly associated with the CD4 co-receptor. We found that transgenic expression of the CD4 co-receptor onto CD8 T-cells promoted their growth in lower concentrations of IL-7. Conversely, inhibition of LCK activity in CD4 T-cells restored their responsiveness to high doses of IL-7 as indicated by the activation of the transcription factor STAT5, in a manner similar to CD8 T-cells. Interestingly, not all CD8 T-cells expanded in high doses of IL-7 and this effect was specific to CD8 T-cells that expressed an activated memory phenotype. We found that IL-7 promoted the proliferation of CD8 T-cells through Cdc25A, a phosphatase required for cell cycle progression. Expression of a constitutively active Cdc25A could maintain T-cell survival and proliferation in the absence of IL-7, demonstrating that Cdc25A is a crucial transducer of IL-7 growth signals. Inhibition of Cdc25A was sufficient to decrease proliferation and down-regulate the expression of activation/

memory markers on CD8 T-cells in the presence of IL-7. Upon further study, we identified a novel role for IL-7 through Cdc25A in the regulation of CD62L, an adhesion molecule required for lymph node entry. Culture with high doses of IL-7 down-regulated the expression of CD62L, suggesting that high doses of IL-7 could affect the ability of T-cells to enter or re-enter the lymph nodes. Collectively, our findings demonstrate that IL-7 administration at the supraphysiological doses currently used in the clinical trials could have a negative impact on the growth of CD4 T-cells and the homing of CD8 T-cells to the lymph nodes, effects which can impede the generation of an effective immune response.

ACKNOWLEDGMENTS

The pursuit of a Ph.D. is truly a collaborative effort and I am grateful to a number of people for their support and encouragement. First and foremost, I must thank my mentor Dr. Annette Khaled, who always had time to answer my questions, big or small, scientific or otherwise. I have learned so much under her guidance; I am deeply indebted to her for providing me with the opportunity to study and work in her laboratory. A very special thank you to all of my lab mates past and especially present: Dr. Kathleen Nemec, Dr. Mounir Chehtane, Rebecca Boohaker, Shannon Ruppert, and Ge Zhang. My lab family has been an invaluable source of both moral support and scientific expertise whose contributions are present throughout this work. I would also like to thank my committee members Dr. Alexander Cole, Dr. James Turkson, and Dr. Antonis Zervos for providing their insight and critiques as I developed my project. And lastly, but most importantly, I must acknowledge my mother who has been and continues to be my greatest supporter.

TABLE OF CONTENTS

LIST OF FIGURES

CHAPTER 1: INTRODUCTION

Cytokines are the signaling proteins of the immune system and have critical roles in mediating immunity and inflammation. They act by binding to specific receptors on the membrane of target cells, providing signals for growth, survival, proliferation, activation, and differentiation. Of therapeutic interest are the cytokines that signal through the common γ chain (γc) which include interleukins 2, 7, 15, and 21 (IL-2, IL-7, 15 and 21), regulators of lymphocyte homeostasis. Defects in γc signaling leads to severe combined immunodeficiency (SCID) in humans, characterized by the loss of T-cells and natural killer cells[1]. However, only IL-7 has been shown to be non-redundant and absolutely required for normal lymphocyte development and growth[2]. Mice lacking IL-7, the IL-7 receptor unique α chain (IL-7Rα), or any components of its signaling pathway have severe lymphocyte deficiencies and are immunocompromised[2, 3]. In humans, loss of IL-7 signaling is the main cause of SCID[4]. In contrast, excess levels of IL-7 as induced by transgenic expression in mice or abnormal regulation in humans lead to the development of lymphomas and malignancies[5, 6, 7]. Based on such findings, IL-7 has been recognized as a key regulator of T-cell growth and homeostasis, leading to immense clinical interest in the biology of this cytokine.

IL-7 is not produced by lymphocytes but rather by stromal and epithelial cells present in lymphoid as well as extralymphoid tissues[8, 9]. While circulating serum levels of IL-7 in healthy individuals are low (0.3- 8.4 pg/ml)[10], IL-7 production can be induced and its levels increased, in response to inflammation[11, 12]. The receptor for IL-7, consisting of IL-7Rα and γc, is expressed on most T-cells, but IL-7Rα can be down-regulated in response to antigenic stimuli and IL-7 itself. Binding of IL-7 induces the dimerization of its two receptor chains, leading to the

activation of the receptor associated tyrosine Janus kinases, JAK1 (IL-7Rα) and JAK3 (γc). The activated JAK proteins in turn phosphorylate specific residues on IL-7Rα, creating docking sites for STAT5 (signal transducers and activators of transcription 5). The STAT5 proteins, specifically STAT5a and STAT5b, become phosphorylated by JAKs, inducing their dimerization and translocation to the nucleus where they modulate the expression of a number of genes involved in cell survival and proliferation (reviewed in[13]).

The function of IL-7 in supporting T-cell survival has been well established and less is known about how it promotes proliferation. As a survival factor, IL-7 up-regulates the expression of the anti-apoptotic protein BCL-2 and transgenic expression of BCL-2 partially protects T-cells from death in the absence of IL-7[14]. These cells however, are growth arrested, demonstrating that they require additional replicative signals from IL-7. Culture with IL-7 *in vitro* or transgenic expression of the cytokine *in vivo* leads to an increase in T-cell numbers, while IL-7 withdrawal induces G_1/S cell cycle arrest and ultimately cell death[15-18]. Intriguingly, the proliferative activity of IL-7 can be uncoupled from its anti-apoptotic effects based on the dosage of the cytokine. Lower doses of IL-7 sustain T-cell survival, while higher doses are required to induce cell cycling[19, 20]. Although this dosage effect of IL-7 is well known, it has not been extensively studied.

One mechanism by which high levels of IL-7 could induce proliferation is through the regulation of key proteins involved in the G_1/S cell cycle transition. We found that T-cells cultured with high doses of IL-7, contained more nuclear Cdc25A, a critical cell cycle phosphatase. Cdc25A is required to remove inhibitory phosphorylations on cyclin-dependent kinase 2 (cdk 2), promoting progression through the G_1/S phase of the cell cycle. Hence, higher

doses of IL-7 would serve as a strong proliferative signal. Furthermore we have shown that in the absence of IL-7, Cdc25A is targeted for proteolytic degradation through a mechanism involving the stress kinase p38 MAP kinase (MAPK)[17]. Loss of IL-7 signaling, therefore, would create a pool of inactive cdk 2, essentially arresting T-cells in the G_1/S phase of the cell cycle.

In addition to mediating T-cell growth, a recent study with rhesus macaques showed that IL-7 could also affect the trafficking of T-cells. This study showed that following IL-7 injection, the T-cells which proliferated in response to IL-7 migrated out of the blood and into various tissues such as the intestines and skin[21]. In contrast, T-cells which were not cycling remained in the blood, suggesting that there was a correlation between the induction of proliferation and T-cell trafficking. In our own studies, we have found that *in vitro* culture of T-cells with higher doses of IL-7 down-regulated the expression of the lymph node homing molecule CD62L. This effect would essentially alter the homing pattern of T-cells, promoting their trafficking away from the lymph nodes and into extralymphoid organs. In addition, we demonstrated that this IL-7 mediated down-regulation of CD62L was dependent on the activity of Cdc25A. Such findings have significant physiological implications because inadvertent effects on T-cell homing and localization as induced by IL-7 treatment could prevent the generation of an effective immune response or at the other end of the spectrum, lead to the development of autoimmunity.

As more information is acquired about the biological activities of IL-7, the cytokine has emerged as a promising therapeutic agent for the treatment of clinical conditions such as immunodeficiencies and cancers. IL-7 is listed among the top five agents for cancer therapy by the National Cancer Institute (NCI) and is currently in clinical trials. Although preclinical animal models demonstrated that IL-7 supported the proliferation and persistence of tumor-

specific T-cells[22], no anti-tumor effects have been observed in the clinical trials [23]. While clinical administration of IL-7 did expand T-cells in a dose-dependent manner, demonstrating a potential use for immune reconstitution, it should be noted that high supraphysiological doses of IL-7 are being used[24]. In fact, this clinical dosing regiment can increase circulating levels of IL-7 by 100-fold in humans and notably an initial depletion of T-cells in the blood have been observed following IL-7 administration[24]. Currently, it is not known whether such a high dosage of IL-7 is optimal for therapeutic use nor have the physiological impact of this dosage been extensively evaluated.

The studies presented here are derived from four manuscripts and demonstrates that exposure to high levels of IL-7 can produce an inflammation-like response by promoting the activation, cell cycling, and trafficking of CD8 T-cells. In contrast, the growth of CD4 T-cells is impaired at high concentrations of IL-7, indicating that there are intrinsic molecular differences between CD4 and CD8 T-cells that mediate their responses to IL-7. The first manuscript is the development of the IL-7 *in vitro* culture method, a technique which is utilized in subsequent studies to expand T-cells *ex vivo*. We demonstrate here that high doses of IL-7 preferentially expand CD8 T-cells with an activated/ memory phenotype such as occurs in response to antigen. In the second manuscript we show that CD4 T-cells grow optimally at lower doses of IL-7, an effect of the cytokine's regulation of the src kinase LCK. The final two manuscripts are based on our initial findings that IL-7 regulates the stability and hence activity of the cell cycle phosphatase Cdc25A. As previously stated, in addition to supporting T-cell proliferation, we show that Cdc25A also has a novel homing effect on T-cells and this is due to its regulation of the Foxo1 transcription factor. Specifically we demonstrate that T-cells expanded *ex vivo* with

high doses of IL-7 acquire a memory effector T-cell phenotype ($CD69^{hi}$, $CD44^{hi}$, and $CD62L^{lo}$), resembling antigen activated T-cells that migrate to the extralymphoid organs. Collectively, these findings show the cellular and molecular consequences of exposing T-cells to high levels of IL-7 such as administered clinically and demonstrate that there is still much unknown about the activities of this multipotent cytokine.

CHAPTER 2: *EX VIVO* EXPANSION OF MEMORY CD8 T-CELLS FROM LYMPH NODES OR SPLEEN THROUGH *IN VITRO* CULTURE WITH INTERLEUKIN-7

Introduction

IL-7 increases lymphocyte numbers, a critical feature of immune reconstitution, through poorly defined proliferative mechanisms. The replicative function of IL-7 has been mainly examined through *in vivo* studies, and few *in vitro* systems have evaluated this activity of the cytokine. *In vitro* studies can be problematic because primary T-cells placed in single-cell suspensions die within a few days of standard culture [25] or fail to proliferate when maintained with IL-7 alone[26]. In fact, many IL-7 *in vitro* studies rely on additional stimuli such as T-cell receptor (TCR) signaling to support proliferation. Hence in the absence of other signals, *in vitro* studies of IL-7 have only revealed a survival function, while it is the *in vivo* studies that have shown a proliferative activity.

Although *in vivo* experiments have yielded important findings, analysis of the data can be challenging. For example, it is difficult to attribute the proliferation observed in *in vivo* studies solely to IL-7. Contributions from other environmental components, such as co-stimulation or TCR:MHC signaling, must also be taken into account. Moreover, most studies examining IL-7 proliferation utilize the technique of adoptive transfer into immunodeficient mice. Because of the paucity of lymphocytes in these animals, signaling by various cytokines, self-peptide/ MHC complexes, or foreign antigens may be atypical due to reduced T-cell competition[27]. Mice such as those lacking components of the IL-7 signaling pathway may also have abnormal lymphoid tissues, impacting lymphocyte trafficking[28, 29]. Finally, IL-7 treatment increases thymic output,

making it difficult to distinguish recent thymic emigrants (RTE) from preexisting (proliferating) naïve T-cells[20, 24].

In order to study the proliferative activity of IL-7 independent of other factors and identify specific subsets of T-cells that respond to IL-7 by proliferating, we developed an *in vitro* culture system for the *ex vivo* expansion of primary T-cells. Previous *in vitro* systems failed to reveal the proliferative activity of IL-7 for multiple reasons. The dose of IL-7 was not optimal (usually 25 ng/ml or less). Cell concentrations varied but were usually low (~10^6 cells/ml). Lastly, the duration of culture with IL-7 rarely exceeded 7 days. The methodology we developed relies on using a greater density of T-cells with a high concentration of IL-7 under extended cell culture conditions. Using this method, we were able to distinguish subsets that proliferated in response to IL-7 from those in which only survival was maintained. This is an important distinction that needs to be made to fully develop the therapeutic uses of IL-7; application of IL-7 could result in the preferential expansion of a specific T-cell subset, potentially leading to a significant skewing of the T-cell repertoire.

Materials and methods

Mice used and cell isolation techniques

C57BL/6 mice were purchased from Jackson Laboratory (Bar Harbor, Maine) and C57BL/6-Tg(OT-I)-RAG1^{tm1Mom} mice were purchased from Taconic (Hudson, NY). Mice were housed in the animal facility at the University of Central Florida and used at 2-3 months of age. STAT5b-CA mice were generously provided by Dr. Michael Farrar (Department of Laboratory Medicine and Pathology, University of Minnesota, Minneapolis, MN) and Bim deficient mice

were a kind gift from Dr. Scott Durum (Laboratory of Molecular Immunoregulation, National Cancer Institute-Frederick, Frederick, Maryland). Animal studies were reviewed and approved by the Institutional Animal Care and Use Committee (IACUC) at the University of Central Florida.

Lymph node and spleen cells were isolated by gentle crushing of organs through a 70μM pore filter (BD Falcon) and pooled. Spleen cells were further treated with ACK lysis buffer (Quality Biological, Inc.) to lyse red blood cells (RBCs) and enriched for T-cells by negative selection with a commercially available kit, the Mouse T-lymphocyte Enrichment kit (BD Biosciences). T-cell enrichment was confirmed by analysis of surface markers by flow cytometry.

In vitro culture with IL-7

Culture conditions, for the *ex vivo* expansion of IL-7-responsive cells, were established as follows: cells were maintained at a density of 3-5 x 10^6 cells/ml in complete medium (RPMI 1640 Medium (Invitrogen) supplemented with 10% Fetal Bovine serum (Hyclone), 2-βmercaptoethanol (1000X, Life Technologies), and 50 U/ml penicillin/ streptomycin) in 24 well plates. Recombinant human IL-7 (Peprotech) was added at the start of culture at a concentration of 150ng/ml and refreshed every other day. This concentration of IL-7 was established experimentally after testing a dose range from 10-200 ng/ml for optimal effects upon cell growth and viability. Cultures were maintained with or without IL-7 for >14 days or until noticeable cell death was apparent and confirmed by Trypan Blue exclusion staining.

Cell surface protein analysis

Surface expression of membrane proteins expressed on T-cells was assessed by flow cytometry using the following fluorochrome-conjugated antibodies: PE-conjugated anti-CD4 (clone GK1.5), PerCP-conjugated anti-CD8 (clone 53-6.7), FITC-conjugated anti-CD44 (IM7), and FITC-conjugated anti-CD69 (clone H1.2F3) (BD Biosciences). Cells were incubated with saturating amounts of the appropriate antibodies for 20 minutes on ice, washed in buffer (PBS + 0.1% bovine serum albumin (BSA)) and analyzed by flow cytometry on a FACSCalibur flow cytometer (BD Biosciences). Data was analyzed using FCS Express software (Ontario, Canada).

Proliferation assays

For CFSE labeling, 5 x 10^6 lymph node or splenic T-cells were washed and resuspended in 2 μM CFSE (Molecular Probes) staining solution (PBS supplemented with 0.1% BSA). After 10 minutes, labeling was stopped and cells washed. The division status of cells was determined by measuring CFSE fluorescence by flow cytometry at 48 hours after culture with or without IL-7. The generation number for the population was determined from a best fit of these data to a Gaussian curve using the Proliferation Add-on module for the FCS express software. Unstimulated, freshly-labeled CFSE-containing cells were used to verify the peak corresponding to the undivided population. To measured DNA synthesis, 5 x 10^6 cells were pulsed with BrdU (10μM) for 48 hours and BrdU incorporation was detected with a commercially available kit (BD Biosciences) according to manufacturer's protocol. Briefly, cells were typed for surface markers CD4 or CD8 as described above, washed, fixed, and permeabilized prior to incubation

with a FITC-conjugated anti-BrdU antibody. The cells were analyzed by flow cytometry as described above.

Results

Phenotype of T-cells from STAT5b-CA mice

In order to develop an *in vitro* culture system for the *ex vivo* expansion of IL-7 responsive T-cells, we first needed to identify the types of T-cells that result from a constitutive IL-7 signal. Hence, we examined the distribution of T-cells isolated from STAT5b-CA mice[30]. The signal transduced through the IL-7 receptor is typically mediated through the JAK/ STAT pathway and expression of a constitutively activated STAT5 (STAT5b-CA) is sufficient to promote IL-7 dependent growth in the absence of the cytokine[30]. We analyzed the phenotype of T-cells isolated from the spleen (by negative selection) and lymph nodes from STAT5b-CA mice. Results are shown in Fig. 1. In agreement with the previous study[30], we observed that the CD4:CD8 ratio of T-cells either enriched from the spleen (Fig. 1A) or isolated from the lymph nodes (Fig. 1B) were significantly skewed towards CD8 T-cells. Few CD4 T-cells were detected (less than 16%). Moreover, the CD8 T-cell subsets that were being generated by constitutive STAT5b signaling did not up-regulate expression of the activation marker, CD69, but displayed elevated expression of CD44 (Fig. 1A and B). This was most prominent in the T-cells enriched from the spleen (Fig. 1A). Therefore, these results indicate that IL-7 promotes the expansion of a specific subset of T-cells, implicating that its replicative function may not extend to all T-cell types.

IL-7 promotes the proliferation of CD8 T-cells

To demonstrate that IL-7 can cause cell division under *in vitro* culture conditions, T-cells were enriched from the spleens of wild-type (WT) C57BL/6 mice and labeled with the intracellular dye, CFSE. Splenic T-cells were cultured with or without IL-7 for 48 hours. Cell division was assessed after two days of culture because beyond this significant cell death was observed in the IL-7 withdrawn cells. Fig. 2A shows that a greater percentage of T-cells divided in the presence of IL-7 compared to cells maintained in the absence of the cytokine. Forty-eight hours of CFSE labeling revealed that there were two major proliferating populations: (1) A slow dividing population (that underwent 1–2 cell division cycles) and (2) A rapidly dividing population (that underwent up to 4 more cell division cycles). The slow dividing population was IL-7 independent, and these were detected in both the presence and absence of the cytokine (Fig. 2A). In contrast, the rapidly dividing population was IL-7 dependent in that two fold more cells were detected in the presence of IL-7 (19%) compared to the absence (8.5%) and these cells underwent up to four more cell division cycles (Fig. 2A). Note that undivided cells only remained in the cultures lacking IL-7. Similar results were observed with cells isolated from lymph nodes, given that these cells, though not enriched for T-cells like those from the spleen, still contained a major population of T-cells (Fig. 2B).

We next determined whether the proliferation observed in *in vitro* cultures resembled that observed within the STAT5b-CA mice in terms of the preferential expansion of CD8 T-cells. Since only a limited number of cell divisions can occur within 2 days, which may not be enough to detect a skew in CD4:CD8 ratios, we extended the culture period with IL-7 to 7 days and measured DNA synthesis by BrdU incorporation. Splenic T-cells were pulsed with BrdU for the

final 48 hours, and Fig. 2C shows that 21% of the CD8 T cells as compared to 7% of CD4 T-cells incorporated BrdU. These results along with the CFSE findings (Fig. 2A) formed the basis for the development of the *in vitro* proliferative assay for the expansion of IL-7 responsive cells.

Ex vivo expansion of memory phenotype CD8 T-cells by IL-7

To identify the type of cell expanded by IL-7, we developed an *in vitro* culture system based on optimizing culture conditions and IL-7 dosage. Previously, we found that low doses of IL-7 only supported survival while high doses promoted cell division[19]. Moreover, IL-7 proliferative effects were detected in cells from lymphopenic or IL-7 transgenic mice[31], which are *in vivo* conditions of higher than normal IL-7 concentration. Using this information, we optimized the *in vitro* culture conditions and IL-7 dosage and assessed the phenotype of cells from C57BL/6 WT mice following long-term culture with the cytokine. Starting with cells isolated from lymph nodes, we examined the CD4:CD8 ratio. The starting CD4:CD8 ratio was approximately 1:1 and by day 7 had shifted to 1:6 and by day 14 to 1:8 (Fig. 3A, top panels). Next the expression of activation and memory markers was examined. We observed an increase in the expression of CD69 on the expanding CD8 T-cells that was sustained through 14 days of culture (Fig. 3A, middle panels). Similarly, the percentage of $CD8^{hi}CD44^{hi}$ T-cells increased upon *in vitro* culture with IL-7, becoming a predominant population by day 14 (Fig. 3A, bottom panels).

To rule out the contributions of additional factors possibly present in the lymph node cultures, we isolated T-cells from the spleens of WT mice by negative selection. This enrichment typically yielded 95% or greater T-cells (Fig. 3B, Day 0 data). Results from T-cell

cultures were comparable to those observed with the lymph node cells. After 14 days of growth with IL-7, CD8 T-cells, expressing the memory-phenotype marker, accumulated (Fig. 3B). Note that a small population of $CD8^{neg}CD44^{hi}$ cells, observed in lymph node cultures (Fig. 3A), were not present in splenic T-cell cultures, suggesting that these $CD44^{hi}$ lymph node cells were likely not lymphocytes. Our results with splenic T-cells were consistent with those observed with the STAT5b-CA mice. We found that culture with IL-7 supported the expansion of CD8 T-cells with a memory phenotype ($CD44^{hi}$). However, our results were also different since we detected up-regulation of the CD69 activation marker; an outcome not observed with T-cells from STAT5b-CA mice (Fig.1). Use of the *in vitro* culture system was successful in that we could expand, in the absence of other signals, the type of T-cells, CD8 memory, supported by IL-7. However, unlike results from *in vivo* studies [16, 30], the *ex vivo* amplified T-cells had an activated phenotype, as indicated by increased CD69 expression, more typical of antigen-activated cells.

To determine whether the *in vitro* culture conditions with IL-7 were artificially inducing the expression of CD69 and CD44, we isolated lymph node cells from OT-1/$Rag1^{-/-}$ mice. This mouse line is homozygous for a transgene that encodes a TCR specific for ovalbumin (OVA) and is also deficient in rag1 (recombinase reactivating gene 1). These mice do not develop T or B cells expressing endogenous receptors, while peripheral CD8 T-cells express the TCR-OVA transgene. In the absence of OVA, most CD8 T-cells from the OT-1/$Rag1^{-/-}$ mice are of a naïve phenotype. Fig. 4 shows lymph node cells from OT-1/$Rag1^{-/-}$ mice cultured for 14 days with IL-7. Unlike the findings with WT cells (Fig. 2), the OT-1/$Rag1^{-/-}$ cells did not proliferate to IL-7, as indicated by the absence of BrdU incorporation after 14 days of culture (Fig. 4A). These cells also did not substantially up-regulate the expression of either CD69 or CD44 (Fig. 4B), as

was observed with WT lymph node or splenic T-cells (Fig. 3). We can therefore conclude from these findings that culture conditions with IL-7 do not result in spontaneous proliferation or the artificial induction of activation or memory markers. Further, we can establish that the IL-7-driven accumulation of memory-phenotype CD8 T-cells results not from the conversion of naïve cells to memory cells, but more likely from the expansion of an already existing population.

Use of the IL-7 in vitro culture system to differentiate survival from proliferative effects

To demonstrate the usefulness of the IL-7 *in vitro* culture system, we applied our methodology to determine whether the proliferative activity of IL-7 results as a default of its survival function. T-cells were enriched from the lymph nodes and spleen of mice which were deficient for the apoptotic protein, Bim ($Bim^{-/-}$). Bim has a role in the death of antigen-activated T-cells[32] and deficiency of Bim rescued the T-cell depleted phenotype of IL-7 receptor deficient mice[33]. Moreover, we observed that $Bim^{-/-}$ deficient T-cells, unlike WT T-cells, survived but did not proliferate in cultures lacking IL-7 (data not shown), suggesting that we could replace the survival (but not proliferative) activity of IL-7 by ablating Bim. Moreover, unlike WT T-cells, we could culture $Bim^{-/-}$ T-cells in the absence of IL-7 for extended periods of time. Fig. 5A shows that the starting populations of $Bim^{-/-}$ T-cells from spleen or lymph nodes were predominantly small-sized cells with few larger blasts as indicated by forward scatter (FSC) and side scatter (SSC) analysis. This trend was reversed upon extended culture with IL-7 in that by day 7 and day 14, blast-sized cells became the major population, and subsequently, when phenotyped, we found that these cells were mainly CD8 T-cells (Fig. 5A).

Starting populations of Bim$^{-/-}$ lymph node cells revealed a significant number of CD4 T-cells (30%), which dropped to 4% by day 14 in culture with IL-7 (Fig. 5B, top panel). Conversely, we observed that CD8 T-cells from Bim$^{-/-}$ mice, cultured with IL-7, increased from 41% to 61% by day 14 (Fig. 5B, top panel). Hence, IL-7 *in vitro* culture conditions selectively expanded CD8 T-cells from a mixed population of cells isolated from Bim$^{-/-}$ mice in a manner similar to that observed with cells from WT mice. This trend was not observed with Bim$^{-/-}$ lymph nodes cells cultured without IL-7 (Fig. 5B, top panel), indicating that the maintenance of survival through Bim deficiency was not sufficient to promote the expansion of CD8 T-cells. This also shows that there are no other factors present in IL-7 deprived lymph node cultures that could sustain the growth of CD8 memory T-cells. In fact, the few CD8 T-cells remaining in the absence of IL-7 also expressed low levels of CD4; a cell type not expanded in IL-7 containing cultures. Fig. 5B (middle panel) showed that in the presence, but not absence of IL-7, there were more CD8 T-cells expressing high levels of CD69 (32%) after a 2 week culture of Bim$^{-/-}$ T-cells. Surface staining also showed that the memory marker CD44 was up-regulated only on CD8 T-cells cultured with IL-7, resulting in a significant accumulation of these cells by day 14 of culture (Fig. 5B, bottom panel).

Next, we isolated T-cells from the spleens of Bim$^{-/-}$ mice. Initially, the starting population of Bim$^{-/-}$ T-cells enriched from the spleen was skewed toward a higher percentage of CD4 T-cells (50%) compared to CD8 T-cells (35%). Yet, by day 14 of culture in IL-7, the predominant population was CD8 T-cells, while in the absence of IL-7, CD4 T-cells predominated (Fig. 5C, top panel). Recall that analysis of cell size by FSC/ SSC showed that after 14 days of culture with IL-7, the few remaining CD4 T-cells were small in size and that the

predominant blast-sized population was CD8 (Fig. 5A, lower panels). In the absence of IL-7, few blast-sized cells were detected (data not shown). Similar to the results obtained from culture of WT T-cells with IL-7 (Fig. 3), splenic T-cells from $Bim^{-/-}$ mice expressed high levels of CD69 (26%) and CD44 (42%) in contrast to cells cultured without IL-7 (1% and 3% respectively) (Fig. 5C, middle and bottom panels).

In summary, our results show that *in vitro* culture with IL-7 results in the *ex vivo* expansion of CD8 memory-phenotype T-cells. This expansion is not due to the survival function of IL-7, since Bim deficiency, in the absence of IL-7, could not recapitulate the effects of IL-7. Rather, our *in vitro* culture has demonstrated that IL-7 has a separate proliferative function, resulting in the expansion of a specific subset of T-cells - CD8 memory-phenotype cells - and that this replicative activity may have the hallmark of antigen-activated proliferation.

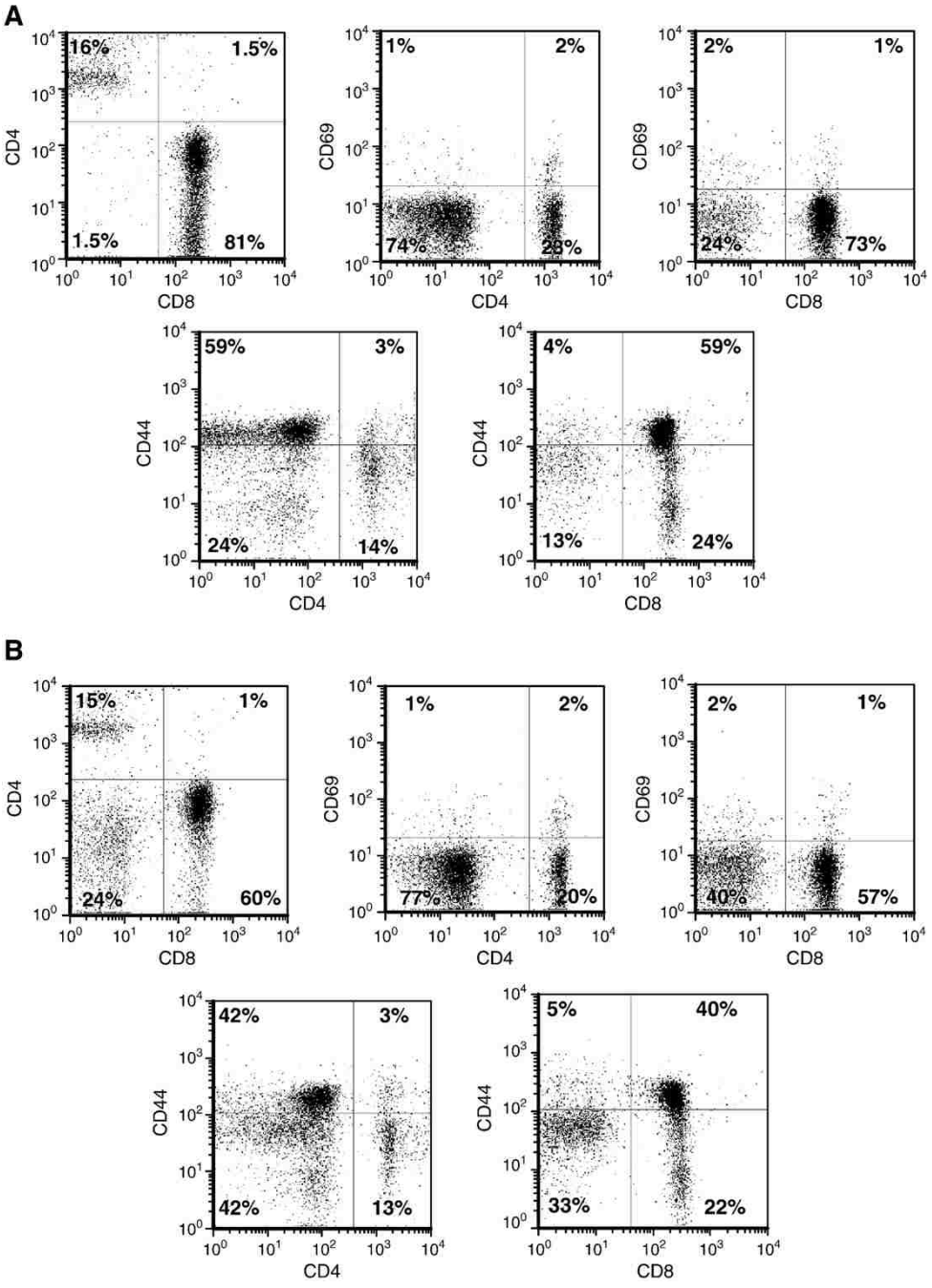

Figure 1. Phenotyping of T-cells isolated from STAT5b-CA mice.
T-cells isolated from spleen (A) and lymph nodes cells (B) of STAT5b-CA mice were analyzed for changes in surface protein expression. Cells were stained with fluorochrome-conjugated antibodies specific for CD4, CD8, CD69 and CD44 and analyzed by flow cytometry. FSC/ SSC gating was used to establish viable gates for lymphocytes. In each dot plot, the numbers shown are the percentages of cells in the indicated quadrant relative to the total cells. Representative data from one mouse is displayed.

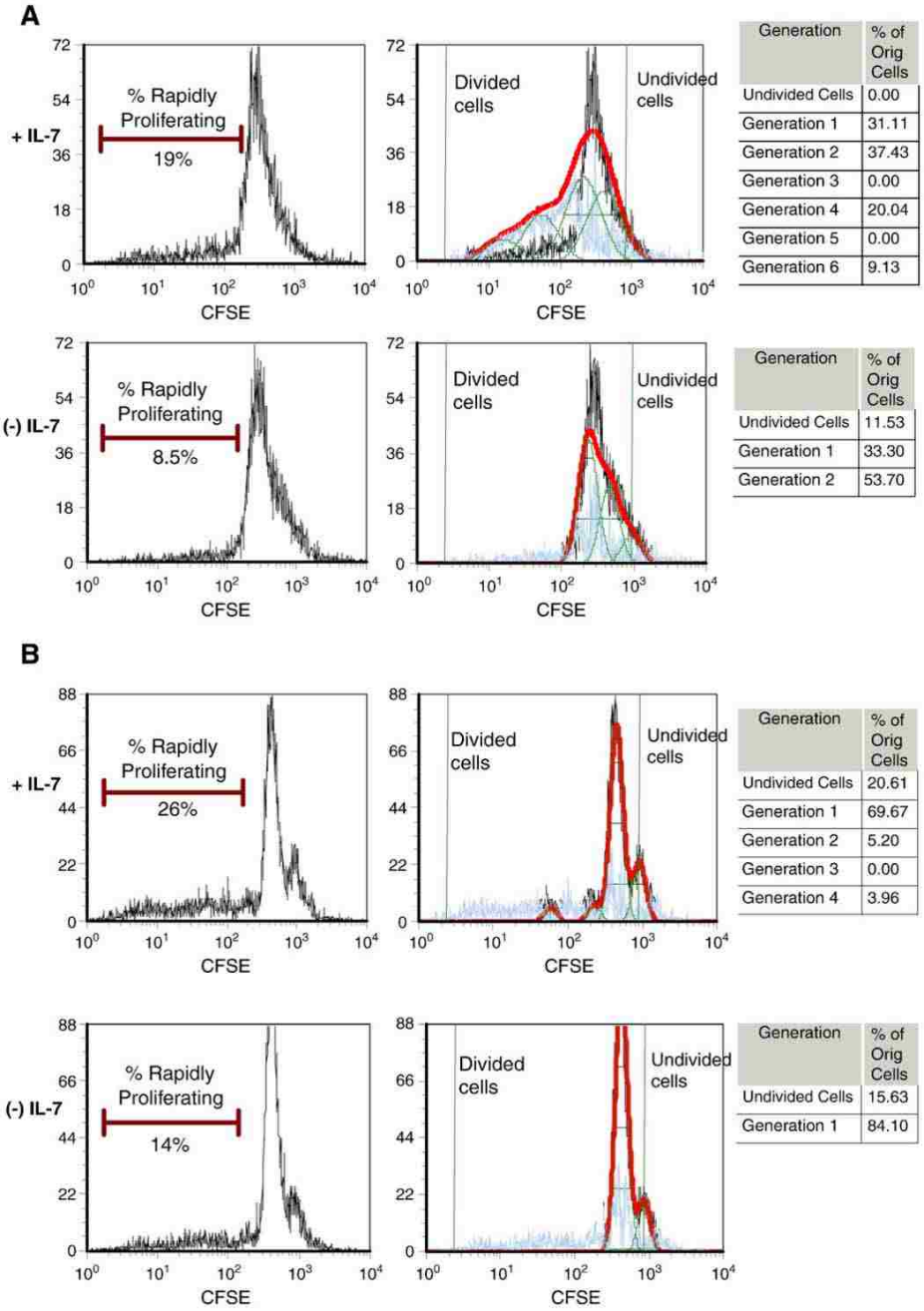

Figure 2. *In vitro* proliferation of T-cells by IL-7.
(A–B) Splenic T-cells (A) and lymph nodes cells (B) of C57BL/6 mice were labeled with CFSE and placed in culture with or without IL-7 (150 ng/ml) for 48 hours. The left panels show the histograms displaying the fluorescence profile of the viable CFSE-labeled lymphocytes. The percent of rapidly proliferating cells is indicated. The right panels show the same histograms subjected to analysis using FCS Express Proliferation software to determine generation time based on loss of CFSE due to cell division. Green lines indicate undivided (rightmost peak) and divided cells (leftmost peak). The tables at the far right display the percent of cells in each generation. A representative experiment of three is shown.

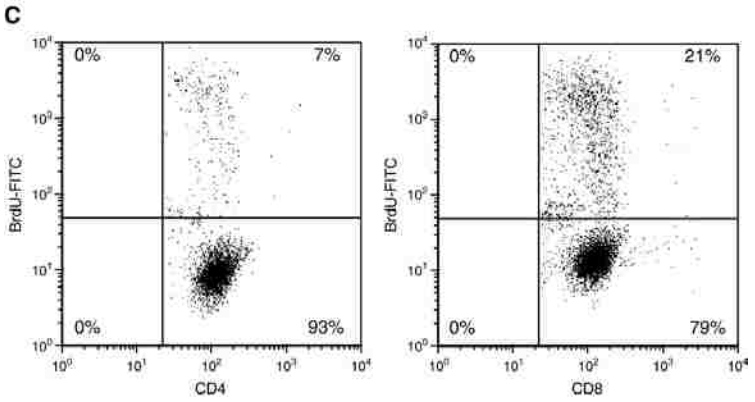

Figure 2. *In vitro* proliferation of T-cells by IL-7.
(C) Splenic T-cells were cultured with IL-7 for 7 days and pulsed with BrdU for the final 48 hours to determine the percentage of cells synthesizing DNA. Cells were stained with PerCP-conjugated antibodies for CD4 or CD8 and a FITC-conjugated anti-BrdU antibody to detect BrdU incorporation and analyzed by flow cytometry. Percentages shown in the dotplots are gated on viable cells (based on FSC/ SSC) and CD4 or CD8 T-cells that incorporated BrdU. Representative results from three experiments are shown.

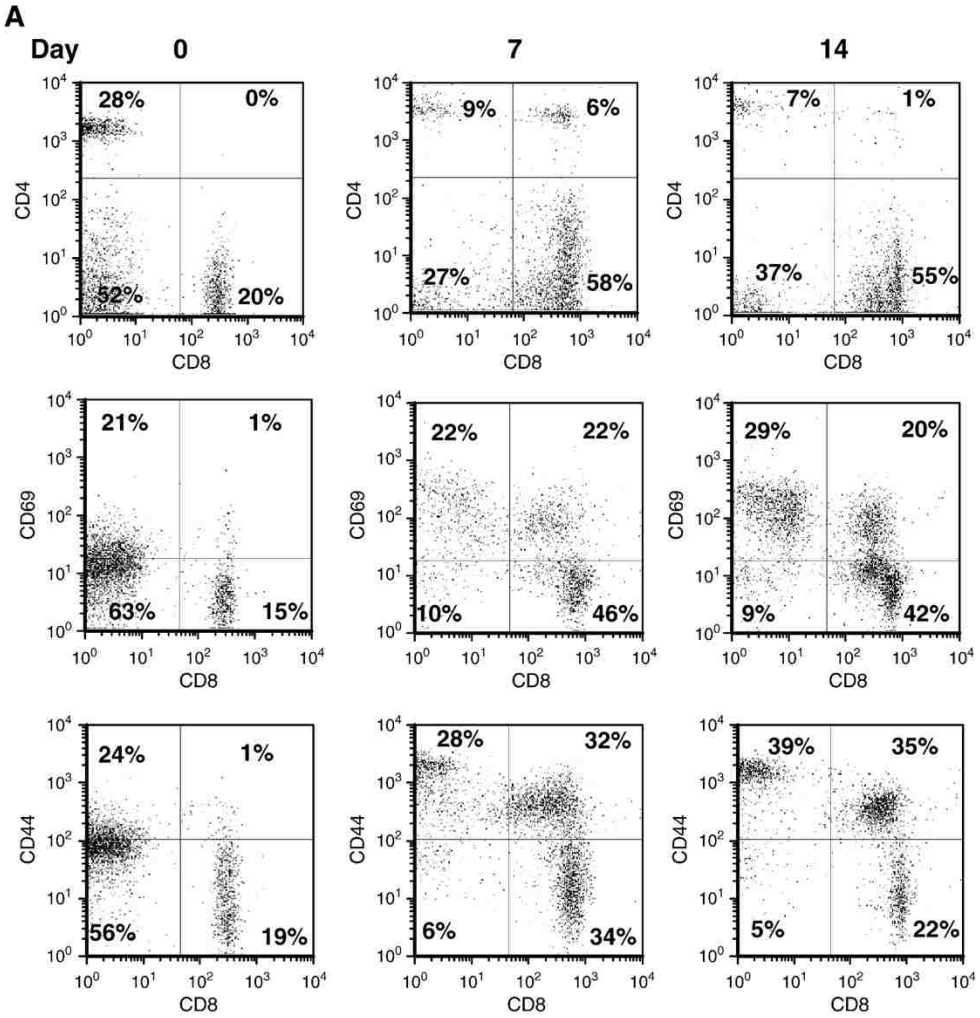

Figure 3. Expansion of memory-phenotype CD8 T-cells by IL-7.
Lymph node cells (A) and T-cells enriched from spleens (B) of C57BL/6 mice were phenotyped for IL-7-dependent changes in surface proteins. Cells were cultured with IL-7 (150 ng/ml) for 0, 7 and 14 days. Cells were stained with fluorochrome-conjugated antibodies specific for CD4, CD8, CD44 and CD69 and analyzed by flow cytometry. FSC/ SSC gating was used to establish viable gates for lymphocytes. In each dot plot, the percentages of cells in each quadrant are shown relative to the total cells. Representative results from four time course experiments are shown.

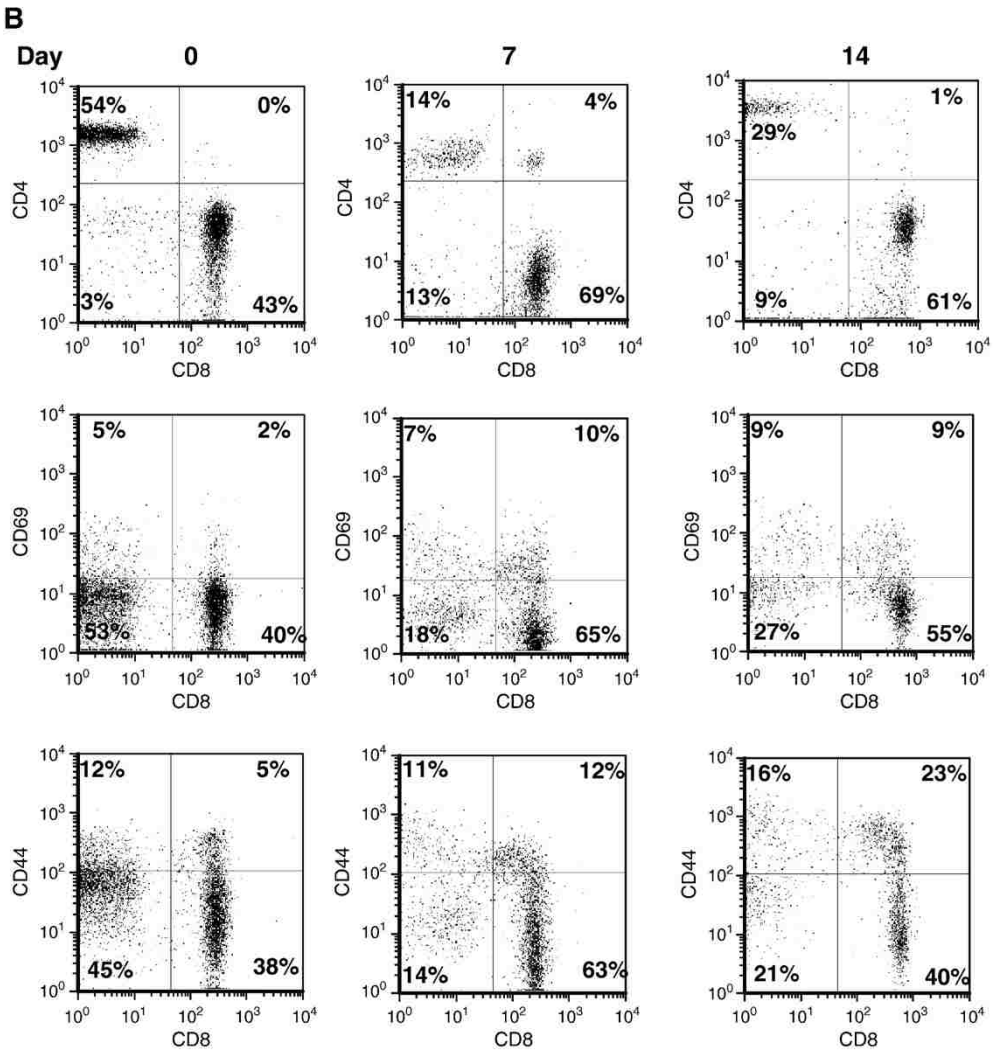

Figure 3. Expansion of memory-phenotype CD8 T-cells by IL-7.

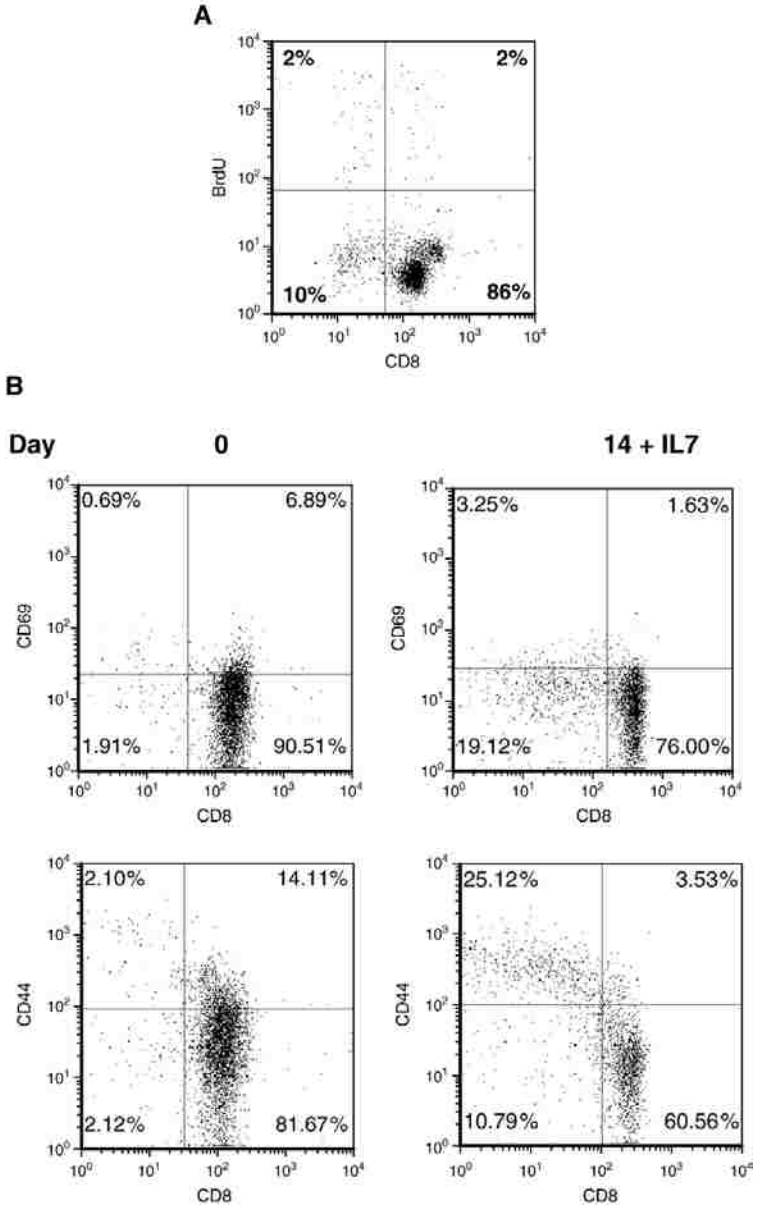

Figure 4. Naive T-cells do not proliferate in response to IL-7.
(A) To examine IL-7 dependent proliferation, cells from the lymph nodes of OT-I Rag1$^{-/-}$ mice were cultured with IL-7 (150 ng/ml) for 14 days and pulsed with BrdU for the final 48 hours. Cells were stained with antibodies for CD8 and BrdU for analysis by flow cytometry. Displayed are the percentages of viable CD8 T-cells (based on FSC/ SSC) that incorporated BrdU during the 48 hours pulse. Representative results from two experiments are shown. (B) Lymph node cells from OT-I Rag1$^{-/-}$ mice were cultured with IL-7 (150 ng/ml) for 0 and 14 days. For analysis by flow cytometry of surface protein changes, cells were stained with fluorochrome-conjugated antibodies for CD8, CD44 and CD69. FSC/ SSC gating was used to establish viable gates for lymphocytes. In each dot plot, the percentages of cells in each quadrant are shown relative to total cells. Time course experiments were performed twice. Representative results are shown.

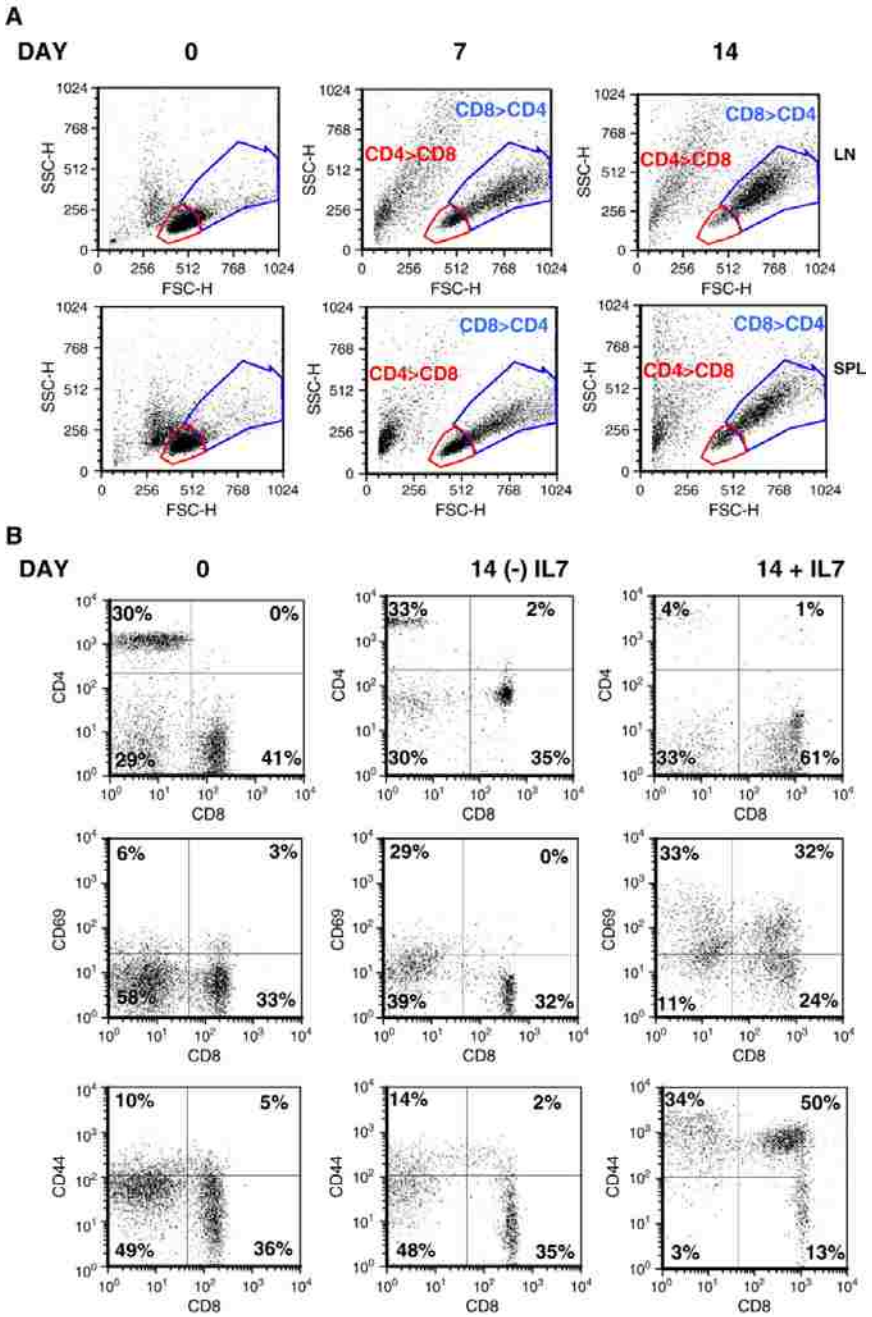

Figure 5. Differentiation of the proliferative from the survival effects of IL-7.
(A) Bim$^{-/-}$ lymph nodes cells and splenic T-cells were cultured with IL-7 (150 ng/ml) for 0, 7 and 14 days. Formation of lymphocyte blasts was assessed by the FSC/ SSC of cell populations by flow cytometry. In dot plots, representing data from day 7 and 14 of culture with IL-7, the red gated populations, predominantly CD4 T-cells, contain the smaller-sized cells, while blue gated populations, predominantly CD8 T-cells, contain the larger blast-like cells. (B–C) Bim$^{-/-}$ lymph nodes cells (B) and splenic T-cells (C) were cultured with IL-7 (150 ng/ml) or without IL-7 for 0 through 14 days. Cells were stained with antibodies for CD4, CD8, CD44, and CD69 and analyzed by flow cytometry. FSC/ SSC gating was used to establish viable gates for lymphocytes. The percentages of cells in each quadrant are shown relative to total cells. Representative data from three experiments is shown.

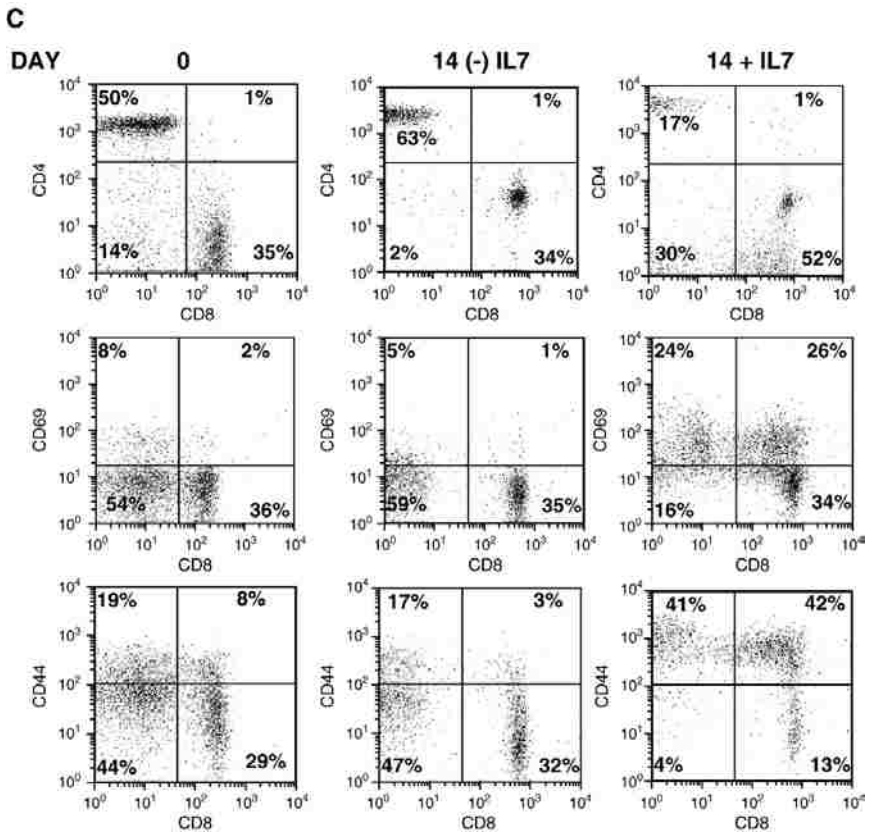

Figure 5. Differentiation of the proliferative from the survival effects of IL-7.

Discussion

We developed an *in vitro* culture system to specifically examine the proliferative activity of IL-7. Results obtained from this approach were independent of other variables that could affect cell growth, such as other cytokines or MHC interactions. The proliferative activity of IL-7 has been demonstrated by *in vivo* studies[25, 34], however, this activity could not be attributed exclusively to the cytokine given the complexity of the *in vivo* environment. Conversely *in vitro* studies that could more specifically study the function of IL-7 resulted in conflicting findings. In some *in vitro* experiments, IL-7 induced proliferation of T-cells[35], while in others it did not[26]. One reason for the different findings made by *in vitro* studies could be that varying culture conditions were utilized. For example, we and others have shown that the concentration of IL-7 used in culture can influence the experimental outcomes - high doses of IL-7 induce proliferation while low doses of IL-7 promote survival[19, 20]. Another factor that could affect *in vitro* results is the type of cell evaluated - naïve T-cells may require multiple growth signals while memory T-cells may not. Such variability in the *in vitro* assay conditions would significantly affect the response of T-cells to IL-7, creating the ambiguous reports of the cytokine's proliferative function.

To address this problem, we developed an *in vitro* IL-7 culture method that would support the expansion of T-cells as has been observed under *in vivo* lymphopenic conditions. Features of our system included an increased dose of IL-7 and extended culture periods. The concentration of IL-7 (150 ng/ml) utilized in our *in vitro* cultures is higher than the levels of IL-7 typically detected in serum (0.3–8.4 pg/ml)[10]. We found that this higher dosage was necessary to support the active cell cycling of CD8 T cells under our *in vitro* conditions. In previous studies

we reported that the induction of proliferation by IL-7 required a stronger IL-7 dose (>50 ng/ml) than the maintenance of survival (<10 ng/ml)[19]. It is possible that a strong proliferative stimulus (as we replicated in our culture system) could be delivered *in vivo* through synergy of IL-7 with additional signals such as TCR engagement of MHC/ peptide as has been demonstrated with naïve T-cells and CD4 memory T- cells[25, 36]. In this regard, IL-7 could function to lower the TCR activation threshold. Although less well-documented *in vivo*, the IL-7 signal could be enhanced by synergy with other cytokines to drive T-cell proliferation. A recent report showed that IL-7 could synergize with IL-6 or IL-21 *in vitro* to promote the proliferation of CD8 T-cells independent of TCR signaling[37] with the resulting enhancement of IL-7 dependent STAT5 activity. Keeping such possibilities in mind, *in vivo* experiments demonstrate that increasing IL-7 levels through the induction of lymphopenia[38, 39], expression of an IL-7 transgene[15], or injecting high doses of IL-7 (relative to physiological doses) as has been done in human clinical trials lead to the expansion of T-cells[24]. We found that using an elevated dose of IL-7 in our *in vitro* experiments mimicked the replicative function of this cytokine observed *in vivo*.

One specific goal was to use the culture method to identify the subset of T- cells that actively proliferate to IL-7 in the absence of other signals. We observed that extended *in vitro* culture with IL-7 selectively expanded CD8 T-cells with a memory phenotype, such as has been seen when T-cells proliferate in IL-7 transgenic hosts[15]. Our *in vitro* culture likely promotes the specific expansion of memory-phenotype CD8 T-cells for the following reasons: 1) The accumulation of $CD44^{hi}$ CD8 T-cells was not immediate but was detectable after 2 weeks of culture in IL-7, suggesting that these cells expanded from a small existing population and not from conversion of naïve cells to memory cells. This was confirmed when we observed that

naïve T-cells from OT-1/Rag1$^{-/-}$ mice did not generate CD44^{hi} cells after culture in IL-7. 2) After 14 days of culture, small populations of CD4 and CD44^{lo} T-cells still remained, indicating that non-specific up-regulation of CD44 was not occurring. 3) Only a subset of T-cells, which were not naïve, rapidly proliferated to IL-7 as indicated by CFSE dilution and BrdU incorporation, demonstrating that IL-7 did not induce the proliferation of all cultured cells.

The proliferative activity of IL-7 has been characterized by others as non-activating in that the activation marker CD69 was not up-regulated[16, 30]. In contrast, we observed that *ex vivo* expansion of T-cells with IL-7 resulted in an increase in CD69 expression as well an increase in the percentage of CD8^{hi} CD69^{hi} T-cells. This outcome is not an artifact of *in vitro* culture conditions. We found that CD8 T-cells from OT-1/Rag1$^{-/-}$ mice did not up-regulate CD69. Moreover, T-cells expressing CD69 have been observed in different tissues. In the bone marrow, CD8 T-cells expressing CD69 have been found[40], and in the gut, intestinal epithelial cells (IELs) retain CD69 expression long after antigen has been cleared[41]. It follows that both the bone marrow and gut are anatomic sites where IL-7 production has been observed[42, 43].

What is unique with our IL-7 *in vitro* culture system is that we have revealed the presence of a population of cells that only rely on an IL-7 signal to induce its proliferation. This is significant because the cell types expanded *in vitro* in our IL-7 assay are phenotypically similar, with the exception of CD69 expression, to the T-cell subset that accumulates *in vivo* in the lymphoid organs of STAT5b-CA mice. Further, the expansion of memory CD8 T-cells results not as a default effect of IL-7's survival function, but rather is a consequence of a distinct proliferative activity. This was shown by using the IL-7 *in vitro* system to culture Bim deficient T-cells in the presence or absence of the cytokine. These conclusions could not have been

reached by traditional adoptive transfer methods using immunodeficient mice. Therefore, the presented method for the *ex vivo* expansion of IL-7 responsive cells incorporates features from *in vivo* and *in vitro* studies to provide a novel methodology to study the diverse activities of this important cytokine.

CHAPTER 3: THE INTERACTION OF LCK AND THE CD4 CO-RECEPTOR ALTERS THE DOSE RESPONSE OF T-CELLS TO INTERLEUKIN-7

Introduction

CD4 and CD8 T-cells differ in their proliferative responses to IL-7 with a preferential expansion of CD8 T-cells[16, 18, 44]. This trend is not limited to *in vitro* studies or animal models as similar effects have been observed in humans. While administration of IL-7 into humans supported the survival of both CD4 and CD8 T-cells by up-regulating the anti-apoptotic protein BCL-2, it had the greatest proliferative effect on CD8 T-cells[24]. Furthermore, lymphopenic conditions in humans which are associated with increased concentrations of IL-7 show a greater inverse correlation with CD4 T-cells numbers than CD8 T-cell numbers[38]. Collectively, these findings suggest that high levels of IL-7 may have different growth effects upon CD4 versus CD8 T-cells.

While the effects of extreme ranges of IL-7 concentrations are well known: immunodeficiency in the absence and lymphoma when overexpressed[5], more subtle dose effects of IL-7 upon T-cell subset growth have also been reported. In one study, by controlling the expression levels of an IL-7 transgene (Tg) in mice, a concentration effect of IL-7 upon T-cell development was revealed[45]. Only low doses of IL-7 could support αβ T-cell development, while high doses effectively blocked development at an early intrathymic stage. We observed, using an IL-7 dependent T-cell line, that a low concentration of IL-7 provided survival signaling, while a high concentration of IL-7 was required to sustain proliferation[18, 19]. Such findings were translated into distinct signaling effects upon the proliferation of naïve versus memory CD4 T-

cells, with naïve T-cells cycling less in response to IL-7[46]. In fact, transgenic expression of IL-7 could enhance the proliferation of both CD4 and CD8 T-cells but not B-cells[31], however the proliferation of CD4 T-cells compared to CD8 T-cells was significantly slower. Moreover, injections with IL-7 resulted in CD4 T-cells increasing their numbers only four-fold as compared to CD8 T-cells which increased 14-fold[16]. These studies suggest that there are IL-7 dose specific effects, and that lymphocyte subsets do not respond equally to IL-7, with CD4 T-cells lagging behind CD8 T-cells in their proliferative response. The molecular basis for this differential response to IL-7 remains to be elucidated but could depend on how the activation of the transcription factor, STAT5, is regulated.

A critical transducer of the IL-7 signal, STAT5 exists in two redundant forms of STAT5a and STAT5b and can be phosphorylated and activated by both JAKs and Src kinases, such as LYN and LCK[47-49]. Recent studies showed that CD8 T-cells but not CD4 T-cells, with the exception of regulatory T-cells, are more dependent on STAT5 activity. Loss of STAT5 severely affected the survival of CD8 T-cells as compared to CD4 T-cells[50], and mice expressing a constitutively active form of STAT5b displayed a striking expansion of CD8 T-cells[30]. Why CD8 T-cells thrive under conditions of high STAT5 activity, but not CD4 T-cells, remains to be fully understood. Answers may lie in a better understanding of the function of the CD4 and CD8 co-receptors and how their modulation of Src kinase activities affects cytokine signaling through STATs.

It is well known that homeostatic proliferation of naïve T-cells requires both an IL-7 signal, since these cells fail to grow when transferred to IL-$7^{-/-}$ recipients[25], and a T cell receptor (TCR) signal transduced though the Src kinase, LCK[51]. However, administration of IL-7 has a

strong biological effect on CD8 T-cells, leaving unexplained why CD4 T-cells fail to grow as abundantly upon receiving the same IL-7 stimulus. One recent explanation is that MHC class II expression on dendritic cells, which also express an IL-7R, is down-regulated by IL-7 and inhibits the expansion of CD4 T-cells, at least *in vivo*[44]. However CD4 T-cells still fail to thrive in STAT5b transgenic mice, in which the transgene was only expressed in lymphocytes[30], suggesting that there also exist inherent differences in CD4 T-cells that account for their inability to respond to IL-7 in the same manner as CD8 T-cells. Our own observations with *in vitro* culture of isolated T-cells with IL-7[18] support this conclusion. To explore the different dose responses of T-cell subsets to IL-7 and reveal a potential mechanism to account for such differences, we studied the expansion of CD4-expressing and non-CD4 expressing T-cells to high and low doses of IL-7. We found that expression of the CD4 co-receptor and the Src kinase, LCK, modulated the responsiveness of CD4 T-cells to IL-7, enabling these to preferentially grow under conditions of low dose, but not high dose, IL-7. CD8 T-cells, in contrast, had no such restrictions. CD4 and CD8 T-cells are thus equipped to respond differently to IL-7, through the interaction of LCK and CD4 co-receptor, which has significant implications for the use of the cytokine in a therapeutic setting.

Materials and methods

Mice, cells and cell isolation techniques

C57BL/6 mice were purchased from Jackson Laboratory (Bar Harbor, Maine) and OT-1/Rag1$^{-/-}$ mice were purchased from Taconic. Mice were housed in the animal facility at the University of Central Florida and used at 2-3 months of age. STAT5b-CA mice were generously provided by Dr. Michael Farrar (Department of Laboratory Medicine and Pathology, University of Minnesota, Minneapolis, MN). IL-7R transgenic mice were generously provided by Dr. Alfred Singer (NEI, NIH). Animal studies were reviewed and approved by the Institutional Animal Care and Use Committee (IACUC) at the University of Central Florida.

Lymph node and spleen cells were isolated by gentle crushing of organs through a 70μM pore filter (BD Falcon) and pooled. Spleen cells were further treated with ACK lysis buffer (Quality Biological, Inc.) to lyse red blood cells (RBCs) and enriched for T-cells by negative selection with a commercially available kit, the IMag Mouse T-lymphocyte Enrichment kit (BD Biosciences). CD4 or CD8 T-cell subsets were enriched by negative selection using the IMag T-cell enrichment kit supplemented with biotinylated CD4 or CD8 antibodies. Thymocytes were isolated from thymic lobes by gentle disruption with a micropipette after treatment with 0.2% collagenase and double negative thymocytes (CD4$^{-/-}$CD8$^{-/-}$) isolated by negative selection using the IMag system as described above. Naïve T-cells were isolated directly from the lymphoid organs of C57BL/6 mice, while CD44^{hi} memory T-cells were isolated from OT1/Rag1$^{-/-}$ mice after 6 weeks from receiving an interperitoneal injection of 10 mg of ovalbumin (OVA). Isolation of T cells was confirmed by analysis of surface markers by flow cytometry as described below.

The IL-7-dependent T-cell line, D1, was established from pro-T-cells isolated from a $p53^{-/-}$ mouse as previously described[52].

In vitro culture with IL-7

Culture conditions, for the *ex vivo* expansion of IL-7-responsive cells, were previously described[18]. Briefly, primary T-cells isolated from lymphoid organs were maintained at a density of 3-5 x 10^6 cells/ml in complete medium (RPMI 1640 Medium (Invitrogen) supplemented with 10% fetal bovine serum (Hyclone), 2-βmercaptoethanol (1000X, Life Technologies), and 50 U/mL penicillin/ streptomycin) in 24 well plates. Recombinant human IL-7 (Peprotech) was added at the start of culture at a concentration of 10 or 150 ng/ml and refreshed every other day. Previously we established that murine T-cells grow well with human recombinant cytokine. Cultures were maintained with or without IL-7 through 14 days or until noticeable cell death was apparent and confirmed by Trypan Blue exclusion staining. In LCK inhibition experiments, cells were treated with LCK inhibitor II (Calbiochem) at 1μM or with a comparable volume of the vehicle control (DMSO) at the time points indicated in the figure legends. The D1 and D1-CD4 T-cell lines were maintained in complete medium as described above and cultured with 0, 10, or 50 ng/ml of IL-7 as indicated.

Cell surface protein analysis

Surface expression of membrane proteins expressed on T-cells was assessed by flow cytometry using the following fluorochrome-conjugated antibodies: PE-conjugated anti-CD4 (clone GK1.5), PerCP-conjugated anti-CD4 (clone RM4-5), PerCP-conjugated anti-CD8 (clone

53-6.7) (BD Biosciences) and PE-conjugated anti-CD127 (IL-7R) (clone A7R34) (eBiosciences). PE- or PerCP-conjugated isotype matched antibodies were used as controls for non-specific staining. Cells were incubated with saturating amounts of the appropriate antibodies for 20 minutes on ice, washed in buffer (PBS + 0.1% bovine serum albumin (BSA)) and analyzed by flow cytometry on a FACSCalibur flow cytometer (BD Biosciences) or C6 flow cytometer (Accuri).

Viability and proliferation assays

T-cell viability was determined based on cell shrinkage and fragmentation by gating on FSC/ SSC parameters acquired by flow cytometry. To measure DNA synthesis, 5 x 10^6 cells were pulsed with BrdU (10μM) for 48 hours, and BrdU incorporation was detected with a commercially available kit (BD Biosciences) according to manufacturer's protocol. Briefly, cells were typed for surface markers CD4 or CD8 as described above, washed, fixed, and permeabilized prior to incubation with a FITC-conjugated anti-BrdU antibody. The cells were analyzed by flow cytometry as described above. Statistical analysis was performed using Prism software (GraphPad).

Intracellular staining of phospho-STAT5 or LCK

For detection of intracellular phosphorylated STAT5 and total LCK, we used an optimized protocol designed to enhance detection of these intracellular proteins[53]. Prior to fixation, cells were stained with PerCP-conjugated antibodies for CD4 (clone RM4-5) or CD8 (clone 53.6.7) (BD Biosciences) as described above. Cells were washed, fixed, and

permeabilized with the Fix & Perm Cell Permeabilization kit (Caltag) following the manufacturer's protocol. Cells were stained with either PE-conjugated anti-phospho-STAT5 (clone 47), or PE-conjugated anti-LCK (clone MOL 171) or isotype matched control PE-conjugated antibodies (BD Biosciences). Cells were analyzed by flow cytometry using the C6 flow cytometer (Accuri) as described above.

Plasmids and transfection of cells

To generate the D1-CD4 T-cell line, D1 T-cells were transfected with CD4 cDNA by electroporation using standard methodologies. Stable lines were selected by antibiotic resistance to Blastocidin. For transient expression of the CD4 co-receptor on CD8 T-cells, CD8 T-cells were enriched by negative selection with biotinylated anti-CD4 (clone GK1.5) (BD Biosciences). CD8 T-cells were then nucleofected with 4µg of plasmid encoding for the CD4 co-receptor, EGFP or the empty vector (pcDNA), using the Mouse T-cell Nucleofection kit (Amaxa) according to the manufacturer's protocol. Cells were analyzed after 24 hours.

Confocal microscopy and live cell imaging

T-cells were stained with the indicated fluorochrome-conjugated antibody as previously described for cell surface protein analysis. D1-CD4 T-cells were fixed after staining using the fixation protocol that is part of the Fix & Perm Cell Permeabilization kit (Caltag). Images were acquired with LSM 510 using 100x/1.4 Oil DIC objective. The composite images were processed and 3D projections of the Z-stacks were generated using the LSM image browser from Zeiss. For live cell imaging, images were acquired with Axio Observer Z1 using a Plan-

Apochromat 63x/1.4 Oil objective. The images were processed with AxioVision LE (Zeiss). Scanned images were generated and modified within the Zen 2009 image processing program (Zeiss).

Immunoprecipitation and immunoblotting

D1 and D1-CD4 T-cells were lysed using Cell Lysis Buffer (Cell Signaling) in the presence of protease inhibitors (Roche) at 4^{o}C. Lysates were precleared with Preclearing Matrix E (sc-45056; Santa Cruz), following manufacturer's protocol, and incubated overnight at 4^{o}C with CD4 antibody (clone 5B5) or CD3 (clone 5B2) (Santa Cruz) antibody complexed with an immunoprecipitation matrix according to the manufacturer's protocol (ExactaCruz E: sc-45042, Santa Cruz). Next day, the matrix was washed and resuspended in 2x loading buffer (Invitrogen), heated to 94°C and centrifuged to pellet matrix. Supernatants were loaded onto a 12% SDS-PAGE gel and proteins transferred onto nitrocellulose membrane. Immunoblotting was performed with anti-LCK (clone 28/LCK) or anti-CD4 (clone C-18) (Santa Cruz) primary antibody followed by the appropriate ExactaCruz E secondary antibody (for immunoprecipitated lystates) or an HRP-conjugated secondary antibody (for pre- and post-precipitation lysates). Signal was developed by enhanced chemiluminescence (ECL) (Pierce) and visualized on BioMax ML film (Kodak). The relative intensities of the bands were quantitated using the Kodak Image Station 4000MM PRO with band detection and density determined using the Carestream Molecular Imaging SE software.

For detection of phosphorylated LCK, whole cell lysates from primary cells were prepared as described above in the presence of phosphatase inhibitors (Roche). Supernatants

were loaded onto a 12% SDS-PAGE gel and proteins transferred onto nitrocellulose membrane. Immunoblotting was performed with Phospho-LCK (Tyrosine 505) antibody (Cell Signaling), followed by the appropriate HRP-conjugated secondary antibody.

Csk gene expression analysis by real-time PCR

For RNA extraction, D1 cells (2.0×10^7) were centrifuged and cell pellets were resuspended in 1 ml TRIZOL (Invitrogen). One μg of RNA was converted into cDNA using iScript cDNA synthesis kit (BioRad). Real-time PCR reactions were performed using Fast SYBR® Green Mix (Applied Biosystems) on a 7500 Real-time PCR system (Applied Biosystems). Primers sequences for Csk were Forward: 5'-ATGAAGAACTGCTCGCACCT-3' and Reverse: 5'-GGCTCAGTTCAAGTTCAGGC-3.' β-actin was used as an endogenous control.

Results

IL-7 has been described as a growth factor for T-cells; however the reported proliferative effects of IL-7 upon different lymphocyte subsets vary considerably. Consistent with this observation, we reported that *ex vivo* culture of T-cells with a high dose of IL-7 (in the absence of TCR stimulation) resulted in the preferential expansion of CD8, but not CD4, T-cells[18]. This bias of IL-7 on the proliferation of CD8 T-cells over CD4 T-cells under high dose conditions was also apparent upon IL-7 administration to humans[24] or mice[15]. In this study, we sought to examine the basis for the differential responses of CD4 T-cells versus CD8 T-cells to IL-7, focusing on why CD4 T-cells grow optimally at a lower dose of IL-7.

IL-7 dose responsiveness is different between CD4 and CD8 T-cells

Using the IL-7 *ex vivo* culture system that we previously developed[18], we compared the growth of CD4 and CD8 T-cells cultured in different concentrations of IL-7. These doses of IL-7 was chosen after examining the effect of low and high concentrations of IL-7 upon the expansion of IL-7 dependent cells[18]. T-cells were isolated from the lymphoid organs of wild type mice and cultured with 150 or 10 ng/ml of IL-7 for 5-14 days. Figure 6A shows that expansion of T-cells occurred at both doses of IL-7 tested, with slightly more cells recovered in response to the higher 150 ng/ml dose. This was indicated by an approximate doubling of T-cell numbers from 5 through 14 days of culture (Fig. 6A). Assessment of the viability of the cell cultures revealed that after 5 days, cells grown with 10 or 150 ng/ml IL-7 were 62-64% viable (Fig. 6B). However, after 14 days of culture, more death was observed with cells grown at the 150 ng/ml dose of IL-7 (39% viable) compared to the lower dose of 10 ng/ml (53% viable) (Fig.

6B). Immunostaining revealed that the majority of the T-cells that expanded at the higher dose of IL-7 were CD8 T-cells (Figs. 6C, 6E). In contrast, the CD4 T-cell population, when cultured with 150 ng/ml of IL-7, was significantly diminished relative to CD8 T-cells (Figs. 6D, 6E). While CD8 T-cell numbers more than doubled when cultured with 150 ng/ml of IL-7, CD4 T-cells were maintained at the lower dose of 10 ng/ml of IL-7 (Figs. 6C, 6D). Initially, CD4 T-cells were detected in approximately equal ratio with CD8 T-cells (typical CD4:CD8 ratios for C57Bl/6 mice range from 1.3-1.0:1.0) (Fig. 6E), but after 5 and 14 days CD4 T-cells were increased only in culture with the lower dose of IL-7 tested (Fig. 6E). Hence, relative to CD8 T-cells, CD4 T-cell numbers decreased over time when maintained with the higher dose of IL-7. The apparent loss of the CD4 T-cells when cultured with 150 ng/ml of IL-7 could result from increased cell death or loss of proliferation.

Previously, we found that CD4 T-cells incorporated less BrdU (synthesized less DNA), compared to CD8 T-cells, under conditions of high dose IL-7[18], suggesting that their proliferation was impaired. However, we also detected decreased viability in total T-cell cultures grown with 150 ng/ml of IL-7 for 14 days that could be due to increased CD4, but not CD8, T-cell death (Fig. 6B). To examine this, we enriched T-cells isolated from lymphoid organs for either CD4 or CD8 subsets and assayed for viability of each subset grown under conditions of high dose IL-7. Figure 6F shows that enrichment yielded cultures of either CD4 or CD8 T-cells without measurable cross-contamination. After seven days of culture with high dose IL-7, we observed fewer viable CD4 T-cells (69% viable) and more viable CD8 T-cells (90% viable), indicating that CD4 T-cells were dying (dead cells indicated by shrinkage and fragmentation) under conditions of 150 ng/ml of IL-7 (Fig. 6F). Moreover, an approximate

doubling of enriched CD8 T-cells occurred at the higher dose of IL-7 that was not noted with CD4 T-cells (data not shown). These results suggested that CD4 T-cells were inhibited for both proliferation and survival when the amount of IL-7 was increased and are therefore intrinsically different from CD8 T-cells in their response to the cytokine.

To rule out potential competitive advantages due to differential expression of IL-7R, we isolated T-cells from mice transgenically engineered to express IL-7R (IL-7RTg). While IL-7RTg CD4 and CD8 T-cells express higher levels of IL-7R than their wild-type counterparts, both IL-7RTg CD4 and CD8 T-cells express similar levels of the receptor (data not shown). Despite the fact that IL-7R levels were elevated on both T-cell subsets, culture of IL-7RTg T-cells in high dose IL-7 still skewed the CD4:CD8 ratio to mostly CD8 T-cells (Fig. 6G). BrdU incorporation showed that, in contrast to CD8 T-cells, IL-7RTg CD4 T-cells proliferated poorly in response to IL-7 (Fig. 6G). We conclude therefore that CD4 T-cells were inhibited for growth in high dose IL-7 irrespective of the level of IL-7R.

Expression of CD4 alters the IL-7 dose responsiveness of T-cells

As our findings showed that IL-7R expression could not fully account for the variation in responses of CD4 versus CD8 T-cells to high dose IL-7, we examined the contribution of the CD4 co-receptor and tested whether expression of CD4 on CD8 T-cells could reverse IL-7 high dose responsiveness. We transiently expressed the CD4 co-receptor on freshly isolated naïve CD8 T-cells, that is T-cells that had not been exposed to exogenous antigen, using the technique of nucleofection and cultured the nucleofected naïve T-cells in high dose (150 ng/ml) or low dose (10 ng/ml) IL-7 for 24 hours. Nucleofection efficiency, as measured by the expression of

GFP that is independent of any IL-7 effects (Fig. 7A), averaged about 32%, and we detected the expression of CD4 in about 56% of the total cells nucleofected with the CD4 cDNA (Fig. 7A). Note, that we observed a small percentage of naïve CD8 T-cells (5–6%) that also endogenously expressed CD4 in cells nucleofected with the empty vector, pcDNA (Fig. 7B). In naïve CD8 T-cells nucleofected with the CD4 co-receptor, we observed few CD8 T-cells (11%) cultured with 150 ng/ml of IL-7 (Fig. 7B). However, at 10 ng/ml of IL-7, these cells composed almost 34% of the total naïve T-cell population (Fig. 7B).

To account for the loss of naïve CD8 T-cells co-expressing CD4 at the higher dose of IL-7, we examined cell viability. Note that the short nature of the nucleofection experiment would not allow for significant proliferation to have occurred. Overall viability for all nucleofected cells (pcDNA and CD4) ranged from 40–50% and equal numbers of cells were analyzed in each experimental set (data not shown). Fig. 7C is gated on naïve CD4-expressing CD8 T-cells and shows that there were fewer viable cells (12%) in 150 ng/ml of IL-7 compared to 10 ng/ml of IL-7 (32%). This result shows that there was increased cell death (identified by shrinkage and fragmentation) of naïve CD4-expressing CD8 T-cells at the higher dose of IL-7. Furthermore, the amount of CD4-expressing CD8 T-cells detected at 10 ng/ml of IL-7, 34% (Fig. 7C), correlated well with the percentage of CD8 T-cells that were nucleofected as indicated by EGFP expression (Fig. 7A). This data suggested that expression of the CD4 co-receptor altered the IL-7 dose response of naïve CD8 T-cells, adapting them for growth in low dose IL-7.

To determine whether the effect of CD4 altering the IL-7 dose responsiveness of naïve CD8 T-cells could occur in other subsets of T-cells, we isolated $CD44^{hi}$ memory CD8 T-cells from OT-1/$Rag1^{-/-}$ mice previously primed with ovalbumin and nucleofected with CD4 cDNA.

Nucleofection efficiency and CD4 expression were optimal in these cells (Fig. 7D). Fig. 7D shows that expression of CD4 on these memory CD8 T-cells (note that OT-1 mice do not have endogenous CD4 T-cells) also significantly shifted the dose response to the lower concentration of IL-7. We confirmed, therefore, the observation made with naïve T-cells (Fig. 7B and C) that CD4 expression alters the capacity of CD8 T-cells to respond to IL-7. We also examined a third subset of T-cells that are highly responsive to IL-7 - the double negative (DN) thymocytes ($CD4^{-/-}CD8^{-/-}$) found in the thymus. DN thymocytes were very difficult to nucleofect with gene expression efficiencies of 11-13% (Fig. 7F). Nevertheless we observed minimal differences in CD4-expressing cells cultured with high or low dose IL-7, suggesting that thymocytes at this stage of development may be independent of the effects of CD4 expression upon IL-7 signaling. Given the findings observed with naïve and memory peripheral CD8 T-cells, we concluded that there were no significant intrinsic differences between CD4 and CD8 T-cells, in regards to IL-7 dose responsiveness, other than co-receptor expression. Our data thus far supported a role for the CD4 co-receptor in modulating the responses of T-cells to different concentrations of IL-7.

To examine how the expression of CD4 versus CD8 co-receptor could affect IL-7 signaling, we analyzed co-receptor distribution. Using confocal microscopy, we acquired images using unfixed, live cells to observe the distribution of the co-receptors. Fig. 8A shows two representative images of multiple cells that were visualized showing that the CD8 co-receptor (green fluorescence) is evenly distributed on the surface of freshly isolated naïve T-cells. In contrast, when freshly isolated naïve CD4 T-cells were imaged, distinct patches or brighter aggregates of the co-receptor (red fluorescence) could be seen at or near the surface of these cells (Fig. 8A, right), perhaps localizing to membrane proximal vesicles. These results suggested that

there were significant differences in the segregation of the membrane-associated CD4 co-receptor, but not the CD8 co-receptor, that could influence intracellular signaling cascades.

In order to examine the contribution of the CD4 co-receptor to IL-7 signaling at the mechanistic level, we used a T-cell line, called D1, that is IL-7 dependent and does not express any co-receptors but retains TCR:CD3 expression[17]. Previously, we showed that D1 T-cells begin to die between 24 and 48 hours after IL-7 withdrawal[17]. To study the role of the CD4 co-receptor, we stably transfected D1 T-cells with CD4 cDNA (D1-CD4) and selected for cells expressing the co-receptor. These experiments were possible because CD4, unlike CD8, is a single transmembrane protein that can be expressed from a single stably integrated plasmid.

We observed significant levels of CD4 expression on 70–80% of the D1-CD4 T-cells, but not D1 T-cells (Fig. 8B and data not shown). Composite images in Fig. 8B show surface expression of the CD4 co-receptor and IL-7R on D1-CD4 T-cells that were fixed and analyzed by confocal microscopy. We noted that while the IL-7R seemed equally distributed on the cell surface, the CD4 co-receptor appeared to aggregate within patches in the membrane (Fig. 8B) similar to that observed on naïve CD4 T-cells (Fig. 8A, right). No significant overlay of the CD4 co-receptor and the IL-7R was noted (Fig. 8B, overlay). Interestingly, while the parental D1 T-cells grew optimally at an IL-7 dose of 50 ng/ml[52], we observed decreased viability of D1-CD4 T-cells at this dosage (data not shown). In fact, the D1-CD4 T-cells grew best at a lower dose of 10 ng/ml of IL-7. We thus routinely maintained the D1-CD4, but not the D1 T-cells, at an IL-7 concentration of 10 ng/ml. As we observed for primary T-cells (Fig. 6) and CD4-expressing CD8 T-cells (Fig. 7), expression of the CD4 co-receptor enabled D1 T-cells to grow at a lower dose of IL-7 compared to the parental D1 cell line.

Association of LCK with CD4 is observed in an IL-7 dependent T-cell line

Our data suggests that the CD4 co-receptor modulates the dose response of a T-cell to IL-7. We ruled out a contribution from the IL-7R by showing that transgenic expression of the IL-7R did not generate comparable responses to IL-7 between CD4 and CD8 T-cells (Fig. 6G) nor did CD4 directly associate with the IL-7R (Fig. 8B). Therefore to understand the contribution of the CD4 co-receptor to the IL-7 signal, we examined the intracellular association of CD4 with the Src kinase, LCK[54]. It is known that LCK has a different affinity for CD4 versus CD8[55]. The proportion of LCK associated with the CD4 co-receptor was documented to be 10–20-fold higher than the amount associated with the CD8 co-receptor[56]. In fact, a range of 75–95% of cellular LCK has been reported to be associated with CD4 co-receptor while only 5–10% is associated with CD8[57]. Such findings led us to determine whether the association of LCK with the CD4 co-receptor or the CD3/TCR complex could be detected in D1 and D1-CD4 T-cells. We directly examined the association of LCK with either the CD4 co-receptor or the CD3/ TCR complex by co-immunoprecipitation. Using D1 and D1-CD4 T-cells, we performed immunoprecipitation experiments using antibodies against either CD4 or CD3 and immunoblotted for the presence of LCK. Representative pre-precipitation lysates are shown in Fig. 8C to demonstrate that LCK was present in all the lysates assayed. Fig. 8D shows the amount of LCK that co-precipitated with either CD3 or CD4 with results from a densitometry scan below. Results from two representative experiments (Precipitate #1 and Precipitate #2) are shown (Fig. 8D). Moreover, since multiple bands at the approximate size of LCK and CD4 immunoprecipitated, we used two methods to define the band for the protein of interest: (1) whole lysates containing LCK or CD4 were run along size molecular marker lanes in an SDS-

PAGE gel to determine upon immunoblotting the location of the protein of interest (data not shown) and (2) for an unbiased determination of the protein band of interest, we used the Carestream Molecular Imaging SE software to identify and calculate the density of the unique band corresponding to our protein of interest, LCK or CD4. In the panels shown in Fig. 8D, arrows indicate the location of LCK or CD4 determined as described above. We observed that in D1 T-cells, detectable amounts of LCK associated with CD3 when cells were stimulated with 50 ng/ml of IL-7 (Fig. 8D). No CD3-bound LCK was measured in lysates from D1-CD4 T-cells (Fig. 8D). Likewise, no LCK was co-immunoprecipitated with CD4 in D1 cells, since these cells lack expression of CD4 (Fig. 8D). As a control, we only detected CD4 protein by immunoblot in D1-CD4 T-cells that were co-immunoprecipitated with anti-CD4 antibody. This co-immunoprecipitation experiment clearly demonstrated that LCK was associating with CD4 when the co-receptor was over-expressed. In cells, lacking CD4, LCK could be either "free" or associated with CD3, the latter more so in the presence of IL-7.

LCK modulates the dose response to IL-7 in primary T-cells

IL-7 signaling involves activation through phosphorylation of JAK3 and STAT5. In addition, LCK has been shown to promote the direct[49] or the indirect, through JAK3[58], phosphorylation of STAT5. Phospho-STAT5 levels therefore serve as an indication of a cell's signaling status. To determine whether CD4 and CD8 T-cells differed in their ability to generate phosphorylated STAT5, we measured the intracellular levels of phospho-STAT5 using an optimized flow cytometry-based methodology[53] with an antibody specific for the Tyr694 phosphorylation on STAT5a and STAT5b. We found that a short 20 minute pulse with either

high or low dose IL-7 could induce the phosphorylation of STAT5 in both CD4 and CD8 T-cells (data not shown).

Culturing primary T-cells for 5 days with high dose or low dose IL-7 enabled us to examine the basal levels of phospho-STAT5 and total LCK in response to the cytokine. We previously compared untreated samples to vehicle (DMSO)-treated samples and no differences were noted (data not shown); hence to minimize duplication of data we show the results for vehicle-treated cells. Extended culture of primary T-cells with either 150 ng/ml IL-7 or 10 ng/ml IL-7 did show a concentration dependent effect upon the levels of phospho-STAT5. In vehicle-treated CD8 T-cells, we found increased levels of phospho-STAT5 when cultured with high dose IL-7 (peak median, 1830) compared to low dose IL-7 (peak median, 1108) (Vehicle, Fig. 9A). Consistent with the preferred growth of CD4 T-cells in low dose IL-7, we detected more CD4 T-cells with elevated phospho-STAT5 at 10 ng/ml of IL-7 (peak median, 1437) as compared to high dose IL-7 (peak median 1193) (Vehicle, Fig. 9A). Fig. 9B shows the total intracellular LCK in the cultured primary cells. CD8 T-cells had higher levels of total LCK compared to CD4 T-cells, and these levels were independent of the concentration of IL-7 in the medium (Fig. 9B).

Next, we treated the high dose or low dose IL-7-cultured primary T-cells with an LCK inhibitor overnight and assayed for intracellular phospho-STAT5. We noted that LCK inhibition reversed the observed effects of high dose IL-7 upon phospho-STAT5 levels. In CD4 T-cells, LCK inhibition restored responsiveness to high dose IL-7, with STAT5 levels increasing (peak median 1193, increased to 1889), while in CD8 T-cells, LCK inhibition decreased phospho-STAT5 (peak median 1830, decreased to 1411) (Fig. 9A). At low dose IL-7 (10 ng/ml), LCK

inhibition effects were less significant with decreased phospho-STAT5 in CD4 T-cells, but increased phospho-STAT5 levels in CD8 T-cells (Fig. 9A).

CD4-associated LCK confers responsiveness to low dose IL-7

Results from primary CD4 and CD8 T-cells indicated that LCK was influencing the response to an IL-7 dose (Fig. 9A). To determine whether the CD4 co-receptor was sufficient to modulate the IL-7 dose response, we examined basal levels of phospho-STAT5 and LCK using D1 and D1-CD4 T-cells following culture with IL-7. Previously we established that a 20 minute pulse with high or low dose IL-7 could induce the phosphorylation of STAT5 in D1 and D1-CD4 T-cells, indicating that both cells lines were equipped to respond to an IL-7 signal (data not shown). Fig. 10A (vehicle control) shows that phospho-STAT5 levels were highest in D1 T-cells cultured with 50 ng/ml of IL-7 and in D1-CD4 T-cells cultured at 10 ng/ml of IL-7, paralleling the results obtained with primary cells in that phospho-STAT5 levels peaked in CD8 T-cells cultured at a higher dose of IL-7 and in CD4 T-cells cultured at a lower dose of IL-7 (Fig. 9A). In the absence of IL-7, we also detected significant basal levels of phospho-STAT5 in D1 cells but not D1-CD4 cells (Fig. 10A). Total LCK levels for D1 T-cells decreased in an IL-7 dose dependent manner, with the lowest levels detected in the absence of the cytokine (Fig. 10B). Minimal changes were detected in the total LCK levels for D1-CD4 T-cells, although these were also slightly decreased in cells deprived of IL-7 (Fig. 10B).

As observed with primary T-cells, the effect of LCK inhibition reversed the IL-7 dose responsiveness of D1 and D1-CD4 T-cells. When we compared the effect of LCK inhibition in D1 T-cells (Fig. 10A, D1), we detected decreased levels of phospho-STAT5 in response to 50

ng/ml of IL-7 (peak median 1898 decreasing to 1457 upon LCK inhibition) as well as a significant decrease in basal phospho-STAT5 in D1 cells cultured without IL-7. In D1-CD4 T-cells, LCK inhibition effectively eliminated most of the increased phospho-STAT5 detected at the 10 ng/ml dose of IL-7 (peak median 1655 decreasing to 887 upon LCK inhibition) (Fig. 10A, LCK INH). Therefore, we concluded that LCK modulated the levels of phosphorylated STAT5 and that the sequestering of LCK by the CD4 co-receptor could be in part responsible for the optimal growth of CD4-expressing cells at low dose IL-7.

To identify a mechanism by which LCK could attenuate the IL-7 signal through decreased phosphorylation of STAT5 in CD4-expressing cells maintained in high doses of IL-7 (Figs. 9 and 10), we examine the potential role of Csk (c-src tyrosine kinase). Csk negatively regulates the activity of LCK through phosphorylation of LCK at tyrosine 505. We propose that one function of the CD4 co-receptor may be to localize LCK within proximity of Csk, which is found in membrane lipid rafts (see Fig.12 for schematic diagram). Therefore, inhibition of LCK activity by Csk could result in decreased STAT5 phosphorylation in CD4 expressing T-cells, at high dose IL-7. To test whether IL-7 directly controls the expression of Csk, we measured Csk synthesis by quantitative PCR (preliminary data shown in Fig. 11A). We observed that increases in Csk gene expression could be detected as soon as two hours after IL-7 treatment and also in D1 T-cells maintained in IL-7 for 18 hours (Fig 11A). Next we determined whether we could detect differences in the phosphorylation of LCK at tyrosine 505 in primary T-cells cultured with high or low doses of IL-7. Note that after 14 days of culture, the cells maintained with 150 ng/ml IL-7 had more CD8 T-cells relative to CD4 T-cells (53% CD8 T-cells to 17% CD4 T-cells) (Fig. 11B). In contrast, cell cultures maintained in 10 ng/ml IL-7 contained approximately

equal ratios of CD4 to CD8 T-cells (Fig. 11B). Figure 11C (preliminary data) shows that there was slightly more phospho- LCK (tyrosine 505) and total LCK detected in lysates prepared from cells maintained at 10 ng/ ml IL-7. This could be due to the increased presence of CD4 T-cells in those cultures, relative to cultures of high dose IL-7 (Fig. 11B). Current studies are underway to test this idea by immunoblotting for phospho-LCK in lysates prepared from purified cultures of either CD4 or CD8 T-cells.

In summary, our results suggest that the dose responsiveness of CD4 T-cells to IL-7 depends on the ability of the co-receptor to bind and sequester LCK. We propose that CD4 T-cells are engineered to attenuate a strong IL-7 signal and that this is achieved through the activity of LCK upon the phosphorylation of STAT5. One possibility is that the CD4 co-receptor sequesters LCK in manner that optimizes IL-7 signal transduction at low doses, while conditions at high doses inhibit the activation of the STAT5 pathway. Support for the idea that a strong IL-7 signal is detrimental for CD4 T-cells comes from data acquired from STAT5b-constitutively active (CA) transgenic mice [30]. We found that few CD4 T-cells localized to the lymphoid organs of STAT5b-CA mice[18] and that *in vitro* culture of the remaining CD4 T-cells with IL-7 did not induce their growth (data not shown). In contrast to CD4 T-cells, CD8 T-cells may contain more "free" or CD3-bound LCK, and are thus able to respond proportionally to the strength of an IL-7 signal. Therefore, the ability of a T-cell to respond to IL-7 is not only determined by expression of the IL-7R but may also depend on the localization of the Src kinase, LCK, and whether it is bound to a co-receptor.

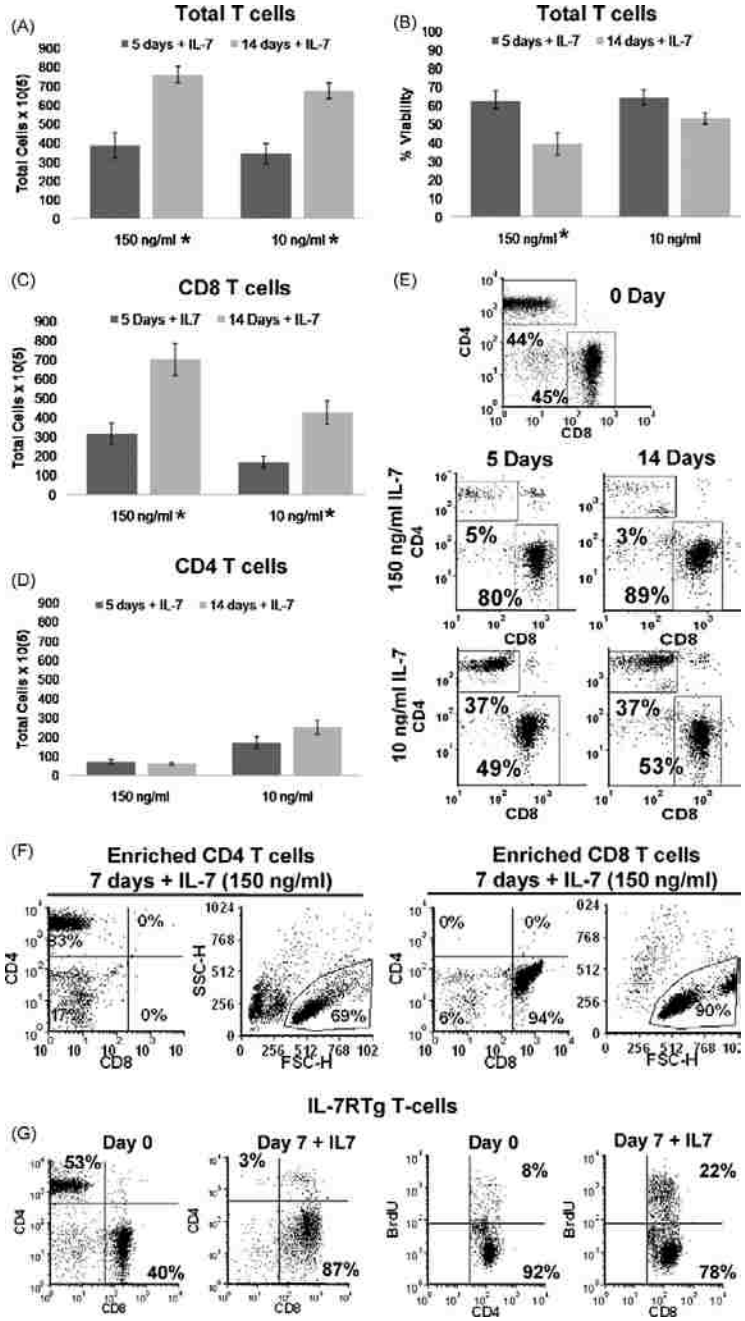

Figure 6. High dose IL-7 supports the growth of CD8 T-cells but not CD4 T-cells.
(A–D) Splenic T-cells from C57Bl/6 mice were cultured with 150 or 10 ng/ml of IL-7 for 5 and 14 days. Total number of T-cells recovered (A), total T-cell viability (B), and the number of cells in the individual subsets of CD8 T-cells (C) and CD4 T-cells (D) were determined by flow cytometry. (E) Ratio of CD4:CD8 T-cells is shown for the cells in (A–D). (F) CD4 T-cells and CD8 T-cells were enriched from spleens of C57Bl/6 mice. CD4 or CD8 T-cells were cultured with 150 ng/ml of IL-7 for 7 days, and the ratio of CD4:CD8 T-cells and viability of each subset were determined by flow cytometry. (G) Splenic T-cells from IL-7R transgenic mice were cultured with 150 ng/ml of IL-7 for 7 days. Ratio of CD4:CD8 T-cells is shown. Proliferation was determined by measuring BrdU incorporation. Representative experiments of three or more performed are shown. *$p < 0.05$.

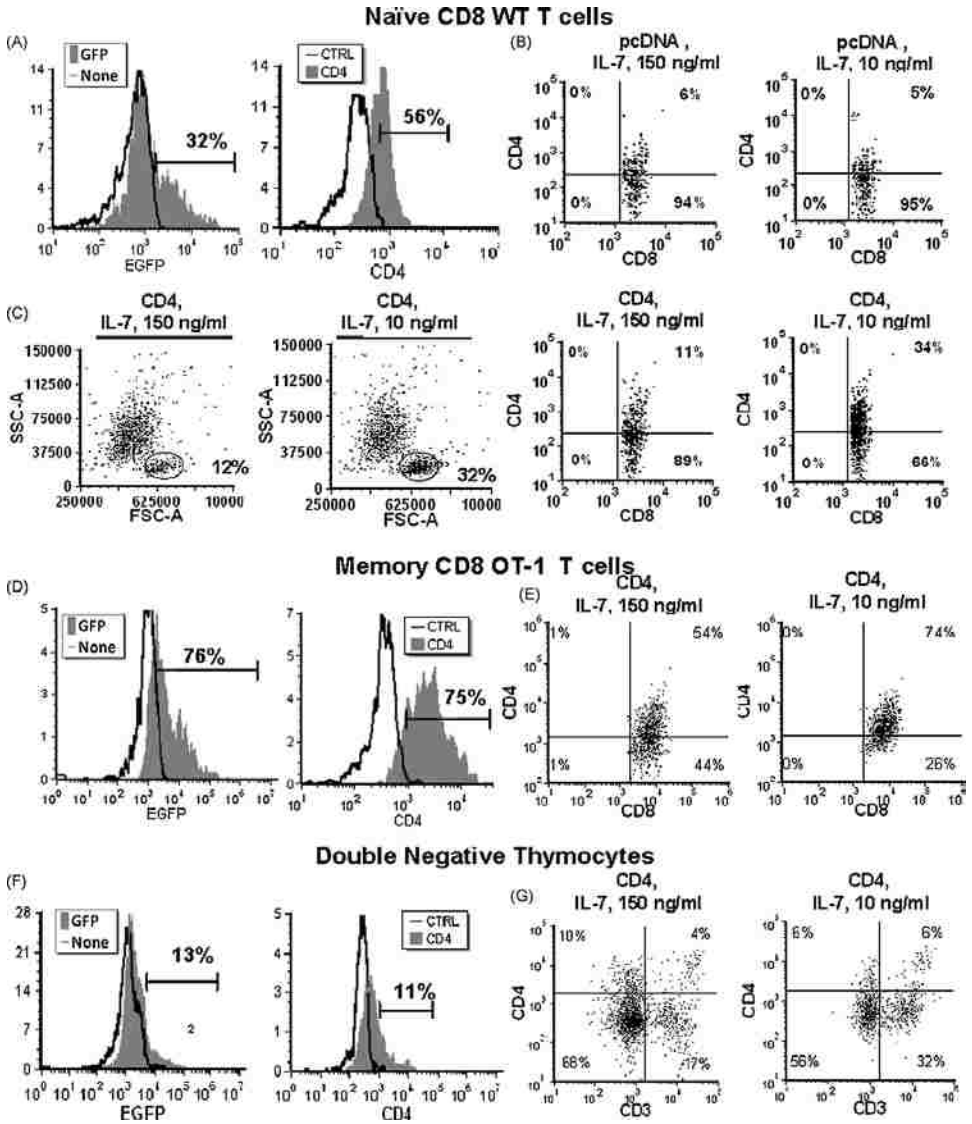

Figure 7. Low dose IL-7 maintains CD8 T-cells that also express the CD4 co-receptor.
(A–C) Naïve splenic CD8 T-cells isolated from C57Bl/6 mice and nucleofected with empty vector (pcDNA) or the cDNA for murine CD4. Nucleofected CD8 T-cells were cultured for 24 hours with either 10 or 150 ng/ml of IL-7 and assayed for cells retaining the CD4 co-receptor using specific antibodies by flow cytometry. The expression of CD4 on CD8 T-cells (shown in the percentages in bold) was determined by staining with specific antibodies for CD4 and CD8 T-cells. (A) Naïve splenic CD8 T-cells were nucleofected, as described above, with the cDNA for EGFP as an indicator of nucleofection efficiency. (B). Naïve splenic CD8 T-cells were nucleofected, as described above, with the cDNA for pcDNA or CD4 as indicated in the figure. (C) Viability (shown by percentage of encircled cells) was determined by examining morphological changes that accompany death, such as cell shrinkage and fragmentation, using forward (FSC) and side scatter (SSC) gating. (D and E) Memory CD44^{hi} CD8 T-cells were isolated from OT-1 mice previously primed with ovalbumin. Cells were nucleofected with EGFP cDNA (nucleofection control) or CD4 cDNA and the expression of CD4 on CD8 T-cells cultured with IL-7 determined as described above. (F and G) DN thymocytes were isolated from WT mice by negative selection. Cells were nucleofected with EGFP cDNA (nucleofection control) or CD4 cDNA and the expression of CD4 on CD8 T-cells cultured with IL-7 determined.

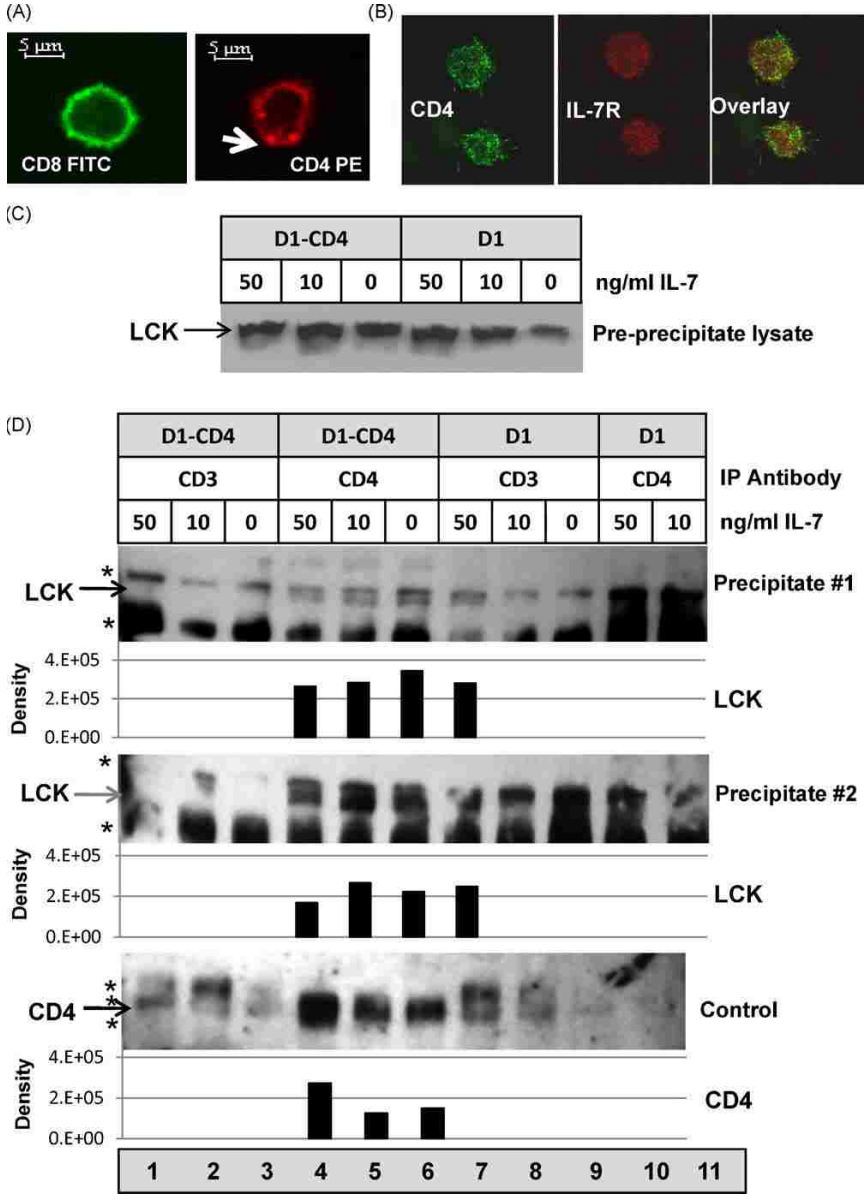

Figure 8. LCK associates with the CD4 co-receptor.
(A) Surface expression of CD8 and CD4 on unfixed lymph node T-cells was visualized by confocal microscopy. Arrows indicate aggregation of the CD4 co-receptor. Representative experiments of two or more performed are shown. (B) Surface expression of IL-7R and CD4 on D1-CD4 T-cells was visualized by confocal microscopy. Composite images were generated from Z-stacks. (C–D) Immunoblots display the results of co-immunoprecipitation of LCK with CD4. Whole cell lysates were prepared from D1 and D1-CD4 T-cells cultured with 50, 10 and 0 ng/ml IL-7. LCK levels in pre-precipitation D1 and D1-CD4 T-cell lysates were determined (C). Pre-cleared D1 and D1-CD4 T-cell lysates were incubated with anti-CD3 or anti-CD4 antibodies to immunoprecipitate CD3- or CD4-associated proteins and then precipitates were immunoblotted for LCK (D). Two representative experiments are shown. As control, the immunoprecipitated amounts of CD4 are shown. Band detection and density were determined using the Carestream Molecular Imaging SE software and results displayed in the accompanying bar graphs. Arrows indicate protein of interest and (*) denotes non-specific protein bands. Confocal images shown in (A) and (B) were acquired with the assistance of Ms. Rebecca Boohaker.

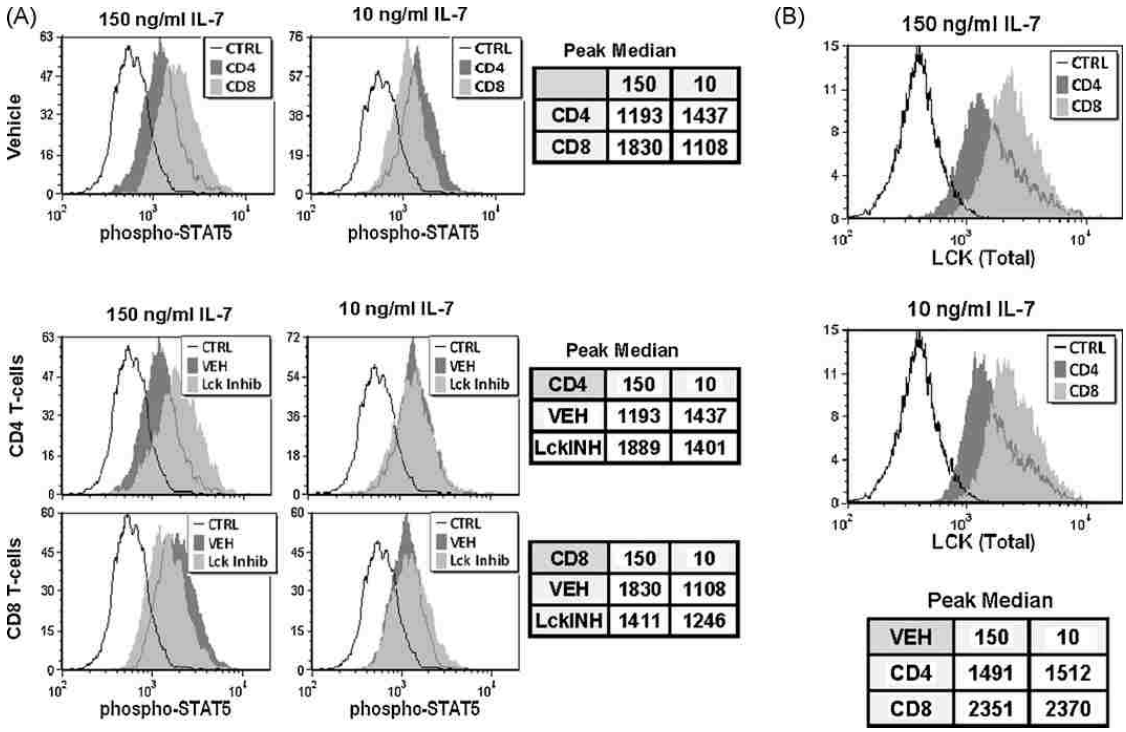

Peak Median	150	10
CD4	1193	1437
CD8	1830	1108

CD4	150	10
VEH	1193	1437
LckINH	1889	1401

CD8	150	10
VEH	1830	1108
LckINH	1411	1246

VEH	150	10
CD4	1491	1512
CD8	2351	2370

Figure 9. Phospho-STAT5 levels in primary T-cells are dependent on IL-7 dose and LCK activity.
(A) Lymph node T-cells were isolated from C57Bl/6 mice and cultured for 5 days with 150 or 10 ng/ml IL-7. T-cells were treated with either vehicle (VEH) control DMSO, or 1μM LCK inhibitor II (LCK Inhib) for 18 hours prior to analysis. Surface expression of CD4 or CD8 was determined using a PE-conjugated anti-CD4 antibody or a PerCP-conjugated anti-CD8 antibody and cells were gated for display. Intracellular phospho-STAT5 was measured using a PE-conjugated phospho-STAT5 (pTyr694) antibody. Levels of surface CD4, CD8 or intracellular phospho-STAT5 were determined by flow cytometry. Isotype matched antibodies were used as controls for non-specific staining. Shown is the matched isotype control (CTRL) antibody for PE-conjugated phospho-STAT5. (B) Using the samples from (A), total intracellular LCK was measured using a PE-conjugated antibody that detects both unphosphorylated and phosphorylated forms of LCK. A matched isotype control (CTRL) for PE-conjugated LCK is shown. Surface expression of CD4 or CD8 was determined as described in (A) and cells gated for display as described above. Medians for each histogram peak were determined using FSC Express software and displayed in the table alongside each histogram set. Representative experiments of three or more performed are shown.

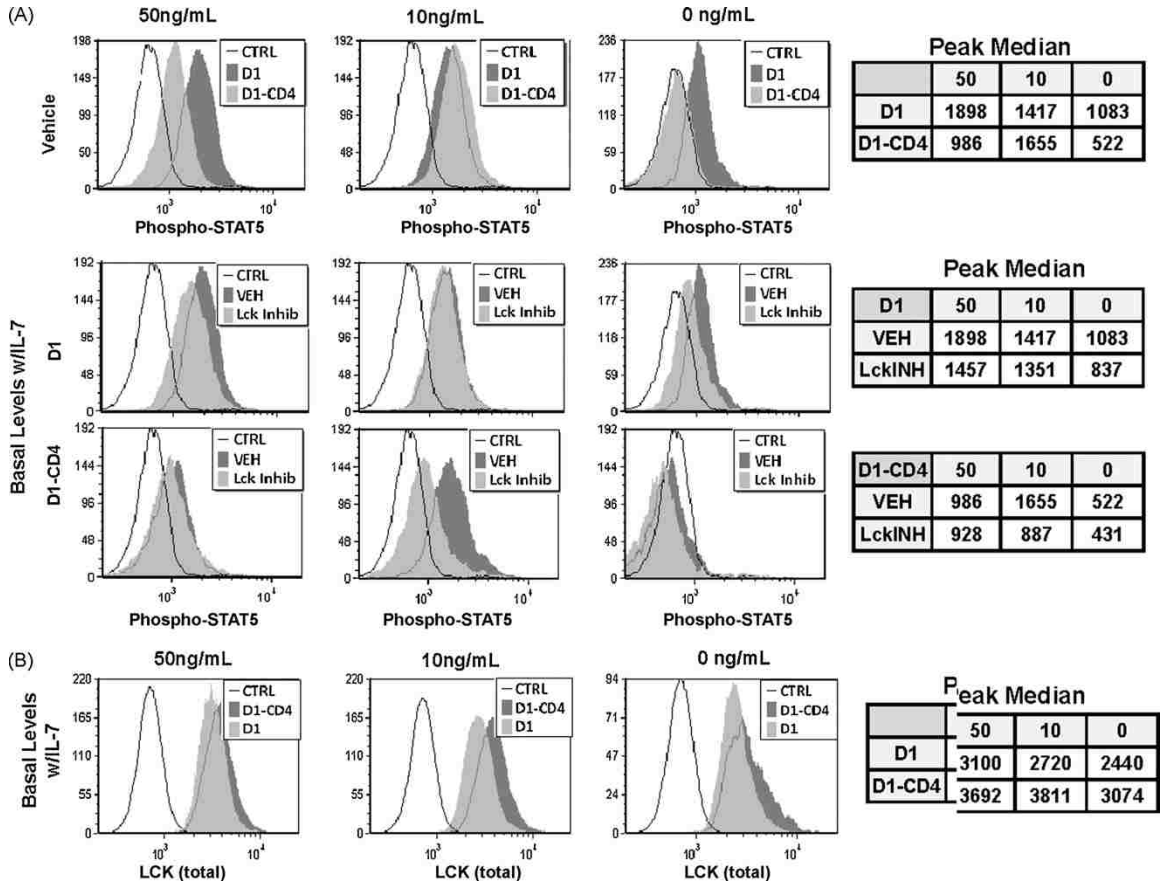

Figure 10. CD4 associated LCK modulates IL-7 dose responsiveness in D1 T-cell line.
(A) D1 and D1-CD4 T-cells were cultured in 50, 10 or 0 ng/ml IL-7 for 24 hours and treated with either vehicle (VEH) control DMSO or 1μM LCK inhibitor II (LCK Inhib) for 18 hours prior to analysis. Surface expression of CD4 in D1-CD4 T-cells was confirmed using a specific PE-conjugated anti-CD4 antibody. Intracellular phospho-STAT5 was measured using a PE-conjugated antibody specific for phospho-STAT5 (pTyr694). Levels of intracellular phospho-STAT5 were determined by flow cytometry. Shown is the matched isotype control (CTRL) antibody for PE-conjugated phospho-STAT5. (B) D1 and D1-CD4 T-cells were cultured in 50, 10 or 0 ng/ml IL-7 for 24 hours as in (A) and total LCK measured using a PE-conjugated antibody that detects both unphosphorylated and phosphorylated forms of LCK. A matched isotype control (CTRL) for PE-conjugated LCK is shown. Medians for each histogram peak were determined using FSC Express software and displayed in the table alongside each histogram set. Representative experiments of three or more performed are shown.

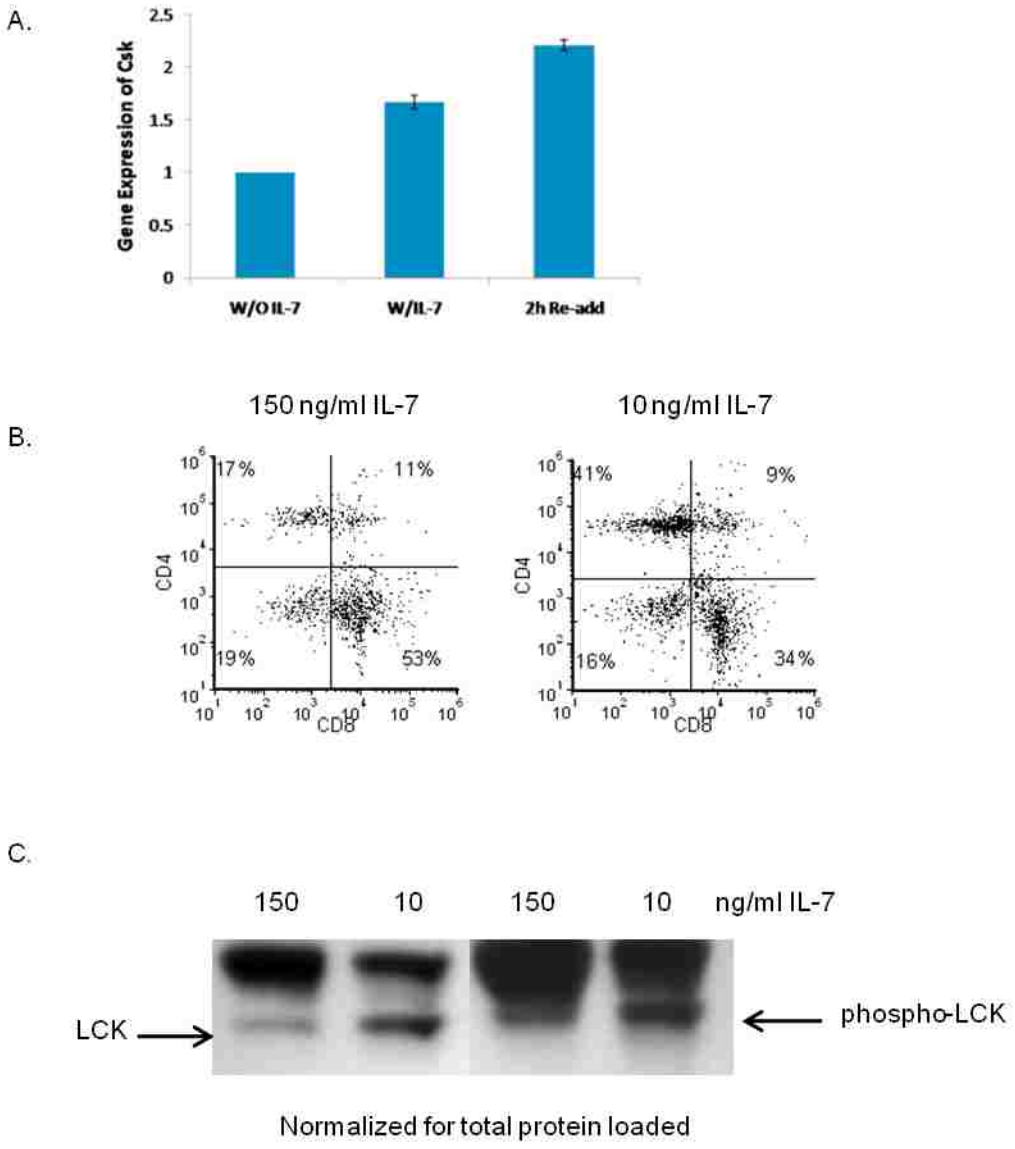

Figure 11. IL-7 regulates the negative phosphorylation of LCK by Csk.
(A) D1 T-cells were cultured with or without IL-7 for 18 hours or IL-7 was readded for 2 hours after IL-7 withdrawal. Csk mRNA was measured with specific primers by qPCR. (B) Splenic T-cells were isolated from C57Bl/6 mice and cultured with 150 or 10 ng/ml of IL-7 for 14 days. Ratio of CD4:CD8 T-cells was determined by staining with fluorochrome-conjugated antibodies specific for CD4 or CD8 T-cells and analyzed by flow cytometry. (C) Immunoblots display levels of total LCK or phosphorylated LCK at tyrosine 505, the Csk target site. Whole cell lysates were prepared from the splenic T-cell cultures maintained with 150 or 10 ng/ml IL-7 as shown in (B). qPCR data in (A) was acquired with the assistance of Mr. Mounir Chehtane. *Unpublished prelimimary data.*

Discussion

We and others have shown that *in vitro* and *in vivo* conditions in which IL-7 concentrations are high favor the growth and proliferation of CD8 but not always CD4 T-cells. In this study, we found that T-cells, which express the CD4 co-receptor, preferentially expanded at lower doses of IL-7 relative to CD8 T-cells because the activity of LCK, which contributed to the phosphorylation of STAT5, was in part controlled through association with the CD4 co-receptor. Furthermore, we established a direct correlation between the amount of phospho-STAT5 and the optimal dose of IL-7 for growth and showed that the LCK-induced phosphorylation of STAT5 significantly contributed to the overall levels of the active transcription factor.

Evidence found in the literature indicates that JAK signaling is likely an evolutionarily recent addition to a primordial Src/ STAT pathway[47] and suggests that interactions between Src kinases and JAKs are at times necessary for the full activation of STATs[59]. Older studies showed that the Src kinases, FYN, LYN and LCK can directly associate with the IL-7 receptor complex[60, 61] and more recently that JAK3 can be phosphorylated upon TCR stimulation independently of γc receptor engagement[58], indicating that direct associations between IL-7 signaling and Src kinases exist. Moreover, expression of a constitutively active LCK kinase induced the phosphorylation and activation of STAT5b and promoted proliferation[49]. These studies and others support our findings that LCK contributes to the phosphorylation of STAT5 in T-cells. We found, in non-CD4 T-cells deprived of IL-7 or CD4 T-cells cultured with low dose IL-7 that increases in phospho-STAT5 were due to the activity of LCK. This is in line with what others have reported in that a proliferative response to an IL-7 signal does not require LCK[62].

The conclusion that can be drawn from our findings is that repression of LCK activity is inherent in the IL-7 signal. Only when IL-7 is limiting does LCK contribute to the phosphorylation of STAT5 in a yet to be described manner.

The activity of JAKs and Src kinases can be inhibited by inactivating phosphorylation. For the Src kinases, this inactivation is mediated through the negative regulatory kinases Csk/Crk. LCK has a C-terminal tyrosine (Y505) that, when phosphorylated by Csk, inhibits its kinase activity, causing the protein to adopt a nonfunctional closed conformation[63]. The transmembrane adaptor protein called Cbp (Csk-binding protein) serves the function of localizing Csk to the plasma membrane where LCK is found[64]. Moreover, Cbp is known to localize to membrane lipid rafts[65].

Among other signaling molecules that also localize to lipid rafts is the CD4 co-receptor[66]. The interaction of LCK with the co-receptors is mediated through an N-terminal dicysteine motif that forms a unique zinc "clasp" like structure[67]. Additionally, the longer CD4 tail provides a larger interface for interacting with LCK. In part this explains why 75–95% of the intracellular LCK is associated with the CD4 co-receptor [68]. Using either HIV infected CD4 T-cells or an anti-CD4 antibody, researchers found that the distribution of LCK to lipid rafts was inhibited upon pre-engagement of CD4[69]. Such findings support a potential mechanism in which the CD4 co-receptor can "sequester" and negatively regulate the activity of LCK. This scenario was proven in an elegant study in which both the CD4 and CD8 co-receptors were deleted and such cells were found to respond to non-MHC ligands[70]. Hence co-receptors not only function to initiate TCR signaling but also to prevent inappropriate TCR-independent T-cell activation by binding and potentially inhibiting the kinase. Taken in total, such studies support our

observations that T-cells, in which CD4 is over expressed, had detectable CD4-bound LCK, and that the CD4 co-receptor itself localized to discreet patches on the cell surface- unlike the CD8 co-receptor that was more evenly dispersed. It is therefore likely that the negative regulation of LCK activity is mediated by signaling proteins such as the CD4 co-receptor or Csk/Cbp that are brought together in lipid rafts.

In earlier published work[52], we performed a cDNA microarray using D1 T-cells and found that, after 2 hours of IL-7 re-addition to deprived cells, a number of factors involved in regulating signal transduction activity were increased. Of significance to our current studies, results from the microarray revealed that IL-7 signaling induced synthesis of the negative regulator of LCK, Csk[52], suggesting that a strong IL-7 signal could be expected to provide a negative regulatory mechanism for the inactivation of LCK. Given this information, we propose that, in CD4-expressing T-cells, a high dose of IL-7 would increase the levels of Csk found at the membrane lipid rafts associated with Cbp. At the same time, the CD4 co-receptor, also located in the lipid rafts, would recruit LCK to the membrane complex for phosphorylation by Csk. As a result, the level of LCK phosphorylated at Y505 would increase and the total amount of phospho-STAT5 available to transduce an IL-7 growth signal would decrease- thereby attenuating the response of the CD4 T-cell to IL-7. This idea is described in model shown in Fig. 12. Only when the concentration of IL-7 drops, and the level of Csk decreases, would active LCK be available to contribute to the phosphorylation of STAT5. In T-cells lacking co-receptors (like D1 T-cell line) little or no LCK could be brought to the membranes for phosphorylation by Csk, and thus more active LCK would be available to generate phospho-STAT5. An in between scenario likely occurs in CD8 T-cells, with the IL-7 dose-dependent increase in LCK inhibitory

phosphorylation by Csk being balanced by reduced recruitment of the kinase to the membrane lipid rafts.

As a result of our studies, we have identified a novel role for LCK bound to the CD4 co-receptor in the dose response of T-cells to IL-7. Our findings on the relationship between LCK and STAT5 not only explain the differential response of CD4 and CD8 T-cells to IL-7 but could also be extended to explain the outcome of cytokine signaling in terms of cell cycling. We previously showed that the cell cycle inhibitor, $p27^{kip}$, increased upon IL-7 loss[71] and that the cell cycle activator, Cdc25A, decreased due to p38 MAP kinase-targeted degradation[17]. It remains possible that in CD4 T-cells, exposed to high dose IL-7, cell cycle arrest could occur upon CD4-coupled LCK inactivation due to a combination of increased $p27^{kip}$ as well as the decreased stability of Cdc25A. As the clinical use of supraphysiological amounts of IL-7 (>10μg/kg/dose) in the treatment of immunodeficiencies and cancer therapy increases[23], the need for a better understanding of the effects that can be expected when a T-cell encounters higher than normal doses of IL-7 becomes absolutely necessary. Studies such as ours serve to provide select answers but also provoke questions that illustrate the complex nature of this unique and critically important cytokine.

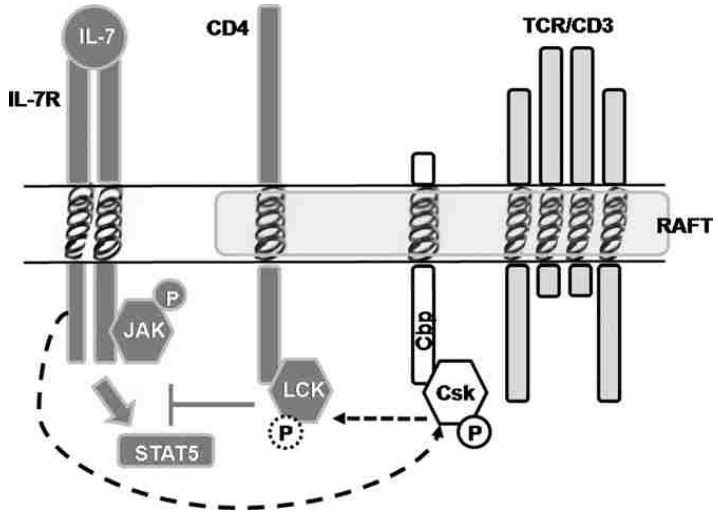

Figure 12. Model for proposed high dose IL-7 signaling events in CD4 T-cells.
Model for proposed high dose IL-7 signaling events in CD4 T-cells. In CD4 T-cells, the co-receptor sequesters cytosolic LCK and brings it into the lipid raft membrane complex. Within the lipid rafts, Csk, anchored to the membrane by Cbp, is activated and negatively regulates the activity of LCK through inhibitory phosphorylation of tyrosine 505. The inhibition of LCK then decreases the total amount of active phospho-STAT5. IL-7 increases the amount of active Csk that inhibits LCK in a dose-dependent manner. Solid gray lines indicate pathways supported by data and broken lines indicate proposed mechanisms.

CHAPTER 4: CYTOKINE DRIVEN CELL CYCLING IS MEDIATED THROUGH CDC25A

Introduction

Cytokines are known to prevent cell death through the induction of the anti-apoptotic proteins BCL-2 or BCL-XL and the inhibition of pro-apoptotic proteins like BAX, BAD, or BIM[52, 72-75]. Overexpression of *bcl-2* protects cells from apoptosis after IL-7 or IL-3 withdrawal, however cells also undergo growth arrest, indicating that these cytokines, in addition to promoting survival, induce replication[14, 72, 74]. IL-7 has been shown to be required for *homeostatic* T-cell proliferation in mice[16, 34]. It therefore appears that the replication of lymphocytes in the presence of IL-7 (and similarly IL-3) may not be merely a default pathway reflecting the survival effect of the cytokine, but rather may be a distinct replication signal from the cytokine receptor.

Cell cycle progression is normally mediated by enzymatic complexes containing cyclin-dependent kinases (Cdks), which phosphorylate substrates such as the Retinoblastoma (Rb) protein, releasing E2F and inducing transcription of genes needed for cell division[76]. Cdks are partially activated by binding to specific cyclins and then are fully activated by phosphorylation of a threonine (T160) located in a conserved domain, the T-loop. Progression through G1 and S phase of the cell cycle requires G1-Cdk/ cyclins, like Cdk4, Cdk6, and cyclin D, as well as the G1-S Cdk/ cyclins, like Cdk2 and cyclin E, and later cyclin A. Though transcriptionally regulated, Cdk activity is primarily controlled through phosphorylation of two conserved residues found in the ATP binding loop, T14 and Y15, mediated by Wee1 kinase and Myt1[77]. In this manner, a pool of phosphorylated Cdks can accumulate during the G1 and G2 phases.

Activation of Cdks, through dephosphorylation of T14 and Y15, is mediated by members of the phosphatase family, Cdc25A, B, and C[78]. Cdc25A is necessary for promoting the G1-S phase transition by removing an inhibitory phosphate on Cdk2, promoting Cdk2-cyclin E/A activity[79,80], but may also have a role during mitotic entry, activating Cdk1[81]. Throughout the cell cycle, Cdc25A is tightly regulated at the protein level through phosphorylation which induces ubiquitination leading to degradation[82], a process that ultimately contributes to cell cycle arrest through the absence of active Cdks. In addition to inhibitory phosphorylations, Cdks are also inhibited by negative regulation mediated through the p16 (INK4) family (p16, p15, p18, and p19) and the p21 (Cip/Kip) family (p21, p27, and p57), which bind to and inhibit the enzymatic activity of the Cdks[83].

Though inhibition of lymphocyte cell death has been accorded the major function of IL-7, an activity in cell cycle progression also is observed. Naive T-cells proliferated *in vitro* when stimulated with IL-4, IL-7 or IL-15, but only IL-7 was essential for the homeostatic proliferation of naive T-cells *in vivo*[25, 34]. In our previous studies, we found that withdrawal of IL-7 induced growth arrest in dependent cells[52]. The present study examines the mechanisms by which IL-7 and IL-3 induce replication in lymphocyte lines and concludes that a key pathway involves the stress kinase p38 MAPK inactivating the phosphatase Cdc25A.

Materials and methods

Cell lines, cells, and treatments

The IL-7-dependent cell line, D1, was established from $CD4^-CD8^-$ mouse thymocytes isolated from a $p53^{-/-}$ mouse as previously described[52]. The IL-3 dependent cells are murine pro-B cell line, FL5.12A[74]. Pharmacological inhibitors of p38 MAPK, PD169316, and SB202190 (Calbiochem), MEK1 inhibitor, PD98059 (Calbiochem), JNK Inhibitor II (Calbiochem), Cdk2 Inhibitor II (Compound 3; Calbiochem), and Cdc25 inhibitor (NSC 95397; Sigma-Aldrich) were made as 20 mM stocks in DMSO. Inhibition of Chk1 was achieved by introducing chemically synthesized small interfering RNA (Santa Cruz Biotechnology, Inc.) using a lipid reagent, *Trans-IT* TKO (Mirus) following the manufacturer's protocol. Cells were treated as described in figure legends. Lymph node cells from 12-wk-old C57Bl/6 mice were isolated by mechanical teasing and placed in culture, $5\text{-}10^6$ cells/ml, in the presence of 100 ng/ml IL-7 (Peprotech) and 0.25 ng/ml Con A (Sigma-Aldrich) from 48 hours before IL-7 withdrawal.

Plasmids, site-directed mutagenesis, and transfections

For dominant negative inhibition of p38 MAPK, pCMV-Flag-p38 (agf; a gift from R. Davis, University of Massachusetts Medical Center, Worcester, MA) was used to transfect cells. Overexpression of cyclin D1 was achieved with pCMV-HA-cyclin D1 (a gift from P. Kaldis, National Cancer Institute at Frederick). The pCMV-HA-Cdc25 WT plasmid (a gift from J. Bartek, Danish Cancer Society, Copenhagen, Denmark) was used to generate mutants pCMV-HA-Cdc25 S75A and/or S123A, as previously described[84]. For expression in the D1 cells, the1.6-kB EcoR1 fragment from either pCMV-HA-Cdc25 WT or pCMV-HA-Cdc25 S75, 123A

mutant was subcloned into pcDNA 6/V5-HisB (Invitrogen) for selection with Blastocidin. Cells were transfected by electroporation (BTX model 830) using standard methodologies. Before electroporation, cells were incubated in a hypoosmolar electroporation buffer (Eppendorf) to slightly swell the cells and improve transfection efficiency. Primary lymphocytes were isolated from lymph nodes as described, treated with IL-7 and Con A for 48 hours, and transfected with *TransIT*-LTI Transfection reagent (Mirus) following the manufacturer's guidelines. Transfected cells (4–6%) were selected by GFP coexpression and assayed for cell cycling and DNA synthesis after 48 hours with or without IL-7.

Cell cycle analysis and BrdU incorporation

For cell cycle analysis, DNA content was measured by propidium iodide (PI) or 7AAD staining. Cells, withdrawn from cytokine and/ or treated with pharmacological inhibitors (as described in figure legends), were placed in detergent buffer[52] with 50 µg/ml Rnase (Invitrogen) at a concentration of $1–2x10^6$ cells/ml with an equal volume of PI (50µg/ml) or 7AAD. Samples were mixed and incubated at RT for 1 hour before analysis, then assayed by flow cytometry using a FACSCalibur flow cytometer (Becton Dickinson) and CellQuest software. Listmode data was acquired and analyzed using ModFit LT software (Verity), excluding apoptotic cells and cell aggregates. DNA synthesis was assessed by BrdU incorporation, using FITC-anti-BrdU or PE-anti-BrdU antibody for detection, and 7AAD staining for DNA content with a commercially available kit following the manufacturer's instructions (BD Biosciences). BrdU incorporation in primary T-cells was measured using an anti-BrdU-PE–labeled antibody, gating on the GFP-positive cells.

Immunoblotting and RPA

For detection of Cdc25A, cell lysates and the making of specific antibodies have been previously described[84]. For analysis of phospho-Rb and phospho-Cdk2, nuclear cell lysates were made using a modified Dignam protocol containing phosphatase inhibitors and protease inhibitors [85,86, 87]. Cells lysates were resolved by SDS-PAGE and immunoblotted. For detection of Cdc25A, mAbs were used (Ab-3, NeoMarkers). For detection of the phosphorylated form of Rb, cyclin D3, and Cdk4, specific antibodies were used: a rabbit polyclonal for detecting phospho-Rb (Serine 780; Cell Signaling Technology) and mouse monoclonals for detecting cyclin D3 and Cdk4 (Cell Signaling Technology). Cdk2 was detected using a rabbit pAb (M2; Santa Cruz Biotechnology, Inc.). To detect the phosphorylated forms of Cdk2 and Cdk1, blots were probed for phospho-Cdks (Tyr15) with a rabbit pAb to phospho-Cdk1 (Tyr15; Cell Signaling Technology), which can also detect Cdk2 when catalytically inactivated by phosphorylation at Tyr15, and for phospho-Cdk (Thr160) with a rabbit pAb specific for Cdk2 and Cdk1 when activated and phosphorylated at this site (Cell Signaling Technology). Appropriate secondary rabbit or mouse antibodies cross-linked to HRP (Cell Signaling) were used for detection. ECL (Pierce Chemical Co.) was used for visualization following the manufacturer's protocol. For detection of mRNA levels for Cdks and cyclins, RPA was performed with BD Riboquant multi-probe kits, mCC-1, mCYC-1, and mCYC-2 (BD Biosciences) following the manufacturer's guidelines. For measurement of p38 activity a commercially available p38 nonradioactive kinase assay kit (Cell Signaling) was used following the manufacturer's protocol. Chk1protein levels were determined by immunoblotting nuclear and cytosolic lysates with a specific antibody (sc8408; Santa Cruz Biotechnology, Inc.) as

described above for Rb, and detection of γ-tubulin with a specific antibody (Sigma-Aldrich) was used as a loading control for nuclear lysates.

Results

The cytokines IL-3 and IL-7 have been previously studied for their anti-apoptotic effects in lymphocytes. We showed that withdrawal of IL-3 or IL-7 induced the translocation of the death protein BAX[73] and that overexpression of the anti-apoptotic proteins BCL-2 or BCL-XL[14,74] prevented cytokine withdrawal- induced death but did not restore proliferation. Recently, we found that IL-7 also promoted the expression of cell cycle regulators such as p55Cdc and Cdk4 and proliferative factors like c-myc[52], furthering supporting a proliferative function, in addition to an anti-apoptotic role, for these cytokines. To identify and characterize components of cell cycle regulation targeted by cytokines like IL-3 or IL-7, we evaluated the effect of these cytokines on the proliferation of two different cytokine-dependent cell lines, as shown in Fig. 13 (A and B) and primary lymphocytes shown in Fig. 13C. Withdrawal of IL-3 from the pro-B cell line, FL5.12A, induced G1 arrest beginning at 8 hours, progressing through 12 hours, and was complete by 17–24 hours, with cells accumulating in G1 as they exited from S-phase (Fig.13A and data not shown). These results indicate that IL-3 is required for cell division. Withdrawal of IL-7 from the thymocyte line, D1, similarly produced a G1 arrest after 24 hours of cytokine withdrawal (Fig. 13B) that initiated after 12 hours of IL-7 deprivation (not depicted). In both the IL-3- and IL-7- dependent cell lines, growth arrest began many hours before the apoptotic processes of mitochondrial breakdown, effector caspase activation and DNA damage, which take place 24–36 hours after cytokine withdrawal[74]. These findings indicate the induction of G1

arrest is an immediate response to cytokine withdrawal that initiates as early as 8 hours after loss of cytokine signal and is complete 17–24 hours later.

To determine if G1 arrest in response to cytokine withdrawal also occurs in primary lymphocytes deprived of IL-7, we isolated lymph node lymphocytes (approximately 70% T-cells) and assayed their proliferative capacity. Most primary T-cells are in G0 until antigen activated[16] and we found that addition of a low concentration of Con A, nonmitogenic on its own, conferred a proliferative response to IL-7 *in vitro*. Lymph node cells were cultured for 48 hours with IL-7 (100 ng/ml) and Con A (0.25µg/ml), which induced 23.4% of the cells to enter S-phase. After 24 hours of IL-7 withdrawal, the number of cells in S-phase was reduced to 12.4% (Fig. 13C) and this declined further to 4% by 48 hours (not depicted). Hence, withdrawal of IL-7 from either cytokine-dependent cell lines or primary lymphocytes induces growth arrest before apoptosis.

Previously, we reported that shortly after withdrawal of IL-3 or IL-7, the MAPK stress pathway was activated (data not shown) and played an important role in inducing the later events of apoptosis[88, 89]. Therefore, we examined whether stress kinases could also be involved in cell cycle regulation, specifically the induction of growth arrest observed in the absence of a cytokine signal. PD169316, a potent inhibitor of the stress kinase p38 MAPK, dramatically increased the number of FL5.12A cells in S-phase after withdrawal of IL-3, and the weaker p38 MAPK inhibitor SB202190 also showed significant effects (Fig. 13A and Fig. 14A). In contrast, inhibition of other MAPKs, ERK or JNK, failed to restore G1-S phase progression (Fig. 14A) after IL-3 withdrawal. An effect of pharmacological inhibition of p38 MAPK was accelerated cell death in the absence of cytokines, as can be noted by the increased number of sub-G1 cells

(Fig. 13, A and B). This was not observed upon inhibition of the ERK or JNK pathway. Thus, potent pharmacological inhibitors of p38 MAPK, in addition to relieving the G1 arrest, also induce some cell death. Perhaps this effect results from mitotic catastrophe or from other drug effects.

To specifically inhibit p38 MAPK without using pharmacological inhibitors, we expressed a dominant negative p38 MAPK, which specifically inhibits p38 MAPK activity, in FL5.12A cells and again observed restoration of cell cycling (approximately 22% in S-phase; Fig. 14A) and DNA synthesis, shown by BrdU incorporation (approximately 18% cells synthesizing DNA; Fig. 14B), in the absence of IL-3. In the IL-7 dependent thymocyte line, D1, G1 arrest after IL-7 withdrawal was also dramatically released by inhibiting p38 MAPK with PD169316, resulting in increased progression into S-phase (Fig. 13B). Primary lymphocytes showed a similar pattern upon inhibition of p38 MAPK, relieving the arrest that followed IL-7 withdrawal (Fig. 13C). These results indicate that activation of p38 MAPK after cytokine withdrawal induces rapid G1-S phase arrest (well before the onset of apoptosis) and that inhibition of p38 MAPK substantially restores S-phase progression, confirmed by measurements of DNA synthesis.

We also assayed for the activity of other checkpoint kinases, specifically CHK1, to determine if these were induced by cytokine withdrawal. Unlike the increased activation of p38 MAPK detected upon cytokine deprivation, we found that protein levels of CHK1 were negligible by 17 hours of IL-3 or IL-7 withdrawal, though detectable in the presence of cytokines (data not shown). Therefore, inhibition of CHK1 by RNA interference (Fig. 14A) did not restore

S-phase progression in the absence of IL-3, suggesting that CHK1 initiated checkpoint regulation was not the mechanism by which cytokine withdrawal induced growth arrest.

Phosphorylation of Rb, which releases E2F and promotes entry into S-phase, was interrupted by IL-3 withdrawal and restored by inhibition of p38 MAPK (Fig. 14C), suggesting that in these cells p38 MAPK acted upstream of the events leading to Rb phosphorylation. One possibility would be that p38 MAPK negatively regulates the synthesis of the Cdk 4/6-cyclin D complexes [90], thereby retaining hypophosphorylated Rb in the absence of these complexes. If so, then we would expect levels of mRNA transcripts for G1-S phase Cdks and cyclins to increase upon p38 MAPK inhibition. However, RNase protection assays (RPAs), to measure mRNA transcripts for Cdks and cyclins, for example Cdk 4, during initiation of G1 arrest showed decline of transcription after 12 hours of IL-3 (Fig. 15A) and IL-7 (not depicted) withdrawal, and minor, if any, increase in transcription as a result of inhibiting p38 MAPK with PD169316. Re-addition of IL-3 or IL-7 after cytokine withdrawal substantially increased the transcription of Cdks and cyclins as would be expected upon restoration of cytokine signaling pathways (unpublished data). In the absence of IL-3, inhibition of p38 MAPK did result in a slight increase in expression of cyclins D2, D3 and E (Fig. 15A), which will be further discussed. RPAs were also performed to measure transcription of Cdks 1, 5, 7, and 8 and cyclins A2, B1, C, B2, F, G1, G2, and H, and no effects of p38 MAPK inhibition were observed (not depicted).

To determine if decreased transcription was reflected by loss of protein, we measured the protein levels for one of the Cdks, Cdk4, and one of the cyclins, cyclin D3. We found that these cell cycle mediators could still be detected by immunoblotting cell lysates even 17 hours after IL-3 withdrawal when cells are fully arrested (Fig. 15, B and C), demonstrating that, though mRNA levels decreased, the proteins themselves were not limiting in the early stages of cytokine withdrawal. Thus, the mechanism through which p38 MAPK regulates cell cycling in cytokine-dependent lymphocytes is not solely based on controlling the synthesis of Cdks and cyclins.

Whereas other growth factors induce the synthesis of cyclin D, we considered the possibility that posttranslational regulation of cyclin D could be regulated by IL-3 and IL-7, because it has been reported that p38 MAPK could phosphorylate cyclin D1, leading to its ubiquitination and degradation[91]. We therefore overexpressed cyclin D1 in FL5.12A cells to determine whether it would mimic the effect of p38 MAPK inhibition in releasing cells from G1 arrest after IL-3 loss. This was not the case because overexpression of cyclin D1 in FL5.12A cells failed to relieve cell cycle arrest in the absence of IL-3 whereas the p38 MAPK inhibitor continued to have this effect as it did in untransfected cells (data not shown). Together, withdrawal of IL-3 leads to G1 arrest by a mechanism unrelated to the levels of cyclin D mRNA (Fig. 15A) or protein (Fig. 15, B and C).

Inhibition of Cdk2, a kinase involved in the transition into S-phase, with a potent and selective pharmacological inhibitor (Cdk2 Inhibitor II- Compound 3), countered the effect of inhibiting p38 MAPK after 17 hours of IL-3 withdrawal (Fig. 16). This effect was evident in the absence of IL-3. Because there were minimal effects of p38 MAPK inhibition on the transcription of Cdk2 (Fig. 15A), we examined a role for regulation of Cdk2 activity, specifically

through the Cdc25 family of phosphatases known to dephosphorylate and activate Cdks[92]. Treatment of FL5.12A cells with a pharmacological inhibitor (NSC 95397) of Cdc25 phosphatases reversed the S-phase progression induced by p38 MAPK inhibition (Fig. 16). These findings suggest that Cdc25 phosphatases, and their activation of Cdks, could be essential components of the pathway through p38 MAPK by which cytokines regulate cell proliferation.

Previous studies had shown that p38 MAPK could directly phosphorylate members of the Cdc25 family, Cdc25B and Cdc25C, inducing their degradation[93, 94]. However, it is Cdc25A that is involved in the G1-S phase transition, dephosphorylating Cdk2 on an inhibitory tyrosine, Y15, thereby activating it. We therefore assayed for Cdc25A and observed that the levels of endogenous (Fig. 17A) and overexpressed HA-tagged Cdc25A rapidly declined 4–8 hours after IL-3 withdrawal (Fig. 17B), suggesting degradation of the protein. Others have shown that the degradation of Cdc25A is proteasome dependent[79] and mediated through ubiquitination [95]. We found that inhibiting p38 MAPK subsequently restored Cdc25A protein levels, both endogenous levels and overexpressed HA-tagged Cdc25A, promoting stability of the phosphatase (Fig. 17B). Hence, p38 MAPK appears to act upstream of the decline of Cdc25A after IL-3 withdrawal, and regulating Cdc25A protein stability may be one of the functions of this kinase.

Two critical serines on Cdc25A (S75 and S123) are known to be kinase targets. DNA damage triggers the Chk kinases which phosphorylate Cdc25A on S123 leading to its degradation[96, 97] and in *Xenopus* embryos, phosphorylation of S73 (S75 in the human sequence) is mediated by another unknown kinase[98], perhaps also Chk1 as has been recently shown[99]. However, Chk kinases are known to be activated during cell cycle checkpoints triggered by DNA damage[100], which occurs later in the apoptotic process, and we did not detect Chk1 protein

during cytokine withdrawal (data not shown) nor observed any effects on cell cycle progression upon Chk1 inhibition by RNA interference (Fig. 14A). This demonstrates that cell cycle arrest due to cytokine withdrawal does not involve Chk1 and suggests that phosphorylation of Cdc25A is mediated by a different kinase activity in cytokine-deprived lymphocytes.

The regulatory sites on Cdc25A, S75 and S123, can be direct targets of p38 MAPK as shown by p38 MAPK *in vitro* kinase assays using HeLa cells[84]. These results, together with the increased stability of Cdc25A promoted by p38 MAPK inhibition (Fig. 17B), suggest that p38 MAPK is the kinase principally responsible for phosphorylation of S75 and S123 on Cdc25A, inducing the decline in Cdc25A after cytokine withdrawal.

Having shown that the decrease in Cdc25A proteins correlated with cell cycle arrest after cytokine withdrawal, we tested whether it played an important functional role. Because S75 and 123 were the targets of p38 MAPK, leading to its degradation, we mutated these sites and measured the effect on cell cycling after cytokine withdrawal. Mutation of S75, and S123 to alanines produced a stable form of Cdc25A that significantly restored S-phase entry after 24 hours of IL-3 withdrawal as shown in Fig. 18A. The Cdc25A double mutant (S75,123A) functioned like a dominant-positive (DP), promoting cell cycling in the absence of IL-3 compared with expression of the WT protein. Significantly, that activity of Cdc25A-DP in the absence of IL-3 resulted in DNA synthesis, as shown by incorporation of BrdU, and not just accumulation in S-phase, with cells progressing into G2/M (Fig. 18A). This was not observed in cells expressing WT Cdc25A that accumulated in the G1 phase.

The effect of expressing the Cdc25A-DP in IL-7 dependent D1 cells was even more striking, with increased cells cycling in the absence of IL-7 (24 hours) compared with WT

protein (Fig. 18B). Using BrdU incorporation to measure DNA synthesis, we also observed restoration of S-phase progression by this Cdc25A mutein after IL-7 withdrawal (Fig. 18B). These effects required mutation of both sites (S75 and S123) on Cdc25A, because either one alone had minimal effects on cell cycling (not depicted). Expression of Cdc25-DP (cotransfected with the selection marker GFP) in primary lymphocytes was able to restore DNA synthesis (measured by BrdU incorporation) in primary cells deprived of IL-7 for up to 48 hours (Fig. 18D). Cdc25A-WT also had a positive effect on primary lymphocyte proliferation, though not as striking as that of the DP protein, perhaps due to reduced levels of p38 MAPK in primary cells as compared with cell lines. These findings indicate that Cdc25A is pivotal regulator of IL-7-driven proliferation of lymphocytes, cell lines and primary cells, and a novel target of IL-7 signal transduction through p38 MAPK.

In addition to promoting cell cycling, expression of the Cdc25A-DP was able to extend the life of cells grown in the absence of IL-7. Shown in Fig. 18C, are forward (FSC)/ side scatter (SSC) plots of D1 cells grown in the absence of IL-7 for 48 hours. Cells expressing the Cdc25A WT protein, lacking IL-7, had begun to undergo apoptosis and shrink in size, as indicated by decreased FSC, whereas cells expressing Cdc25A-DP remained viable and did not undergo atrophy. Therefore, expression of Cdc25A-DP replaced the IL-7 signal for cycling and cell maintenance for 2–5 days of cytokine withdrawal, after which cells die likely due to loss of nutrient uptake[101]. Untransfected cells or cells expressing the WT protein shrink and die after 36–48 hours of cytokine deprivation. As comparison, expression of the anti-apoptotic proteins, BCL-2[14] or BCL-XL (data not shown), though protecting cells from death, did not promote cell

cycling, but rather inhibited growth and instead maintained cells in a shrunken, vegetative state, likely undergoing autophagy in the absence of cytokines.

Mutation of S75 and S123 on Cdc25A also mimicked the effect of inhibiting p38 MAPK in stabilizing the Cdc25A protein after IL-3 withdrawal (Fig. 19, A and B) and IL-7 withdrawal (not depicted). Mutation of S75 alone had a partial effect of stabilizing Cdc25A (Fig. 19B), although cell cycle progression was not restored, whereas mutation of S123 alone did not restore protein stability (not depicted). Hence, mutation of both S75 and S123 are required to deregulate Cdc25A, promoting protein stability and function in the context of cytokine deprivation in lymphocytes.

The Cdc25A-DP mutant protein was also fully competent for phosphatase activity. The DP mutant sustained phosphorylation of Rb and Cdks (Cdk2 and Cdk1) after withdrawal of IL-3 or IL-7 (Fig. 19C). Specifically, we detected the accumulation of hyperphosphorylated Cdks at T160 and Y15, correlating with active cell cycling despite cytokine deprivation. It is possible that the increased expression of cyclin E (and perhaps cyclins D2 and D3) transcripts observed during p38 MAPK inhibition (Fig. 15A) resulted from phosphorylated Rb which in turn would result in the release of E2F and the subsequent induction of various genes, such as cyclins, involved in cell cycle progression. Hence, expression of Cdc25A-DP was sufficient to induce cell cycling and maintain cell integrity in the absence of a cytokine growth stimulus, and this in part resulted from the activation of Cdks/ cyclins and the phosphorylation of Rb.

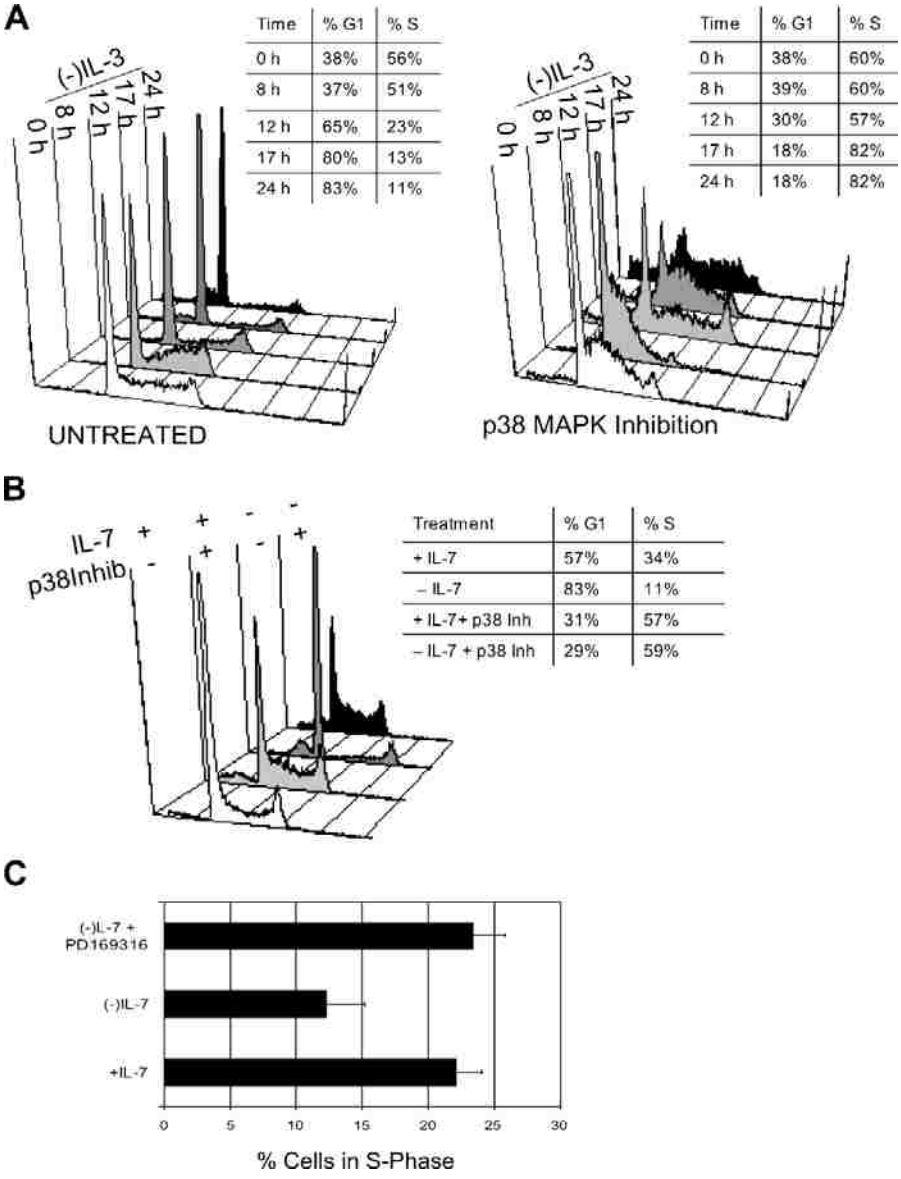

Figure 13. Inhibition of p38 MAPK prevents G1/S arrest after withdrawal of IL-3 or IL-7 from cytokine-dependent lymphoid cells.

Cell cycle was analyzed by incorporation of propidium iodide (PI). Percent of cells in G1 and S phases was calculated using ModFit LT software. (A) IL-3 was withdrawn from FL5.12A, pro-B cells for 8, 12, 17, or 24 hours. The p38 MAPK inhibitor, PD169316 (20 µM), was added at the time of IL-3 withdrawal. Shown is a representative example of four experiments. (B) IL-7 was withdrawn from D1, a thymic cell line, for 24 hours. The p38 MAPK inhibitor, PD169316 (20 µM) was added at the time of IL-7 withdrawal. Shown is a representative experiment. (C) Mouse lymph node cells were isolated and placed in culture with IL-7 (100 ng/ml) and a submitogenic concentration of Con A (0.25 µg/ml) for 48 hours. Cells were then washed and cultured for 24 hours without IL-7 and with PD169316 (20 µM). Shown are the results of two combined experiments, with error bars representing ± SEM.

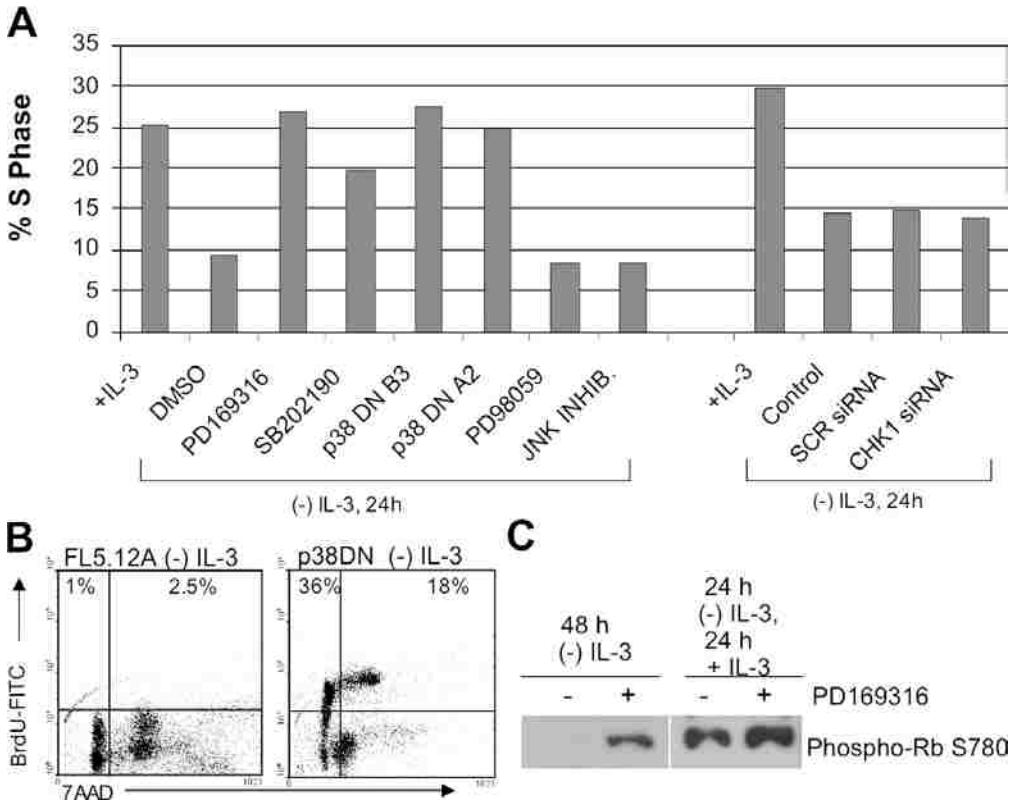

Figure 14. Inhibition of p38 MAPK, but not ERK or JNK, restores S-progression and Rb phosphorylation in the absence of IL-3.

Cell cycle was analyzed by incorporation of PI. Percent of cells in S phase was calculated using ModFit LT software. (A) FL5.12A cells were cultured with or without IL-3 for 17 hours. The p38 MAPK inhibitors, PD169316 (20 µM) or SB202190 (20 µM), the MEK1 inhibitor (activator of ERK), PD98059 (20 µM), and the Jun kinase inhibitor, JNK inhibitor II (20 µM), were added at the time IL-3 was withdrawn. DMSO (0.1%) was included as a negative control. Two different FL5.12A clones B3 and A2, stably transfected with a dominant negative (DN) p38 MAPK, were placed in culture without IL-3 for 17 hours. Results shown are representative of two experiments. (B) FL5.12A-A2 cells, expressing DN-p38 MAPK, incorporated BrdU during 17 hours of IL-3 withdrawal, while untransfected cells arrested. (C) Levels of phosphorylated Rb protein were assayed in FL5.12A cells after 48 hours of IL-3 withdrawal. Nuclear lysates were resolved by SDS-PAGE and immunoblotting using an antibody specific for Rb protein phosphorylated at serine 780.

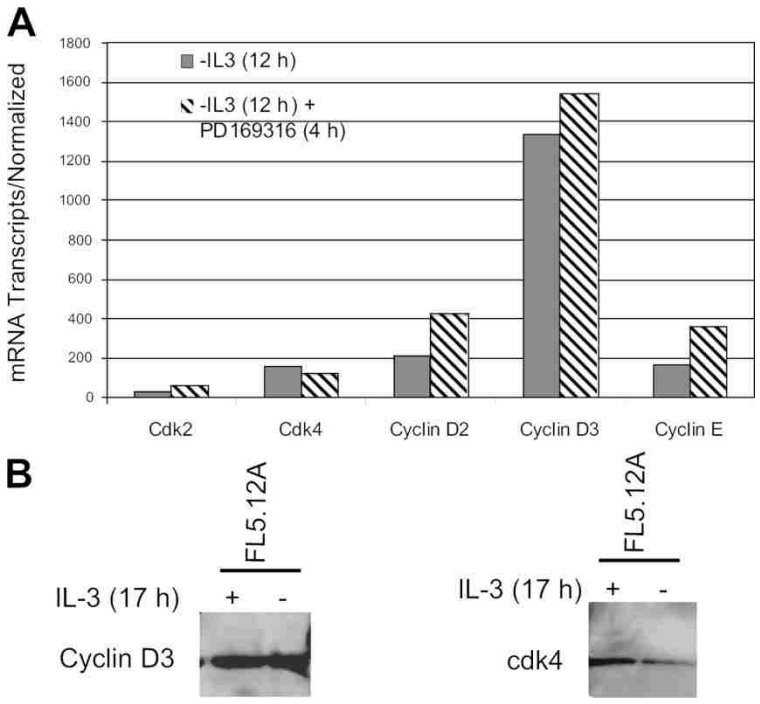

Figure 15. Inhibition of p38 MAPK after IL-3 withdrawal induces minor increases in G1-S Cdks and cyclins in B lymphocytes.

(A) FL5.12A cells were incubated for 12 hours in the absence of IL-3 and then further incubated for 5 hours with either PD169316 (20μM) or IL-3 (not depicted) for a total of 17 hours. Cells were then harvested and total RNA isolated. RPAs were performed as described in Materials and methods. Transcription of L32 was measured as a control for total mRNA expressed. Results were quantified using a Bio-Rad Gel Documentation system, and mRNA transcripts for Cdks and cyclins normalized to the levels of L32 expression. (B) Whole cell lysates were prepared from FL5.12A cells deprived of IL-3 for 17 hours and immunoblotted for detection of Cdk4 and cyclin D3 with specific antibodies. RPAs shown in (A) were performed by Dr. Annette Khaled.

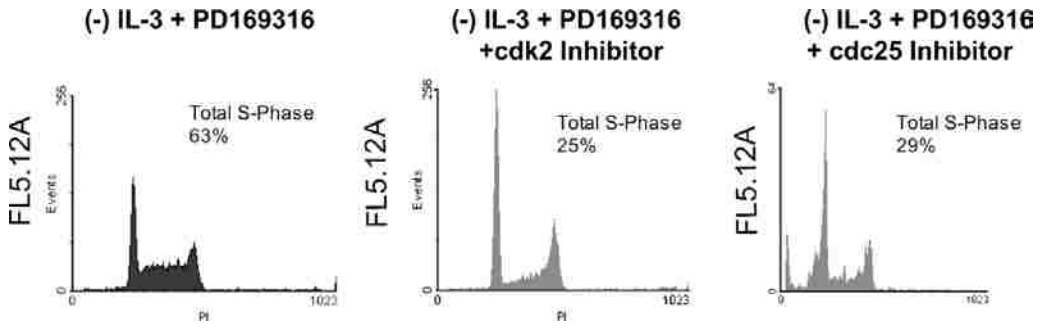

Figure 16. Inhibition of Cdk2 or Cdc25 reverses the effects of p38 MAPK inhibition of the promotion of cell cycling during IL-3 withdrawal.
Cell cycling was analyzed by incorporation of PI and percent of cells in S phase was calculated using ModFit LT software. FL5.12A cells were cultured without IL-3 and PD169316 (20μM) in the presence of 20μM of a pharmacological inhibitor of Cdk2 (Cdk2 inhibitor II) or 20μM of a pharmacological inhibitor of Cdc25 (NSC95397) for 17 hours and effects of cell cycling assessed.

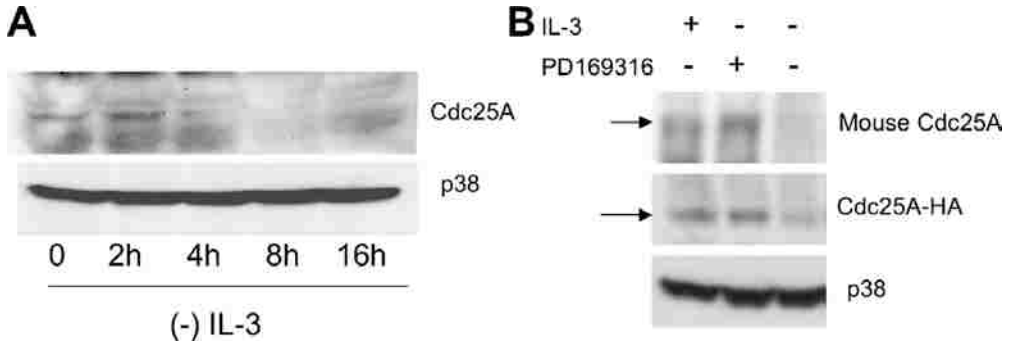

Figure 17. Cdc25A protein is degraded upon cytokine withdrawal and stabilized, in the absence of cytokines, by inhibition of p38 MAPK.
(A) Levels of endogenous mouse Cdc25A protein were measured in FL5.12A cells. Whole cell lysates were made from cells deprived of IL-3 for 2, 4, 8, and 16 hours, then resolved by SDS-PAGE and immunoblotted using an antibody specific for Cdc25A. Total p38 MAPK was measured as a loading control. (B) Endogenous mouse Cdc25A was measured in FL5.12A cells stably overexpressing wild-type (WT) human Cdc25A. Whole cell lysates were made from cells cultured with or without IL-3 and 20 μM of PD169316 for 16 hours, and then resolved by SDS-PAGE and immunoblotted using antibodies specific for mouse Cdc25A and for human Cdc25A. Levels of p38 were detected as a loading control. Shown are representative experiments of three such performed. Immunoblots performed by Mr. Dimitry Bulavin.

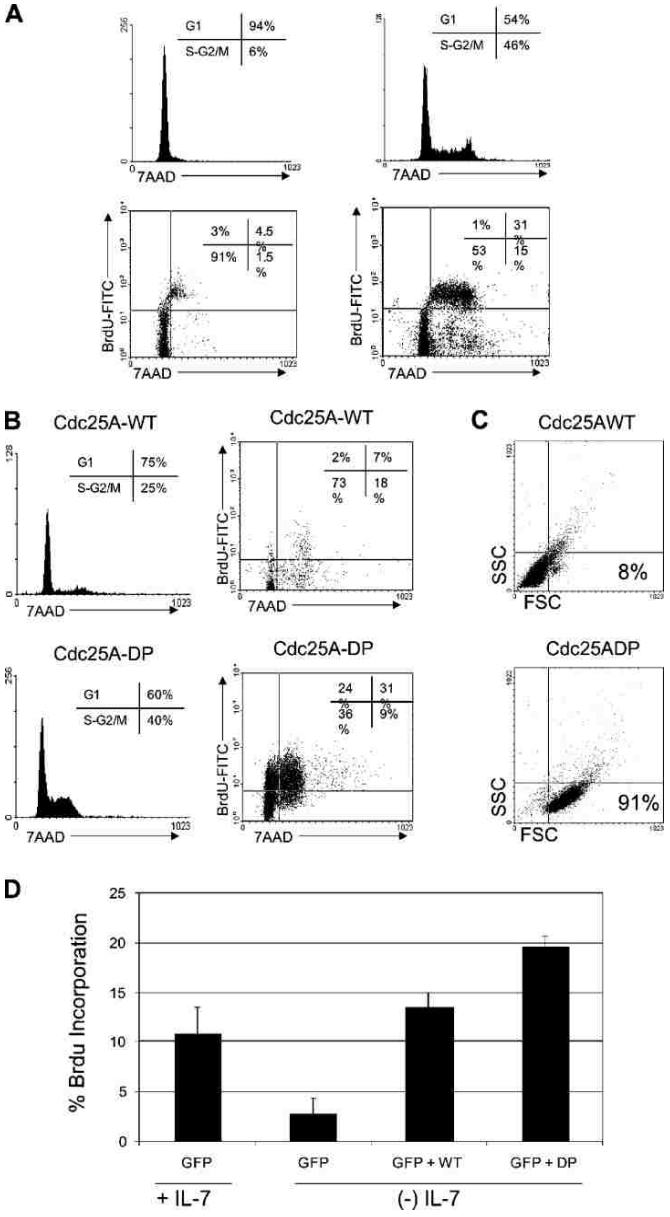

Figure 18. Expression of Cdc25A mutated at S75 and S123 prevents G1 arrest and sustains S-phase progression after withdrawal of IL-3 or IL-7.

DNA synthesis was detected by BrdU incorporation and cell cycle was measured by 7AAD and analyzed by flow cytometry. Percent of cells in G1 and S-phase was calculated using ModFit LT software, excluding apoptotic cells and aggregates. (A) FL5.12A cells stably expressing the dominant-positive (DP) Cdc25A (S75,123A) mutein or Cdc25A-WT were cultured with or without IL-3 for 24 hours. (B) D1 cells stably expressing the Cdc25A-DP (S75, 123A) mutein or Cdc25-WT were cultured with or without IL-7 for 24 hours. (C) Viability and cell size of D1 cells stably expressing Cdc25A-DP or Cdc25A-WT are shown in dot blots displaying forward (FSC) and side scatter (SSC). (D) Lymph node cells were isolated and grown with IL-7 (100 ng/ml) and Con A (0.25 μg/ml). Primary cells were transfected with Cdc25A-DP or Cdc25A-WT and GFP, as a selection marker. Transfected cells, were selected by gating on GFP expression for analysis of DNA synthesis and cycling by BrdU/ 7AAD staining after 24 hours of IL-7 withdrawal. Results shown are representative of three or more experiments performed.

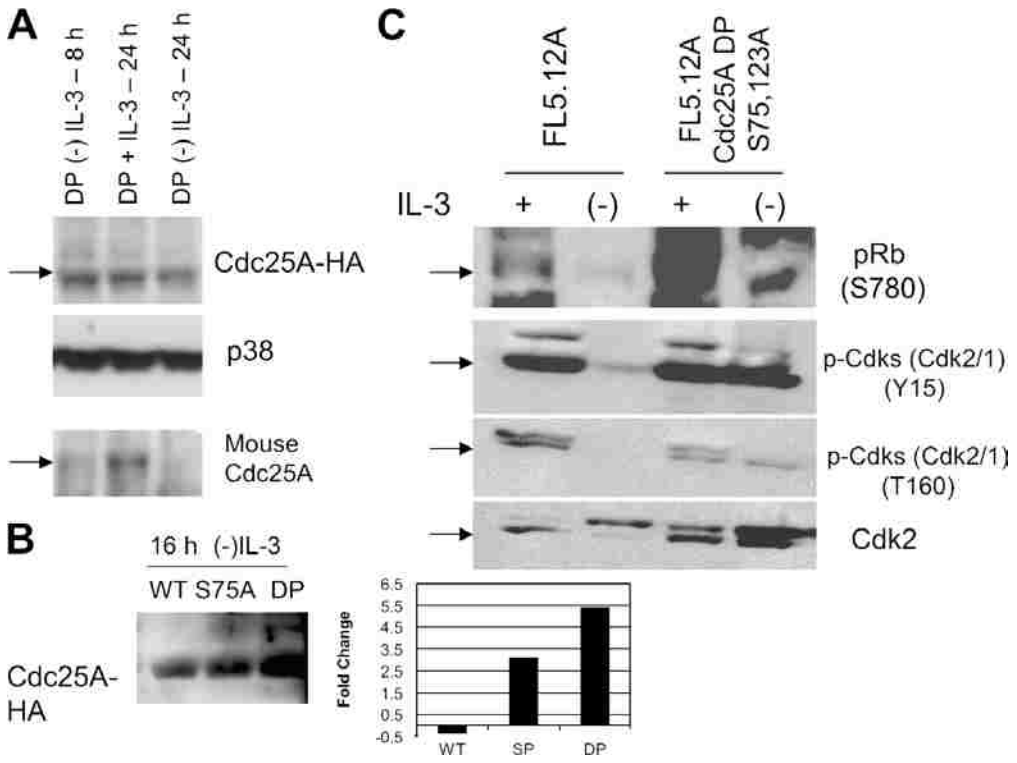

Figure 19. Cdc25A-DP (S75, 123A) remains stable and sustains phosphorylation of Rb and Cdks after IL-3 withdrawal.

(A) Protein levels of Cdc25A-DP (S75,123A) were measured in FL5.12A cells. Cells were deprived of IL-3 for 17 hours, and cytosolic extracts were resolved by SDS-PAGE and immunoblotted using an antibody specific for mouse (to detect endogenous protein) or human Cdc25A (to detect the overexpressed HA-tagged protein). Total p38 MAPK was measured as a loading control. Shown is a representative experiment of two. (B) Stability of Cdc25A was determined in FL5.12A cells overexpressing the Cdc25A-DP mutant (DP) and the Cdc25A single mutant (S75A) (SP) after IL-3 withdrawal. The immunoblot was quantified using a Bio-Rad Gel Documentation system and results shown in the adjacent panel. The graph indicates fold differences in protein levels measured with or without IL-3 for 16 hours. (C) Levels of phosphorylated Rb protein and Cdk2 were measured in FL5.12A cells and FL5.12A cells stably overexpressing the Cdc25A-DP mutein. Nuclear extracts were made from cells deprived of IL-3 for 17 hours, then resolved by SDS-PAGE and immunoblotted using antibodies specific for phospho-Rb protein (phosphorylated at serine 780), phospho-Cdk (tyrosine 15) (detects phospho-Cdk2 and phospho-Cdk1) and phospho-Cdk (threonine 160; detects phospho-Cdk2 and phospho-Cdk1). Total Cdk2 levels were also measured with a specific antibody. Note, the same cell lysates (equally loaded) were used in the phospho-Rb, phospho-Cdks, and Cdk-2 blots. Immunoblots shown in (A) and (C) were performed by Mr. Dimitry Bulavin and Dr. Annette Khaled, respectively.

Discussion

Lymphocytes depend on external signals from cytokines for survival and proliferation. Here we have examined the mechanisms by which IL-3 and IL-7 induce proliferation of lymphoid cell lines and primary lymphocytes and find that this pathway differs from that of better-studied factors that induce growth of mesenchymal cells. Rather than inducing synthesis of cyclins, these cytokines appear to protect lymphocytes from a stress response. Withdrawal of IL-3 or IL-7 induced cell cycle arrest through activation of a stress kinase, p38 MAPK, which occurred in the first few hours after cytokine withdrawal. p38 MAPK then directly phosphorylated the phosphatase Cdc25A at S75 and S123, targeting the phosphatase for degradation. Because Cdc25A is required to remove an inhibitory phosphate (Y15) from Cdk2, the latter kinase was inactive, failed to phosphorylate Rb and the cells arrested at the G1-S boundary. We show that inhibiting either component of this pathway, blocking p38 MAPK activity or expressing a p38 MAPK-resistant form of Cdc25A, prevented growth arrest in the absence of a cytokine receptor signal, restoring cell cycle progression as well as maintaining cell viability and size. We have produced time courses (some are shown) for most of these phenomena. The sequence of events after cytokine withdrawal is: (1–12 hours) p38 activation, Cdc25A phosphorylation and degradation; (12–48 hours) G1 arrest; (24–48 hours) apoptosis. The time points selected for the figures were intended to illustrate each of these phases.

Another mechanism reported for cell cycle arrest after cytokine withdrawal is through an increase in p27kip1, a negative regulator of proliferation through its interactions with Cdks, especially Cdk2[102]. Protein levels of p27kip1 accumulate in serum-starved and growth factor–deprived cells, and we have confirmed this increase occurs in cells deprived of IL-7 or IL-3.

However, we noted that p27kip1 levels also increased after cytokine withdrawal in cells overexpressing Cdc25A-DP (unpublished data) that were not arrested in G1 (Fig. 18); thus these cells replicated normally in the absence of cytokines despite their elevation in p27kip1. This suggests that the positive effect of Cdc25A-DP on cell cycle progression can dominate over the negative effect of p27kip1.

Microinjection of antibodies to Cdc25A have been shown to arrest cells in G1[103], indicating the importance of this phosphatase in the cell cycle. Overexpression of wild-type Cdc25A in rat-1 cells accelerated entry into S-phase and the activation of Cdk2 [104]. However, in the lymphocytes in our studies, overexpressed wild-type Cdc25A was degraded in the absence of IL-3 or IL-7 and did not restore cell cycle progression in cell lines (Figs. 17 and 18), whereas overexpression of the stable Cdc25A-DP sustained cell growth (Figs. 18 and 19). Thus, in our studies, the failure to rescue cell division with overexpressed wild-type Cdc25A in cell lines is presumably because it is rapidly degraded after phosphorylation by p38 MAPK, which is activated by cytokine withdrawal. However, in primary cells, expression of Cdc25A-WT did have growth promoting effects likely because the levels of active p38 MAPK may be reduced in comparison to the cell lines. Even in this case, however, expression of Cdc25A-DP resulted in IL-7 independent DNA synthesis beyond that observed with expression of the WT protein.

In cell lines, Cdc25A-DP supported multiple rounds of cell division in the absence of cytokine. Over the first 2 days a five-fold increase in cell numbers was observed, thereafter, cells continued to divide until the rate of cell death increased to the point that all cells were dead by day 5. The eventual death of cytokine-deprived Cdc25A-DP expressing cells could result both from apoptosis (because they cease expressing BCL-2) and from metabolic depression

because cytokine withdrawal also reduces glucose uptake as we showed for IL-7[101] and others showed for IL-3[105].

If cytokines induce survival via BCL-2 or BCL-XL and proliferation via Cdc25A one might predict that transfecting both BCL-2 and Cdc25A should render cells capable of both survival and proliferation in the absence of cytokine. However we were unable to obtain stable lines of BCL-2/ Cdc25A doubly transfected cells. This could be because, as reported by others[106, 107], overexpression of BCL-2 or BCL-XL, although maintaining the life of the cell, can also inhibit its replication. Or it could be due to lack of glucose uptake, as noted above; thus a cell protected by BCL-2 or BCL-XL may be able to survive in a quiescent state when deprived of cytokine-induced glucose uptake, but when driven to divide by Cdc25A-DP, the cell may die from metabolic stress.

Recent studies in HeLa cells showed that osmotic stress or UV irradiation induced cell cycle arrest. This arrest was accompanied by degradation of wild-type Cdc25A, but not Cdc25A-DP, however, in contrast to our studies, cell cycling was not restored by Cdc25A-DP[84]. This suggests that multiple checkpoints, in addition to Cdc25A regulation, must be involved in the growth arrest from osmotic stress or UV irradiation and ensuing DNA damage. One such pathway would be stabilization of p53 leading to p21 induction; this would occur after UV irradiation but does not occur after cytokine withdrawal, for which we show that Cdc25A destabilization is the major mechanism of growth arrest.

CHK1 and CHK2 are also reported to phosphorylate and destabilize CDC25A. We measured levels of CHK1 in cytokine-dependent cells and found that this protein disappeared after cytokine withdrawal (data not shown). CHK2 is not as critical a regulator of Cdc25A as is

CHK1. We also treated cells with CHK1 small interfering RNA and saw no effect on the G1 arrest induced by cytokine withdrawal (Fig. 14A). In contrast to the disappearance of CHK1, p38 activity dramatically increased after cytokine withdrawal (data not shown). These observations favor a role for p38 MAPK, rather than CHK1 in the down-regulation of Cdc25A after cytokine withdrawal.

We found that p38 MAPK was required to phosphorylate S75 and S123 on Cdc25A and induce its degradation. Others have shown that, in response to DNA damage, phosphorylation of S75, followed by phosphorylation of S82 and S88, leads to βTrCP-dependent ubquitination and degradation of Cdc25A[82]. The kinase that phosphorylates Cdc25A at S82 and S88 is unknown, and it may be active in cytokine deprived lymphocytes in addition to p38 MAPK as we have shown. In other cell types, others have shown that mutation of S75 alone was sufficient to confer stability to Cdc25A[84, 95], however we found only a partial effect, whereas mutation of both S75 and S123 conferred a full stabilizing effect (Fig. 19). Mutation of both sites on Cdc25A also restored proliferation to cells deprived of cytokines (Fig. 18), whereas single mutations had little effect (not depicted), providing the strongest support for the importance of the stability of this phosphatase in regulating lymphocyte proliferation.

We have shown that cytokine withdrawal from lymphocytes results in two distinguishable responses, one after the other. First, cells undergo cell cycle arrest; second, they undergo apoptotic cell death. These two processes, cell cycle arrest and apoptosis are not only distinguishable kinetically and mechanistically, they also appear to require different levels of cytokine receptor occupancy, i.e., a low concentration of the cytokine is sufficient to protect from cell death but is insufficient to induce cell division (unpublished data). These concentration

effects of cytokines, low dose inducing survival, high dose inducing division, presumably account for these two homeostatic activities of IL-7 in the peripheral immune system[108]. Thus, when lymphocyte density is at its maximum, cells would consume the available IL-7 as rapidly as it is synthesized and each cell would encounter just enough IL-7 to protect from cell death but not enough to proliferate. When the lymphoid compartment is relatively empty, IL-7 would be sufficiently abundant to drive proliferation as well as survival. Our studies with lymphoid cell lines and primary cells suggest that, *in vivo*, this homeostatic proliferation of lymphocytes may be regulated by p38 MAPK and Cdc25A and further studies to test this hypothesis are underway.

CHAPTER 5: CDC25A DRIVEN PROLIFERATION REGULATES LYMPHOCYTE HOMING IN RESPONSE TO INTERLEUKIN-7

Introduction

As effective agents of immunity, T-cells transit to widely dispersed areas of the body. To enter a lymph node from the blood, naïve T-cells must express the adhesion molecule, L-selectin (CD62L), which binds to its peripheral node addressins on the high endothelial venules (HEVs) of the lymph nodes[109]. This interaction promotes "rolling" and facilitates the transmigration of naïve T-cells into the lymph nodes. Antigen encounter and activation proceeds with T-cells stimulated to undergo massive clonal expansion. During this process, the newly activated, effector T-cells down-regulate CD62L to prevent activated T-cells from re-entering the lymph nodes and enable migration of activated T-cells to sites of infection. Hence, CD62L controls the entry or re-entry of T-cells into the lymph nodes, and its expression is linked, in a manner still to be fully understood, with their activation and proliferative expansion.

One of the essential cytokines that T-cells encounter upon entering a lymph node is Interleukin-7 (IL-7), likely presented to them by fibroblastic reticular cells (FRC) which express detectable levels of IL-7 mRNA[110, 111]. IL-7 is an important regulator of T-cell development as well as the survival of peripheral T-cells and maintenance of long-term memory T-cells[13, 112]. The receptor for IL-7 (IL-7R) is expressed by T-cells and consists of the IL-7Rα chain and the common cytokine γ chain (γc)[113]. Upon binding of IL-7, the two receptor chains heterodimerize and initiate signaling events through the JAK/ STAT pathway (reviewed in[13]). Mutations in IL-7, its receptor (IL-7R) or components of its signaling pathway lead to severe immunodeficiency[4],

demonstrating that this cytokine is a potent mediator of the homeostatic mechanisms that maintain populations of naïve and memory T-cells in the peripheral immune system[25, 34, 114].

The mechanism by which IL-7 supports the expansion of T-cells is partially characterized. We reported that the activity of the cdk inhibitor $p27^{kip1}$ and the cdk activating phosphatase, Cdc25A, was regulated by IL-7[17, 71]. Over-expression of $p27^{kip1}$ induced G1 arrest in the presence of IL-7 and deletion could partially restore proliferation of T-cells from IL-$7^{-/-}$ mice[71]. Cdc25A levels declined upon cytokine loss due to p38 MAP kinase (MAPK)-targeted degradation[17, 84]. Expression of a constitutively active form of Cdc25A promoted cell cycling of lymphocytes in the absence of IL-7, even in the presence of elevated levels of $p27^{kip1}$ [19]. Hence in the absence of IL-7, expression of Cdc25A could support cell proliferation, suggesting that Cdc25A is a critical transducer of the IL-7 replicative signal.

Survival, proliferative and metabolic[115] activities have all been ascribed to IL-7, revealing the potential therapeutic applications of this cytokine. However, the effect of IL-7-mediated proliferation upon lymphocyte trafficking is poorly understood. To this end, we examined the functionality of IL-7 under conditions in which proliferative activity was regulated by genetic manipulation of Cdc25A and detected phenotypic changes that could alter lymphocyte homing. Specifically, we observed the up-regulation of activation markers like CD69 and the down-regulation of adhesion molecules like CD62L on Cdc25A-expressing T-cells. Expression of constitutively active Cdc25A indicated that proliferation driven through IL-7 could significantly alter lymphocyte homing in the absence of any antigen stimulation.

Material and methods

Mice and cell isolation

Mice were housed in the animal facility at the University of Central Florida and used at 3 months of age. Bim deficient ($Bim^{-/-}$), on a C57Bl/6 background, mice were housed at the National Cancer Institute, Frederick, Maryland. C57Bl/6 mice were purchased from Jackson Labs. Lymph node and spleen cells were isolated by gentle crushing through a 70μM pore filter (BD Falcon) and pooled. Spleen cells were further treated with ACK lysis buffer (Quality Biological, Inc.). T-cells were enriched by negative selection with the Mouse T-lymphocyte Enrichment kit according to the manufacturer's protocol (BD Biosciences). For $CD62L^{hi}$ and $CD62L^{lo}$ enrichment experiments, T-cells were purified from spleen as described above and further enriched for $CD62L^{hi}$ or $CD62^{lo}$ cells with biotinylated anti-CD62L (clone MEL-14; BD Biosciences) according to manufacturer's protocol.

In vitro culture

Cells were maintained at a density of $3\text{-}5x10^6$ cells in complete medium (RPMI 1640 Medium (Invitrogen) supplemented with 10% Fetal Bovine serum (Hyclone), 2-βmercaptoethanol, and penicillin/ streptomycin). Recombinant human IL-7 (rhIL-7) (Peprotech) was added at the start of culture at a concentration of 10 ng/ml or 150 ng/ml and refreshed every other day, except for IL-7 withdrawal experiments in which cell cultures were maintained in complete medium only.

Plasmids and nucleofection of T cells

The constitutively active HA-tagged Cdc25A (Cdc25A-DP) plasmid was previously described[17]. To inhibit Cdc25A activity, a catalytically inactive Cdc25A (Cdc25A-DN) was generated in the background of the Cdc25A-DP plasmid by targeting the active site Cys-$(X)_5$-Arg motif[116]. Cys-430 was mutated to serine and Arg436 was mutated to alanine by using a site-directed mutagenesis approach (QuikChange II site directed mutagenesis kit, Stratagene). To transiently express Cdc25A-DP, Cdc25A-DN, GFP or the empty vector (pcDNA), T-cells were nucleofected with 4µg of plasmid DNA using the Mouse T-cell Nucleofection kit (Amaxa) according to the manufacturer's protocol. For the GFP experiments, cells were immediately maintained in the presence or absence of IL-7 for 24 hours and no differences in transfection efficiency were observed. In the surface staining experiments, cells were maintained in IL-7 overnight and then washed the next day and cultured an additional 24 hours with or without IL-7 prior to analysis. For the BrdU experiments, cells were immediately cultured with or without IL-7 and pulsed with 10µM BrdU (BD Biosciences) and analyzed 24 hours later as described above.

Cell surface phenotyping

Surface expression on T-cells was assessed with PE-conjugated anti-CD4 (clone GK1.5), PerCP-conjugated anti-CD8 (clone 53-6.7), FITC-conjugated anti-CD44 (IM7), FITC-conjugated anti-CD69 (clone H1.2F3), and PE-conjugated anti-L-selectin (CD62L; (clone MEL14) (BD Biosciences). Cells were incubated with the appropriate antibodies for 20 minutes on ice and analyzed by flow cytometry using the C6 flow cytometer (Accuri). The data was analyzed using FCS Express software (Ontario, Canada).

Intracellular BrdU labeling

Cells were pulsed with BrdU (10μM) for 48 hours and BrdU incorporation was detected with a commercially available kit (BD Biosciences) according to manufacturer's protocol. Briefly, cells were surface stained as described above, washed, fixed, and permeabilized prior to incubation with a FITC-conjugated anti-BrdU antibody. Staining with 7AAD was performed following manufacturer's protocol. Cells were analyzed by flow cytometry using the C6 flow cytometer (Accuri). The data was analyzed using FCS Express software (Ontario, Canada).

Intracellular staining of Cdc25A or Foxo1

For detection of intracellular or nuclear Cdc25A or nuclear Foxo1, we used an optimized protocol designed to enhance detection of these intracellular proteins[53]. Nuclei were isolated in extraction buffer (320 mM sucrose, 5mM MgCl2, 10mM HEPES, 1% Triton-X100). Prior to fixation, intact T-cells or nuclei were stained with Foxo1 antibody (Cell Signaling) or Cdc25A antibody (Santa Cruz). Cells or nuclei were washed, fixed, and permeabilized with the Fix & Perm Cell Permeabilization kit (Caltag) following the manufacturer's protocol. Cells were stained with PE-conjugated anti-rabbit secondary antibody. The secondary antibody alone or isotype matched PE-conjugated antibodies (BD Biosciences) were used as controls. Cells were analyzed by flow cytometry using the C6 flow cytometer (Accuri) described above. The data was analyzed using FCS Express software (Ontario, Canada).

IL-7 injections of mice

C57Bl/6 mice were injected once, intraperitoneally, with 200µl PBS (control) or 10µg recombinant human IL-7 (rhIL-7) (Peprotech), or 100µg M25 anti-IL-7 antibody (Amgen) or a premixed combination of 10µg rhIL-7 and 100µg M25 antibody in 200µL PBS. Mice were euthanized after 72 hours and lymphoid organs harvested for analysis of T-cell content as previously described.

Results

Previously, we reported that the phosphatase, Cdc25A, was an essential transducer of cytokine-mediated proliferation in lymphocytes[17]. Using cytokine dependent T and B cell lines, we found that a constitutively active form of Cdc25A (Cdc25A-DP), lacking the p38 MAPK phosphorylation sites that target the phosphatase for degradation, could promote cell division even when levels of the cell cycle inhibitor, $p27^{kip1}$, were elevated[19].

To examine the function of Cdc25A in a biologically relevant scenario, we used primary T-cells freshly isolated from the lymph nodes of C57Bl/6 mice. Our initial observation, using a cell culture method that we optimized to expand IL-7 dependent T-cells[18], was that the dose of IL-7 used for *in vitro* culture had differential effects upon the T-cell subsets expanded. We found that culture of lymph node T-cells with high dose IL-7 (150 ng/ml), as compared to low dose IL-7 (10 ng/ml), for 2 weeks, up-regulated the expression of the CD69 activation marker (a marker typically found increased upon antigen-activation[117] on CD8 more than CD4 T-cells (Fig. 20A). The activation and memory marker, CD44, was also elevated on CD8 but not CD4 T-cells grown with high dose IL-7 (150 ng/mL) (Fig. 20B). These results confirmed our published

findings that CD8 T-cells but not CD4 T-cells optimally respond to high dose IL-7[118] and that the expression of activation/ memory markers is also enhanced in CD8 T-cells cultured with high doses of IL-7[18]. However, we also noted that the expression of the adhesion molecule, CD62L, was significantly down-regulated on $CD44^{hi}$ CD8 T-cells maintained under conditions of high dose IL-7 compared to low dose IL-7 (Fig. 20B). Note that CD4 and CD8 T-cells freshly isolated from murine lymph nodes (Day 0) displayed low levels of CD69 and CD44 and high levels of CD62L, typical of naïve T-cells (Figs. 20A and 20B). The implication of these findings is that the strength of the IL-7 signal may not only drive proliferation and up-regulation of activation/ memory markers but could also affect T-cell lymph node homing by altering the expression of CD62L. Because the doses of IL-7 being used for testing in human clinical trials are supraphysiological (> 10μg/kg/dose)[23, 24], we focused our investigation on the mechanisms by which IL-7 modulates the levels of CD62L using the conditions of high dose IL-7 that lead to the expansion of CD8 T-cells bearing activation/ memory markers.

We next examined the intracellular levels of Cdc25A in response to IL-7. We anticipated that nuclear Cdc25A levels would decrease in parallel with the IL-7 dose. Figure 21A shows that lymph node T-cells, isolated from wild type (WT) C57Bl/6 mice and cultured with IL-7, contained more nuclear Cdc25A when maintained with high dose IL-7 (150 ng/ml) compared to low dose IL-7 (10 ng/ml) (Fig. 21A, left histogram). These findings showed that high dose IL-7 was a strong proliferative stimulus. We and others noted, however, that primary T-cells from WT mice rapidly die in the absence of IL-7[18, 26]. In order to examine the effects of IL-7 deprivation, we used lymph node T-cells from mice deficient in the pro-apoptotic protein, Bim. Others have shown that mice deficient in both the IL-7 receptor and Bim displayed partial

recovery of T-cell numbers[33], indicating that T-cells from these mice could be resistant to death when deprived of IL-7[119]. We examined the amounts of total Cdc25A in lymph node T-cells from $Bim^{-/-}$ mice and found that Cdc25A was elevated in the presence of IL-7 and significantly decreased in the absence of IL-7 (Fig. 21A, right histogram). Taken together with our previous findings that phosphorylation of Cdc25A by p38 MAPK lead to degradation of the phosphatase under conditions of cytokine-deprivation, we concluded that intracellular levels of Cdc25A are increased, and the phosphatase is not degraded, upon receipt of a strong IL-7 signal and as such Cdc25A drives the proliferation of T-cells in response to IL-7.

It follows that Cdc25A is needed to transduce the IL-7-proliferative signal in dependent T-cells. We examined this by expressing either a constitutively active form of Cdc25A (Cdc25A-DP), in which the p38 MAPK target sites (Ser75, Ser123) were mutated to alanines, or a dominant negative form (Cdc25A-DN) in which, in addition to the Ser75A and Ser123A mutations, the enzyme active site was mutated, but all activating phosphorylation sites, were retained. The expectation was that Cdc25A-DP would remain stable and induce proliferation, while Cdc25A-DN would inhibit proliferation independently of IL-7. Using $Bim^{-/-}$ lymph node T-cells, we employed the method of Nucleofection (Amaxa) to transiently express Cdc25A-DP or Cdc25A-DN in cells grown either with high dose IL-7 (150 ng/ml) or deprived of IL-7 (0 ng/ml). Using FSC/ SSC analysis guided by GFP expression, we gated on the population of cells that were nucleofected. In Figure 21B we showed that BrdU incorporation was inhibited in IL-7-maintained T-cells upon expression of Cdc25A-DN, and that BrdU incorporation was induced in IL-7-deprived cells upon expression of Cdc25A-DP.

Subsequently, we determined whether Cdc25A activity could mimic the effect of IL-7 upon the levels of activation/ memory markers displayed by T-cells (shown in Fig. 20). Figure 22 shows representative experiments in which $Bim^{-/-}$ T-cells (initially expanded in IL-7) were nucleofected with Cdc25A-DP and cultured without IL-7 (Fig. 22A), or WT T-cells (freshly isolated) were nucleofected with Cdc25A-DN and cultured with high dose (150 ng/ml) IL-7. Expression of Cdc25A-DP increased the surface levels of both CD69 and CD44 in T-cells deprived of IL-7 (Fig. 22A), while expression of Cdc25A-DN decreased CD69 and CD44 levels in T-cells maintained with high dose IL-7 (Fig. 22B). Note that CD44 levels were already elevated in $Bim^{-/-}$ T-cells due to prior culture in IL-7-containing medium. Furthermore, we observed a trend towards up-regulation of CD62L due to Cdc25A inhibition through expression of Cdc25A-DN (Fig. 22C). Collectively the results shown in Figures 21 and 22 indicate that the proliferative and activating effects of high dose IL-7 upon T-cells can be replicated by inducing Cdc25A or blocked by inhibiting Cdc25A. We concluded that Cdc25A is a critical transducer of IL-7 signals - including those signals that could potentially alter lymphocyte homing through modulation of CD62L.

We next examined the mechanism by which IL-7 down-regulated the expression of CD62L on T-cells. Fig 23A shows a representative histogram in which the nuclear levels of the transcription factor, Foxo1, increased in the absence of IL-7. Previous studies showed that Foxo1 controls the expression of CD62L[120, 121]. We inferred, from our findings (Fig. 23A), that IL-7 signaling controlled the nuclear translocation of Foxo1, retaining the transcription factor in the cytosol when IL-7 engaged its receptor. We then determined whether the IL-7 signal transduced through Cdc25A was responsible for modulating the intracellular localization of

Foxo1. Because expression of Cdc25A-DN by nucleofection was limited to 30-40% of the cells, we examined nuclear Foxo1 levels in WT lymph node T-cells treated with a Cdc25 pharmacological inhibitor. Figure 23B shows the striking results that nuclear Foxo1 levels greatly increased in cells maintained with IL-7 when Cdc25 was inhibited. It follows that the cells, in which Cdc25 inhibition caused an increase in nuclear Foxo1, would also express higher levels of CD62L. Because T-cells freshly isolated from the lymph nodes are predominantly $CD62L^{hi}$, we used T-cells isolated from the spleen and sorted for $CD62L^{lo}$ cells. Overnight treatment of these $CD62L^{lo}$ cells with the Cdc25 inhibitor (in the presence of IL-7) caused a rapid increase in the expression of CD62L that was not observed upon treatment with the vehicle control (Fig. 23C). These results revealed the mechanism underlying our initial observation that high dose IL-7 caused down modulation of CD62L. We demonstrated that it is the dephosphorylating activity of Cdc25A, which activates CDKs and drives cell cycling, that prevents the nuclear translocation of Foxo1, resulting in decreased expression of CD62L.

The prediction that stems from the proposed mechanism would be that in lymph nodes of mice, treated with high dose IL-7, decreased T-cell numbers would result. To test this, C57Bl/6 mice were injected intraperitoneally with one large dose of IL-7 (10 μg), one dose of IL-7 (10 μg) premixed with anti-IL-7 antibody (100 μg, M25), or one dose of M25 (100 μg) alone. We previously observed that under *in vitro* culture conditions the M25 antibody inhibited IL-7 signaling but had little effect *in vivo* (data not shown). We surmised that while IL-7 alone would provide the strongest IL-7 signal, treatment with the M25 antibody and IL-7 could generate conditions of attenuated IL-7 signaling, as a consequence of the interactions of the cytokine with the antibody. Treatment with M25 alone would provide a negative control. We found that

treatment with IL-7/ M25 resulted in the largest recovery of total lymph node cells as well as T-cells, while IL-7 alone caused the greatest loss of total lymph node cells, specifically T-cells (Fig. 24A, left graph). This striking loss of cellularity was apparent when examining the actual size of the lymph nodes recovered from mice injected with IL-7 compared to IL-7/ M25 (Fig. 24A). Differences in total splenic cellularity among mice injected with IL-7 compared to IL-7/ M25 were not as significant (although more total splenic cells were recovered in mice receiving the IL-7/ M25 combination), and in fact little or no differences were observed in regards to splenic T-cell numbers (Fig. 24A, right graph). As anticipated, treatment with M25 alone did not have any notable effects and was similar to the untreated control mice (Fig. 24A). We next examined the ratio of CD4 to CD8 T-cells recovered from the lymph node and spleens of mice injected with IL-7, IL-7/ M25 or M25 alone. In the lymph nodes, IL-7 treatment decreased CD8 T-cells, while the IL-7 /M25 injections resulted in the opposite trend, with more CD8 T-cells accumulating (Fig. 24B). CD4 T-cells did not change appreciably under any of the treatment conditions. In the spleen, we noticed that the IL-7/ M25 treatment caused a loss of both CD4 and CD8 T-cells. We also observed that T-cells remaining in the lymph nodes under all treatment conditions were $CD62L^{hi}$ (data not shown).

Results from the injections with IL-7 or IL-7/ M25 supported our proposed mechanism by which IL-7 controls lymphocyte homing to lymph nodes through Foxo1. A strong IL-7 signal (such as that received with IL-7 alone) could cause the down-regulation of CD62L, enabling T-cells to exit the lymph nodes and remain in circulation, accounting for the decreased number of lymph nodes cells observed in Fig. 24A. An attenuated IL-7 signal (such as that received with IL-7 + M25) could maintain the levels of CD62L, retaining cells within the lymph nodes as seen

in Figure 24A. Because we could not detect CD62L^{lo} cells in the lymphoid organs, as these cells would exit and traffic throughout the body, we examined the levels of Foxo1 in the cells recovered from the injected mice. In correlation with our prediction that the attenuated IL-7 signal, delivered by the combination of IL-7/ M25, would maintain CD62L expression, we observed the highest nuclear levels of Foxo1 in these cells (Fig. 24C). In contrast, Foxo1 levels were decreased in mice receiving IL-7 or M25 alone (Fig. 24C). These *in vivo* studies provide strong evidence that high dose IL-7 could drive T-cell proliferation (through the activity of Cdc25A) and also down-regulate CD62L through the cytosolic retention of Foxo1, enabling T-cell exit but not re-entry into the lymph nodes.

Results from the *in vivo* injections of mice with IL-7 were compelling but T-cells which down-regulated CD62L expression could not be recovered for study. To address this problem and determine whether a strong IL-7 signal causes the down-regulation of CD62L, we performed a series of long term *in vitro* culture experiments with high dose IL-7 to determine whether CD62L^{hi} cells (typical of T-cells found in the lymph nodes) became CD62L^{lo} cells upon IL-7 treatment.

Using splenic T-cells from Bim$^{-/-}$ mice, we sorted for T-cells that were either CD62L^{hi} or CD62L^{lo}. These T-cells were cultured *in vitro* with either low dose IL-7 (10ng/ml) or high dose IL-7 (150 ng/ml) for 7 and 14 days. Results in Figure 25A revealed that T-cells that were initially CD62L^{lo} did not increase in cell number in culture with IL-7. In contrast, cells that started out CD62L^{hi} rapidly expanded, especially with high dose IL-7, more than doubling in number after 14 days of culture (Fig. 25A). We examined the phenotype of the T-cells cultured with high dose IL-7 (150 ng/ml), focusing on the expression of CD62L on CD4 and CD8 T-cells.

We observed that T-cells, initially $CD62L^{hi}$, lost CD62L expression and had become predominantly $CD62L^{lo}$ (Fig. 25B). In contrast, CD62L was not up-regulated on T-cells cultured with IL-7 that were initially $CD62L^{lo}$. We further examined the proliferative status of T-cells that started out either $CD62L^{lo}$ or $CD62L^{hi}$ and found increased BrdU incorporation, indicative of pronounced cell cycling, in the $CD8^{+}$ $CD62L^{hi}$ population. Note that the few remaining CD4 T-cells proliferated slightly. Thus as a consequence of a strong IL-7 signal, T-cells proliferate through the Cdc25A-driven activation of CDKs and also down-regulate CD62L which prevents lymph node re-entry. In support of this effect of IL-7, we isolated $Bim^{-/-}$ lymph node T-cells expressing heterogeneous levels of CD62L and placed them in extended *in vitro* culture with high dose IL-7. Table 1 shows that after 14 days most of the T-cells cultured with IL-7 retained expression of the activation/ memory marker CD44 but down-regulated CD62L, while a much smaller percent maintained detectable levels of CD62L. In contrast, cells deprived of IL-7 expressed a naïve phenotype that was $CD44^{lo}$ and $CD62L^{hi}$.

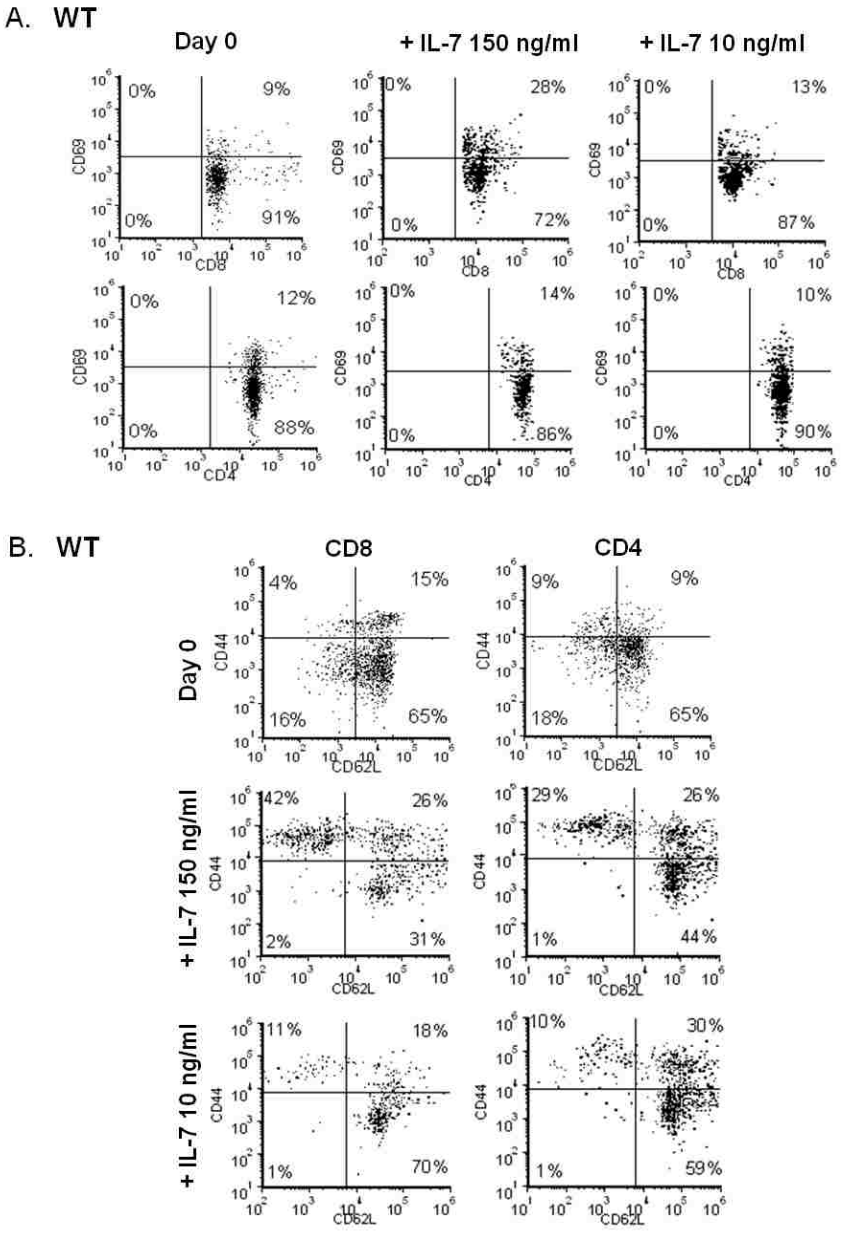

Figure 20. High dose IL-7 promotes expression of CD69 and CD44 and down-regulates CD62L.
(A) Lymph node T-cells were isolated from wild type (WT) C57Bl/6 mice (Day 0) and cultured with 150 or 10 ng/ml of IL-7 for 14 days. Dot plots display CD69 surface expression on CD8 and CD4 T-cells as determined by staining with fluorochrome-conjugated antibodies specific for CD69, CD4 or CD8 and analyzed by flow cytometry. Results shown were acquired from the viable cell gate. Quadrants were established using control antibodies. (B) Lymph node T-cells were isolated from WT C57Bl/6 mice (Day 0) and cultured with 150 or 10 ng/ml of IL-7 for 14 days. Dot plots display CD44 and CD62L surface expression as determined by staining with a fluorochrome-conjugated antibodies specific for CD44 or CD62L and analyzed by flow cytometry. Gating was performed on CD4 or CD8-expressing cells using fluorochrome-conjugated antibodies specific for CD4 or CD8 T-cells, respectively. Results shown were acquired from the viable cell gate. Quadrants were established using control antibodies. A representative experiment of three performed is shown.

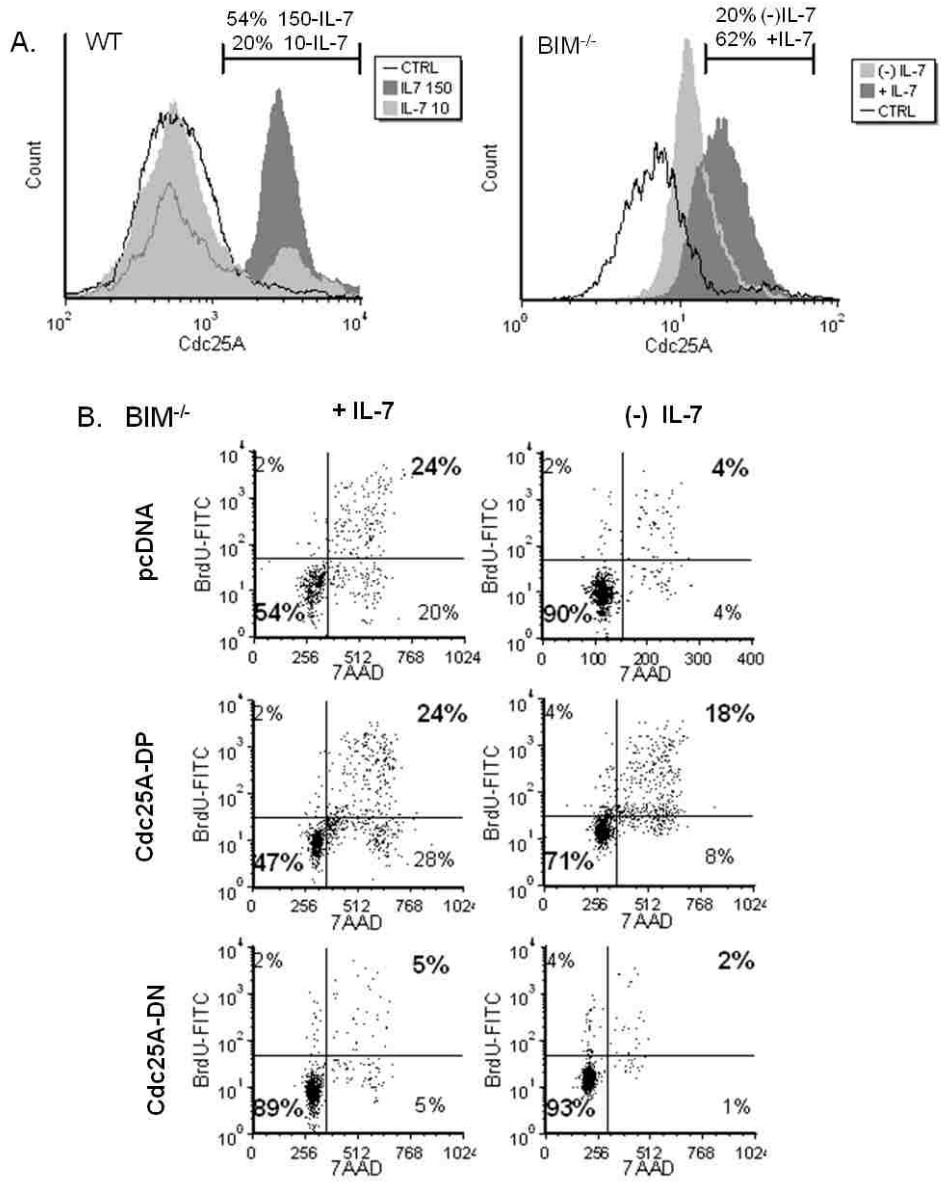

Figure 21. Cdc25A transduces IL-7 proliferative signals.
(A) Lymph node T-cells from WT C57BL/6 mice (left histogram) or BIM$^{-/-}$ mice (right histogram) were isolated and cultured with low dose (10 ng/ml) or high dose (150 ng/ml) IL-7 (left histogram) or with or without IL-7 (right histogram). Intracellular levels of nuclear Cdc25A (left histogram) or total Cdc25A (right histogram) were determined by intracellular staining using a specific Cdc25A antibody followed by a PE-conjugated secondary antibody and analyzed by flow cytometry. Percentages shown represent the population of cells indicated by the marker. CTRL represents use of an isotype matched PE-conjugated secondary antibody control. (B) Nucleofection was used to transiently express the cDNA for Cdc25A-DP, Cdc25A-DN or vector only (pcDNA) in lymph node T-cells from Bim$^{-/-}$ mice that were cultured with (+) or without (-) IL-7 for 24 hours. Cell cycling was assessed by measuring the incorporation of BrdU into replicating DNA with a FITC-conjugated BrdU antibody and DNA content was measured by 7AAD staining using flow cytometry. Quadrants were established using control antibodies. Percentages in bold indicate cells that had incorporated BrdU and were in the G2/S/M phases of the cell cycle. A representative experiment of four performed is shown.

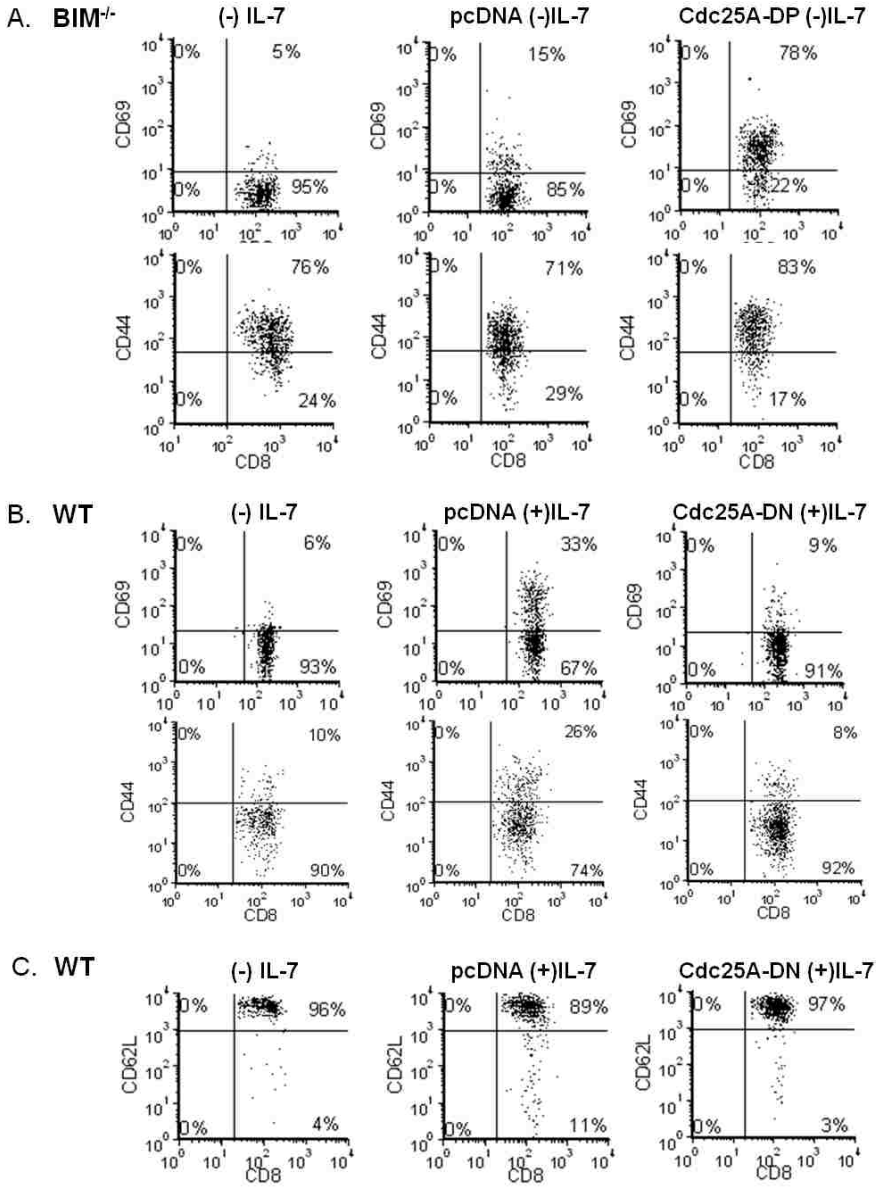

Figure 22. Expression of Cdc25A mimics the effect of high dose IL-7, promoting the growth of activated T-cells that down-regulate CD62L.

(A) Lymph node T-cells were isolated from Bim$^{-/-}$ mice that were expanded with IL-7 (150 ng/ml) for 48 hours. Nucleofection was used to transiently express the cDNA for Cdc25A-DP or vector only (pcDNA) and T-cells were cultured without (-) IL-7 for 24 hours. Untransfected cells are also shown for comparison. Dot plots display CD69 or CD44 surface expression on CD8 T-cells as determined by staining with fluorochrome-conjugated antibodies specific for CD69 and CD44 and analyzed by flow cytometry. (B-C) Lymph node T-cells were isolated from WT C57BL/6 mice, and nucleofection was used to transiently express the cDNA for Cdc25A-DN or vector only (pcDNA). WT cells were cultured with (+) IL-7 for 24 hours. Untransfected cells cultured without IL-7 are also shown for comparison. Dot plots display CD69 or CD44 surface expression on CD8 T-cells as determined by staining with fluorochrome-conjugated antibodies specific for CD69 and CD44 (B) or CD62L and CD8 (C) and analyzed by flow cytometry. A representative experiment of three performed is shown.

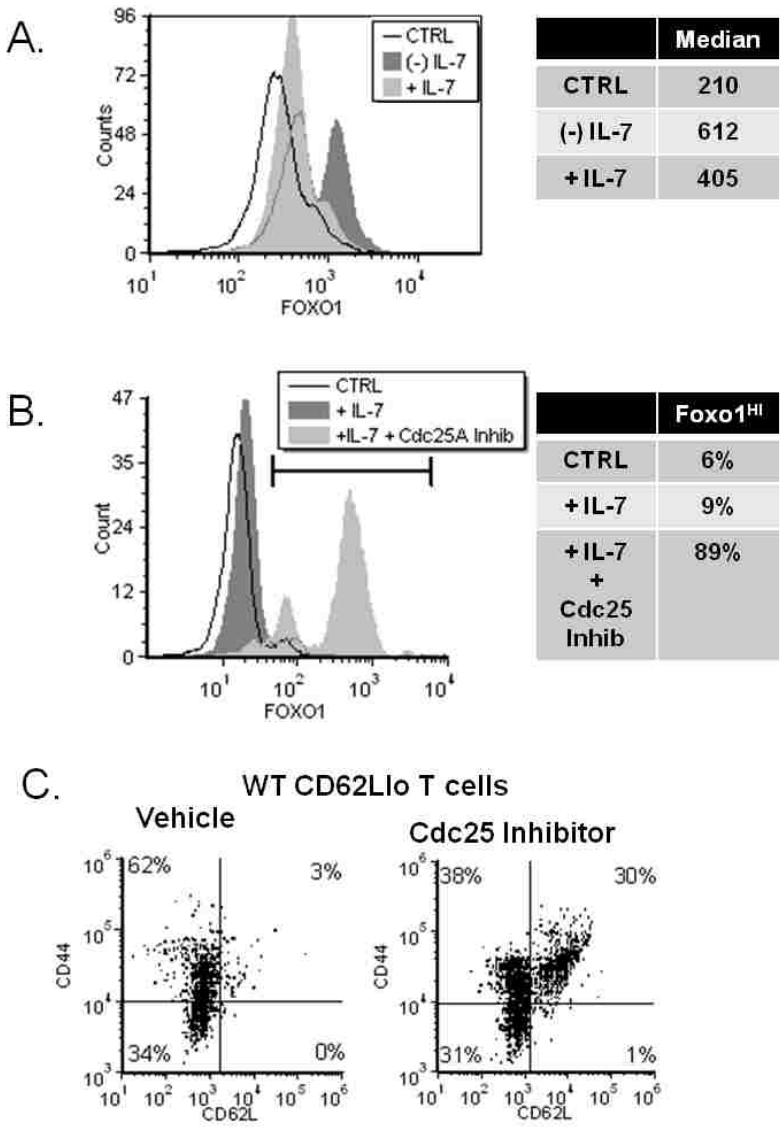

Figure 23. Surface Expression of CD62L depends on the nuclear translocation of Foxo1 which is inhibited by Cdc25A.

(A-B) Lymph node T-cells were isolated from WT C57BL/6 mice and cultured for 24 hours with 150 ng/ml IL-7 or without IL-7 (A) or with a Cdc25 inhibitor (B) Levels of nuclear Foxo1 were determined by intracellular staining using a specific Foxo1 antibody followed by a PE-conjugated secondary antibody and analyzed by flow cytometry. CTRL represents use of an isotype matched PE-conjugated secondary antibody control. Medians for each peak displayed in the histograms were determined using FCS Express software (DeNovo). (C) Splenic CD62L^{lo} T-cells, isolated from WT C57BL/6 mice, were sorted using anti-CD62L antibody and magnetic beads. T-cells were treated with a vehicle control (DMSO) or the Cdc25 inhibitor for 24 hours and analyzed for surface expression of CD44 and CD62L using a FITC-conjugated CD44 antibody and a PE-conjugated CD62L antibody and analyzed by flow cytometry. Quadrants were determined using control antibodies. A representative experiment of four performed is shown.

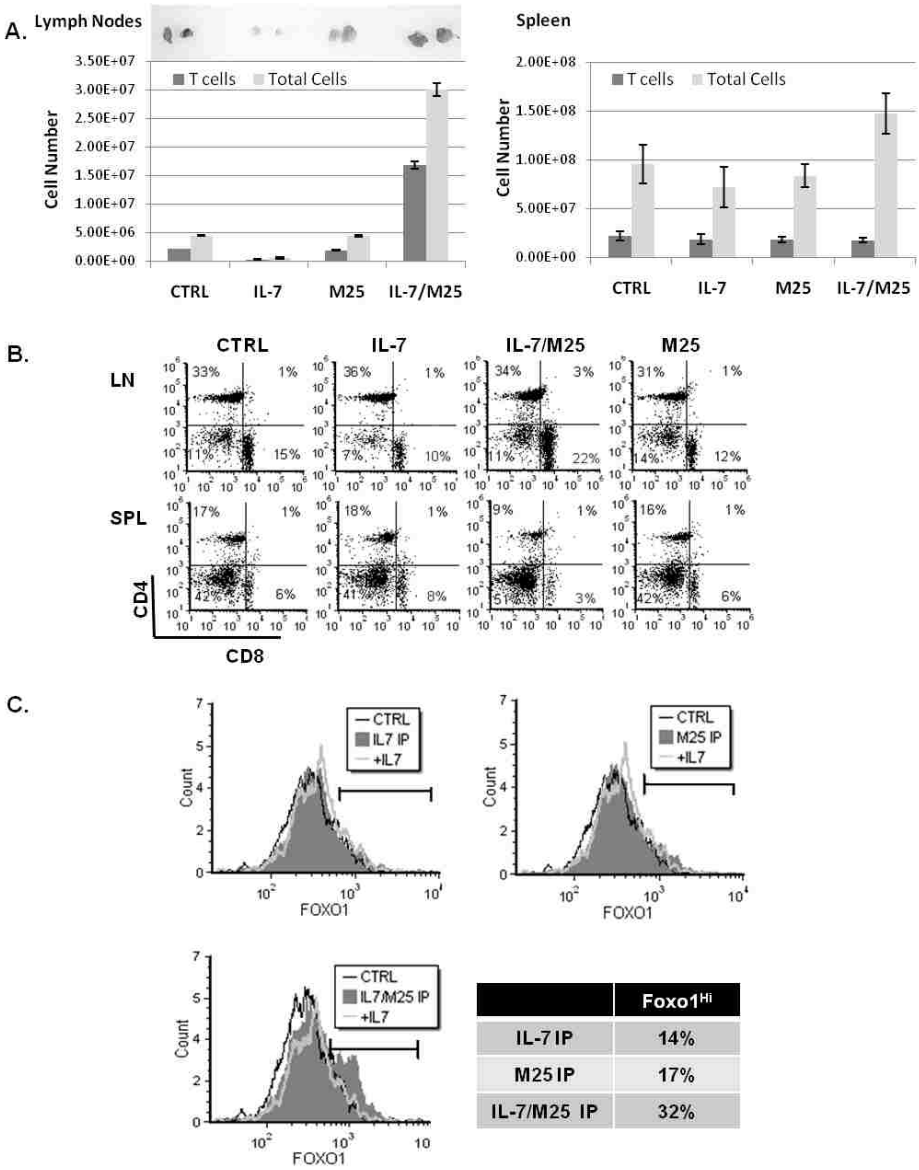

	Foxo1^{Hi}
IL-7 IP	14%
M25 IP	17%
IL-7/M25 IP	32%

Figure 24. ***In vivo*** **administration of IL-7 drives expansion of T-cells that decrease CD62L and exit the lymph nodes.**

C57BL/6 mice were injected once, intraperitoneally, with PBS (CTRL), 10 μg rhIL-7 (IL-7), 100 μg M25 antibody (M25) or pre-mixed 10 μg rhIL-7 and 100 μg M25 antibody (IL-7/M25). Mice were euthanized after 72 hours and lymph nodes and spleen removed for analysis. (A) Total cellularity and T-cell numbers recovered from lymph nodes were determined using the Accuri flow cytometer and confirmed by microscopic evaluation. Images display inguinal lymph nodes removed from representative mice. (B) Dot plots display ratio of CD8 and CD4 T-cells as determined by staining with fluorochrome-conjugated antibodies specific for CD4 or CD8 and analyzed by flow cytometry Results shown were acquired from the viable cell gate. Quadrants were established using control antibodies. (C) Levels of nuclear Foxo1 were determined by intracellular staining using a specific Foxo1 antibody followed by a PE-conjugated secondary antibody and analyzed by flow cytometry. Percentages shown in the table represent the population of Foxo1^{hi} cells indicated by the marker. CTRL represents use of an isotype matched PE-conjugated secondary antibody control. Representative data from four experiments performed is shown.

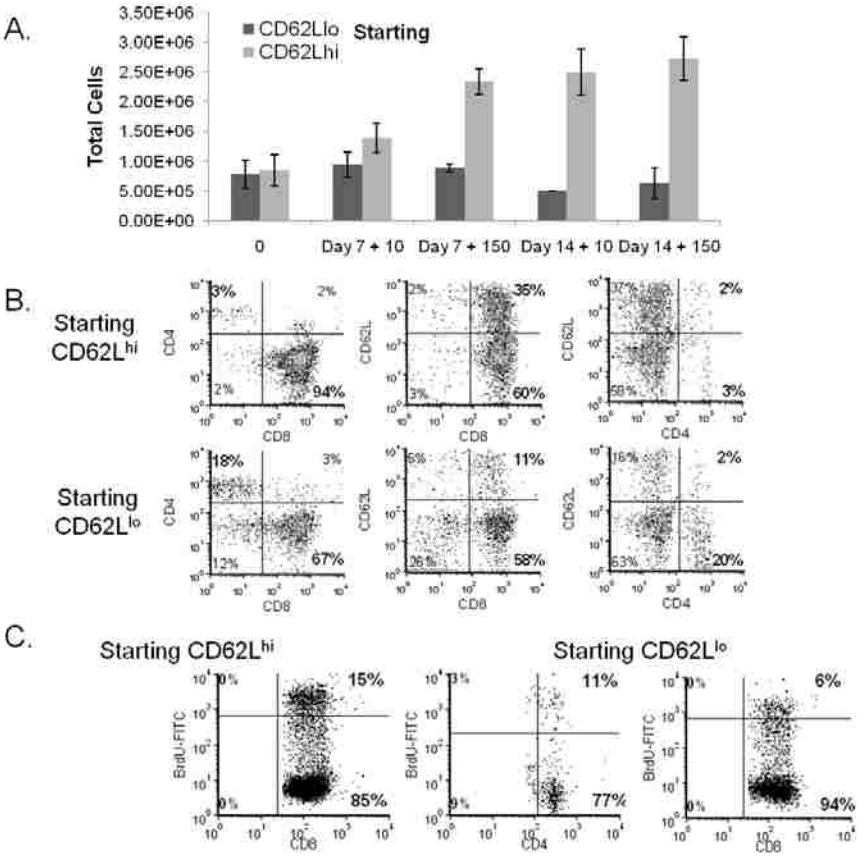

D.

		Naïve CD44loCD62Lhi		Central Mem. CD44hiCD62Lhi		Effector Mem. CD44hiCD62Llo	
Bim-/- LN		+IL7	-IL7	+IL7	-IL7	+IL7	-IL7
Day 0	CD8	78%		4%		2%	
Day 7	CD8	39%	48%	19%	11%	41%	39%
Day 14	CD8	22%	80%	12%	9%	60%	10%

Figure 25. ***In vitro*** **culture with high dose IL-7 promotes proliferation and down-regulation of CD62L on CD8 T-cells.**

(A-C) Splenic CD62L^{lo} or CD62L^{hi} T-cells were isolated from Bim$^{-/-}$ mice and sorted using anti-CD62L antibody and magnetic beads. Cells were placed in culture with 10 or 150 ng/ml of IL-7 or without IL-7 for 7 or 14 days. (A) T-cell numbers from populations of cells that were initially sorted for CD62L^{lo} or CD62L^{hi} expression was determined flow cytometery. (B) Dot plots display ratio of CD8 and CD4 T-cells and surface levels of CD62L of CD62L^{lo} or CD62L^{hi} T-cells after 14 days of culture in 150 ng/ml IL-7. Phenotype was determined by staining with fluorochrome-conjugated antibodies specific for CD4 or CD8 and CD62L. Results shown were acquired from the viable cell gate. (C) Cell cycling of CD62L^{lo} or CD62L^{hi} T-cells was assessed after 7 days of culture in 150 ng/ml IL-7 by measuring the incorporation of BrdU with a FITC-conjugated BrdU antibody and CD4 or CD8 expression determined using flow cytometry. Quadrants were established using control antibodies. Percentages in bold indicate CD4 or CD8 T-cells that had incorporated BrdU. (D) Unsorted lymph node T-cells were isolated from Bim$^{-/-}$ mice and placed in culture with 150 ng/ml IL-7 or without IL-7 for 7 or 14 days. At the indicated time points, cells were stained with antibodies for CD4, CD8, CD44 and CD62L. Surface expression was analyzed by flow cytometry. Table data is gated on CD8 T-cells and is presented as a percentage of total viable cells expressing the indicated phenotype. Results from a representative experiment of two experiments performed are shown.

Discussion

In this study we show that Cdc25A is a critical transducer of IL-7-mediated proliferative and homing signals. Secondary to the effects upon cell growth, expression of either the stable or inhibitory Cdc25A altered the expression of memory and activation markers, changing the phenotype of T-cells independently of IL-7. We found that inhibition of Cdc25 enabled the movement of Foxo1 to the nucleus and up-regulated the expression of CD62L. Thus Cdc25A is not just a mediator of proliferation but also regulates lymph node homing through control of Foxo1 localization and the Foxo1-driven expression of CD62L (Fig. 26). Testing this mechanism both *in vivo* and *in vitro* revealed that high dose IL-7 can deplete the cellularity of lymph nodes by down-regulating the expression of CD62L on responding CD8 T-cells in a Foxo1 dependent manner.

How does manipulation of Cdc25A, a cell cycle activator, affect immune function and specifically CD62L expression? One of the hallmarks of T-cell activation and TCR stimulation is clonal expansion. A strong proliferative signal, as induced by high dose IL-7, could drive the cell cycle machinery in a manner similar to antigen stimulation. Specifically, the dephosphorylating activity of Cdc25A would result in activated CDKs, like CDK2, which can directly phosphorylate Foxo1[122, 123], causing its cytoplasmic translocation and inactivation. In support of this idea, we found that the inhibition of Cdc25 resulted in the nuclear accumulation of Foxo1 protein and increased the surface expression of CD62L in the presence of IL-7.

Of significance, our data also showed that the down-regulation of CD62L, as mediated by IL-7, is most prominent at the highest dose of IL-7 tested, 150 ng/ml. This indicates that merely receiving a survival signal from IL-7, which occurs at the lower dosage of IL-7 (<10ng/ml), is

not sufficient to decrease expression of CD62L. Indeed, the generation of an effector phenotype, involving the down-regulation of CD62L, the up-regulation of the activation markers CD69 and CD44, and acquisition of effector functions, results when T-cells undergo multiple cell cycles[124]. Our findings with $Bim^{-/-}$ T-cells supports this idea. We found that multiple rounds of IL-7-driven cell division, over a period of 7 to 14 days, resulted in the accumulation of $CD62L^{lo}$ T-cells, even when starting with $CD62L^{hi}$ cells, while IL-7 withdrawal maintained a naïve $CD44^{lo}CD62L^{hi}$ phenotype.

Our results indicate that a strong proliferative signal, as supplied by high dose IL-7 or over-expressed Cdc25A, can promote lymph node exit. We found that introduction of exogenous IL-7 lead to decreased cellularity of the lymph nodes and lower T-cell counts. This is most likely an outcome of T-cell redistribution rather than massive cell apoptosis. Others have shown that injection of IL-7 into rhesus macaques did not induce cell death but rather the movement of T-cells into various organs[21], and was linked to their proliferation. Consistent with published reports[125], we found that a combination of IL-7 and M25 resulted in the highest recovery of cells from the lymph nodes. Others have attributed this accumulation of T-cells to antibody-mediated stabilization of the cytokine. However, we propose in our studies that a combination of IL-7 and M25 actually generates an attenuated IL-7 signal (as indicated by increased Foxo1 nuclear expression), which is consistent with the previously described IL-7 neutralizing activity of M25[126] . Hence, an IL-7/ M25 signal would produce a $CD62L^{hi}$ phenotype, enabling T-cell retention in the lymph nodes. In support, we observed the highest levels of nuclear Foxo1 in lymph node T-cells recovered from mice injected with IL-7 and M25.

It is difficult to determine whether T-cells in circulation normally encounter increased amounts of IL-7 comparable to that utilized in our *in vitro* assays or *in vivo* injections. The concentration of IL-7 detected in the serum of healthy individuals is low (0.3-8.4 pg/mL)[10] and reporter assays for IL-7 production did not detect the cytokine outside of primary lymphoid organs [127, 128]. Other reports, however, indicate that migrating T-cells could encounter regions of higher levels of IL-7. Following injections of IL-7, increased levels of the cytokine were detected in extralymphoid tissues such as the intestines[21]. This could be explained by the presence of heparin sulfate proteoglycans, found on stromal cells within various organs that could concentrate the cytokine [129], creating localized microenvironments containing increased IL-7. More significantly, IL-7 production can be induced upon infection as was shown to occur with liver hepatocytes upon TLR engagement [11], and increases in circulating levels of IL-7 have been reported following inflammation [12]. Hence it is possible that physiological conditions exist whereby T-cells encounter elevated levels of IL-7 in tissues, yet serum levels remain undetectable. From a therapeutic standpoint, supraphysiological levels of IL-7 are currently being utilized in human clinical trials. Our findings that the action of Cdc25A upon Foxo1 and CD62L impact the redistribution of T-cells exposed to high dose IL-7 provide a possible explanation for an observed effects of IL-7 application, the transient depletion of circulating T-cells[24], providing insight for optimizing the therapeutic potential of this essential cytokine.

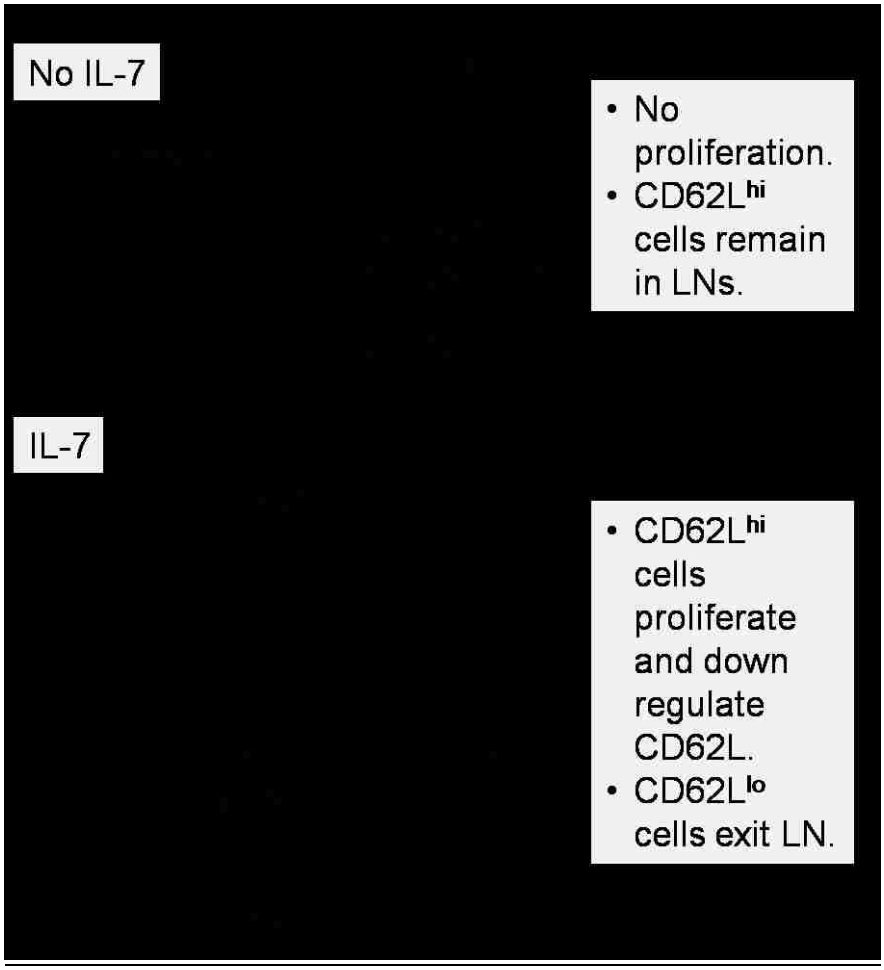

Figure 26. Model of T-cell homing regulation by Cdc25A through Foxo1 and CD62L.
Intracellular levels of Cdc25A are controlled by IL-7 through targeted degradation mediated by the phosphorylating activity of p38 MAPK. In the presence of IL-7, Cdc25A is stable and activates cyclin-dependent kinase 2 (cdk2). In turn, cdk2 phosphorylates Foxo1, leading to the cytosolic localization and inactivation of the transcription factor. Hence Foxo1-dependent expression of CD62L is down-regulated on T-cells, promoting a $CD62L^{lo}$ phenotype.

CHAPTER 6: CONCLUSIONS

As a prototypic homeostatic cytokine with growth promoting activities, IL-7 is well suited to act as a therapeutic stimulator of the immune system. As a therapeutic agent, IL-7 could be used to restore T-cell numbers after lymphodepletion or to augment the body's inherent immune response against cancers. However, clinical administration of IL-7 has only lead to the expansion of T-cells and to date, no anti-tumor effects have been achieved. Our findings show that a thorough understanding about the activity of IL-7 at the molecular level is needed for successful therapeutic development of the cytokine. As proof of principle, clinical assessment of IL-7 function has generally been limited to observational analysis of peripheral blood T-cells. Our studies clearly show that exposure of T-cells to high levels of IL-7 as is currently utilized in the clinical trials could alter the ability of T-cells to home to the lymph nodes. Specifically, these T-cells down-regulate the expression of the lymph node homing marker CD62L, promoting their trafficking away from the lymph nodes and into extralymphoid organs. Indeed, a transient depletion of peripheral blood T-cells following clinical administration of IL-7 has been observed in humans[24], and studies in rhesus macaques support our findings that this effect may be due to the trafficking of proliferating T-cells into extralymphoid organs[21]. Hence an observational analysis of the T-cells present in the patient's blood as is routinely performed clinically would provide an inaccurate overview about the overall T-cell population and their responses to IL-7.

Using our *in vitro* IL-7 culture method, we have been able to study how the introduction (or loss) of the IL-7 signal affected the growth of T-cells in terms of subset distribution, activation status, proliferative response, and trafficking activity. We then affirmed our results by examining *in vivo* models of either transgenic mice expressing constitutively activated STAT5

(STAT5b-CA), which mimics a strong IL-7 signal, or mice that were injected with exogenous IL-7. One of the most important findings from these studies is that IL-7 is not merely a "homeostatic" cytokine that maintains the status quo as it is traditionally defined. Rather at high concentrations, IL-7 acts as an activating stimulus for CD8 T-cells, promoting the expansion of CD8 T-cells with a memory effector phenotype ($CD44^{hi}CD62L^{lo}$), reminiscent of T-cells undergoing an inflammation response. We have shown that this effect is mediated in part through the IL-7 dependent regulation of the cell cycle phosphatase Cdc25A. In contrast to CD8 T-cells, high doses of IL-7 antagonize the growth of CD4 T-cells which favor growth at lower dosages of IL-7. This phenomena is an effect of IL-7's regulation of the T-cell receptor (TCR) kinase LCK, revealing a new link between cytokine and TCR signaling. Perhaps most importantly, these findings show that the signal transduced by IL-7 is a pluripotent one which can be modulated by the concentration of the cytokine as well as the nature of the responding T-cell subset.

Our findings have significant implications for the use of IL-7 in cancer therapy. IL-7 could potentially be used for adoptive immunotherapy in which activated tumor- specific CD8 T-cells are expanded *ex vivo* with IL-7 and then transferred back into the patient. Further studies would be required to test the function and cytolytic activities of these *ex vivo* expanded T-cells. The optimization of IL-7 for systematic administration as performed in the clinical trials is more complex due to the presence of additional *in vivo* factors which must be taken into account. For example, our studies show that injections of high doses of IL-7 into patients as currently performed could interfere with 1) the growth of CD4 T-cells and 2) the ability of CD8 T-cells to home to the lymph nodes, effects which may impede the generation of an anti-tumor response. It

is well known that the activity of CD4 T-cells is required to support and activate CD8 T-cells during an immune response. Furthermore, in response to high doses of IL-7, T-cells down-regulate the expression of CD62L which would promote T-cell localization to potential extralymphoid tumor bearing sites. However, this effect would also interfere with T-cell entry into the lymph nodes, potentially preventing them from encountering the necessary stimulatory signals present there that are required for their proper activation.

As a multipotent cytokine, IL-7 has numerous potential therapeutic applications. While the toxicity has been low, it cannot be over looked that repeated administration of high amounts of the cytokine has produced a number of physiological effects in patients such as skin rashes, erythema at the IL-7 injection site, and hypertension[23, 24]. Moreover, use of high levels of IL-7 presents the risks of contributing to the development of lymphomas or autoimmune conditions as has been observed in transgenic mice over expressing IL-7[6, 130]. Such observations along with our findings demonstrate that the function of IL-7 should not be confined to that of a homeostatic cytokine. Rather, it must be recognized that signaling by IL-7 generates multiple and sometimes opposing effects which is dependent not only on the dosage of the cytokine, but also the nature of the responding T-cell subsets. Hence, an understanding about the molecular functions of IL-7 is absolutely essential for optimizing its therapeutic potential.

REFERENCES

1. Sugamura,K. *et al.* The interleukin-2 receptor gamma chain: its role in the multiple cytokine receptor complexes and T cell development in XSCID. *Annu. Rev. Immunol.* 14, 179-205 (1996).

2. von-Freeden-Jeffry,U. *et al.* Lymphopenia in interleukin (IL)-7 gene-deleted mice identifies IL-7 as a nonredundant cytokine. *J Exp Med* 181, 1519-1526 (1995).

3. Maraskovsky,E. *et al.* Impaired survival and proliferation in IL-7 receptor-deficient peripheral T cells. *J Immunol* 157, 5315-5323 (1996).

4. Puel,A., Ziegler,S.F., Buckley,R.H., & Leonard,W.J. Defective IL7R expression in T(-) B(+)NK(+) severe combined immunodeficiency. *Nat Genet* 20, 394-397 (1998).

5. Fisher,A.G. *et al.* Lymphoproliferative disorders in an IL-7 transgenic mouse line. *Leukemia* 7 Suppl 2, S66-S68 (1993).

6. Rich,B.E., Campos-Torres,J., Tepper,R.I., Moreadith,R.W., & Leder,P. Cutaneous lymphoproliferation and lymphomas in interleukin 7 transgenic mice. *J Exp Med* 177, 305-316 (1993).

7. Yamanaka,K. *et al.* Skin-derived interleukin-7 contributes to the proliferation of lymphocytes in cutaneous T-cell lymphoma. *Blood* 107, 2440-2445 (2006).

8. Mazzucchelli,R. & Durum,S.K. Interleukin-7 receptor expression: intelligent design. *Nat. Rev. Immunol.* 7, 144-154 (2007).

9. Madrigal-Estebas,L. *et al.* Human small intestinal epithelial cells secrete interleukin-7 and differentially express two different interleukin-7 mRNA Transcripts: implications for extrathymic T-cell differentiation. *Hum. Immunol.* 58, 83-90 (1997).

10. Sasson,S.C., Zaunders,J.J., & Kelleher,A.D. The IL-7/IL-7 receptor axis: understanding its central role in T-cell homeostasis and the challenges facing its utilization as a novel therapy. *Curr. Drug Targets.* 7, 1571-1582 (2006).

11. Sawa,Y. *et al.* Hepatic interleukin-7 expression regulates T cell responses. *Immunity.* 30, 447-457 (2009).

12. Unsinger,J. *et al.* IL-7 promotes T cell viability, trafficking, and functionality and improves survival in sepsis. *J. Immunol.* 184, 3768-3779 (2010).

13. Kittipatarin,C. & Khaled,A.R. Interlinking interleukin-7. *Cytokine* 39, 75-83 (2007).

14. Li,W.Q., Jiang,Q., Khaled,A.R., Keller,J.R., & Durum,S.K. Interleukin-7 inactivates the pro-apoptotic protein bad promoting T cell survival. *J. Biol. Chem.* 279, 29160-29166 (2004).

15. Kieper,W.C. *et al.* Overexpression of Interleukin (IL)-7 Leads to IL-15-independent Generation of Memory Phenotype CD8(+) T Cells. *J Exp Med* 195, 1533-1539 (2002).

16. Geiselhart,L.A. *et al.* IL-7 administration alters the CD4:CD8 ratio, increases T cell numbers, and increases T cell function in the absence of activation. *J Immunol* 166, 3019-3027 (2001).

17. Khaled,A.R. *et al.* Cytokine-driven cell cycling is mediated through Cdc25A. *J. Cell Biol.* 169, 755-763 (2005).

18. Kittipatarin,C. & Khaled,A.R. Ex vivo expansion of memory CD8 T cells from lymph nodes or spleen through in vitro culture with interleukin-7. *J. Immunol. Methods* 344, 45-57 (2009).

19. Kittipatarin,C., Li,W.Q., Bulavin,D.V., Durum,S.K., & Khaled,A.R. Cell cycling through Cdc25A: transducer of cytokine proliferative signals. *Cell Cycle* 5, 907-912 (2006).

20. Swainson,L. *et al.* IL-7-induced proliferation of recent thymic emigrants requires activation of the PI3K pathway. *Blood* 109, 1034-1042 (2007).

21. Beq,S. *et al.* Injection of glycosylated recombinant simian IL-7 provokes rapid and massive T-cell homing in rhesus macaques. *Blood* 114, 816-825 (2009).

22. Wang,L.X. *et al.* Interleukin-7-dependent expansion and persistence of melanoma-specific T cells in lymphodepleted mice lead to tumor regression and editing. *Cancer Res.* 65, 10569-10577 (2005).

23. Sportes,C. *et al.* Phase I study of recombinant human interleukin-7 administration in subjects with refractory malignancy. *Clin. Cancer Res.* 16, 727-735 (2010).

24. Sportes,C. *et al.* Administration of rhIL-7 in humans increases in vivo TCR repertoire diversity by preferential expansion of naive T cell subsets. *J. Exp. Med.* 205, 1701-1714 (2008).

25. Tan,J.T. *et al.* IL-7 is critical for homeostatic proliferation and survival of naive T cells. *Proc Natl Acad Sci U S A* 98, 8732-8737 (2001).

26. Rathmell,J.C., Farkash,E.A., Gao,W., & Thompson,C.B. IL-7 enhances the survival and maintains the size of naive T cells. *J Immunol* 167, 6869-6876 (2001).

27. Bourgeois,C. & Stockinger,B. T cell homeostasis in steady state and lymphopenic conditions. *Immunol. Lett.* 107, 89-92 (2006).

28. Kondrack,R.M. *et al.* Interleukin 7 regulates the survival and generation of memory CD4 cells. *J. Exp. Med.* 198, 1797-1806 (2003).

29. Singh,N.J. & Schwartz,R.H. The lymphopenic mouse in immunology: from patron to pariah. *Immunity.* 25, 851-855 (2006).

30. Burchill,M.A. *et al.* Distinct effects of STAT5 activation on CD4+ and CD8+ T cell homeostasis: development of CD4+CD25+ regulatory T cells versus CD8+ memory T cells. *J. Immunol.* 171, 5853-5864 (2003).

31. Bosco,N., Agenes,F., & Ceredig,R. Effects of increasing IL-7 availability on lymphocytes during and after lymphopenia-induced proliferation. *J. Immunol.* 175, 162-170 (2005).

32. Snow,A.L. *et al.* Critical role for BIM in T cell receptor restimulation-induced death. *Biol. Direct.* 3, 34 (2008).

33. Pellegrini,M. *et al.* Loss of Bim increases T cell production and function in interleukin 7 receptor-deficient mice. *J. Exp. Med.* 200, 1189-1195 (2004).

34. Schluns,K.S., Kieper,W.C., Jameson,S.C., & Lefrancois,L. Interleukin-7 mediates the homeostasis of naive and memory CD8 T cells in vivo. *Nat Immunol* 1, 426-432 (2000).

35. Cassese,G. *et al.* Bone marrow CD8 cells down-modulate membrane IL-7Ralpha expression and exhibit increased STAT-5 and p38 MAPK phosphorylation in the organ environment. *Blood* 110, 1960-1969 (2007).

36. Seddon,B., Tomlinson,P., & Zamoyska,R. Interleukin 7 and T cell receptor signals regulate homeostasis of CD4 memory cells. *Nat. Immunol* 4, 680-686 (2003).

37. Gagnon,J. *et al.* IL-6, in synergy with IL-7 or IL-15, stimulates TCR-independent proliferation and functional differentiation of CD8+ T lymphocytes. *J. Immunol.* 180, 7958-7968 (2008).

38. Napolitano,L.A. *et al.* Increased production of IL-7 accompanies HIV-1-mediated T-cell depletion: implications for T-cell homeostasis. *Nat Med* 7, 73-79 (2001).

39. Schuler,T., Hammerling,G.J., & Arnold,B. Cutting edge: IL-7-dependent homeostatic proliferation of CD8+ T cells in neonatal mice allows the generation of long-lived natural memory T cells. *J. Immunol.* 172, 15-19 (2004).

40. Zhang,X. *et al.* Human bone marrow: a reservoir for "enhanced effector memory" CD8+ T cells with potent recall function. *J. Immunol.* 177, 6730-6737 (2006).

41. Masopust,D., Vezys,V., Wherry,E.J., Barber,D.L., & Ahmed,R. Cutting edge: gut microenvironment promotes differentiation of a unique memory CD8 T cell population. *J. Immunol.* 176, 2079-2083 (2006).

42. Maeurer,M.J. *et al.* Interleukin-7 (IL-7) in colorectal cancer: IL-7 is produced by tissues from colorectal cancer and promotes preferential expansion of tumour infiltrating lymphocytes. *Scand. J. Immunol.* 45, 182-192 (1997).

43. Pillai,M., Torok-Storb,B., & Iwata,M. Expression and Function of IL-7 Receptors in Marrow Stromal Cells. *Leuk. Lymphoma* 45, 2403-2408 (2004).

44. Guimond,M. *et al.* Interleukin 7 signaling in dendritic cells regulates the homeostatic proliferation and niche size of CD4+ T cells. *Nat. Immunol.* 10, 149-157 (2009).

45. El,K.N. *et al.* A dose effect of IL-7 on thymocyte development. *Blood* 104, 1419-1427 (2004).

46. Swainson,L., Verhoeyen,E., Cosset,F.L., & Taylor,N. IL-7R alpha gene expression is inversely correlated with cell cycle progression in IL-7-stimulated T lymphocytes. *J. Immunol.* 176, 6702-6708 (2006).

47. Ingley,E. & Klinken,S.P. Cross-regulation of JAK and Src kinases. *Growth Factors* 24, 89-95 (2006).

48. Chin,H. *et al.* Lyn physically associates with the erythropoietin receptor and may play a role in activation of the Stat5 pathway. *Blood* 91, 3734-3745 (1998).

49. Shi,M., Cooper,J.C., & Yu,C.L. A constitutively active Lck kinase promotes cell proliferation and resistance to apoptosis through signal transducer and activator of transcription 5b activation. *Mol. Cancer Res.* 4, 39-45 (2006).

50. Yao,Z. *et al.* Stat5a/b are essential for normal lymphoid development and differentiation. *Proc. Natl. Acad. Sci. U. S. A* 103, 1000-1005 (2006).

51. Seddon,B. & Zamoyska,R. TCR signals mediated by Src family kinases are essential for the survival of naive T cells. *J. Immunol.* 169, 2997-3005 (2002).

52. Kim,K. *et al.* Characterization of an interleukin-7-dependent thymic cell line derived from a p53(-/-) mouse. *J. Immunol. Methods* 274, 177-184 (2003).

53. Van De Wiele,C.J. *et al.* Thymocytes between the beta-selection and positive selection checkpoints are nonresponsive to IL-7 as assessed by STAT-5 phosphorylation. *J. Immunol.* 172, 4235-4244 (2004).

54. Veillette,A., Bookman,M.A., Horak,E.M., & Bolen,J.B. The CD4 and CD8 T cell surface antigens are associated with the internal membrane tyrosine-protein kinase p56lck. *Cell* 55, 301-308 (1988).

55. Veillette,A., Bookman,M.A., Horak,E.M., Samelson,L.E., & Bolen,J.B. Signal transduction through the CD4 receptor involves the activation of the internal membrane tyrosine-protein kinase p56lck. *Nature* 338, 257-259 (1989).

56. Veillette,A., Zuniga-Pflucker,J.C., Bolen,J.B., & Kruisbeek,A.M. Engagement of CD4 and CD8 expressed on immature thymocytes induces activation of intracellular tyrosine phosphorylation pathways. *J. Exp. Med.* 170, 1671-1680 (1989).

57. Julius,M., Maroun,C.R., & Haughn,L. Distinct roles for CD4 and CD8 as co-receptors in antigen receptor signalling. *Immunol. Today* 14, 177-183 (1993).

58. Tomita,K. *et al.* Cytokine-independent Jak3 activation upon T cell receptor (TCR) stimulation through direct association of Jak3 and the TCR complex. *J. Biol. Chem.* 276, 25378-25385 (2001).

59. Garcia,R. *et al.* Constitutive activation of Stat3 by the Src and JAK tyrosine kinases participates in growth regulation of human breast carcinoma cells. *Oncogene* 20, 2499-2513 (2001).

60. Seckinger,P. & Fougereau,M. Activation of src family kinases in human pre-B cells by IL-7. *J. Immunol.* 153, 97-109 (1994).

61. Page,T.H., Lali,F.V., & Foxwell,B.M. Interleukin-7 activates p56lck and p59fyn, two tyrosine kinases associated with the p90 interleukin-7 receptor in primary human T cells. *Eur. J. Immunol.* 25, 2956-2960 (1995).

62. Seddon,B. & Zamoyska,R. TCR and IL-7 receptor signals can operate independently or synergize to promote lymphopenia-induced expansion of naive T cells. *J. Immunol.* 169, 3752-3759 (2002).

63. Sicheri,F. & Kuriyan,J. Structures of Src-family tyrosine kinases. *Curr. Opin. Struct. Biol.* 7, 777-785 (1997).

64. Brdicka,T. *et al.* Phosphoprotein associated with glycosphingolipid-enriched microdomains (PAG), a novel ubiquitously expressed transmembrane adaptor protein, binds the protein tyrosine kinase csk and is involved in regulation of T cell activation. *J. Exp. Med.* 191, 1591-1604 (2000).

65. Xu,S., Huo,J., Tan,J.E., & Lam,K.P. Cbp deficiency alters Csk localization in lipid rafts but does not affect T-cell development. *Mol. Cell Biol.* 25, 8486-8495 (2005).

66. Parolini,I. *et al.* Phorbol ester-induced disruption of the CD4-Lck complex occurs within a detergent-resistant microdomain of the plasma membrane. Involvement of the translocation of activated protein kinase C isoforms. *J. Biol. Chem.* 274, 14176-14187 (1999).

67. Kim,P.W., Sun,Z.Y., Blacklow,S.C., Wagner,G., & Eck,M.J. A zinc clasp structure tethers Lck to T cell coreceptors CD4 and CD8. *Science* 301, 1725-1728 (2003).

68. Molina,T.J. *et al.* Profound block in thymocyte development in mice lacking p56lck. *Nature* 357, 161-164 (1992).

69. Nyakeriga,A.M. *et al.* Engagement of the CD4 receptor affects the redistribution of Lck to the immunological synapse in primary T cells: implications for T-cell activation during human immunodeficiency virus type 1 infection. *J. Virol.* 83, 1193-1200 (2009).

70. Van,L.F. *et al.* Deletion of CD4 and CD8 coreceptors permits generation of alphabetaT cells that recognize antigens independently of the MHC. *Immunity.* 27, 735-750 (2007).

71. Li,W.Q. *et al.* IL-7 promotes T cell proliferation through destabilization of p27Kip1. *J. Exp. Med.* 203, 573-582 (2006).

72. Maraskovsky,E. *et al.* Bcl-2 can rescue T lymphocyte development in interleukin-7 receptor-deficient mice but not in mutant rag-1-/- mice. *Cell* 89, 1011-1019 (1997).

73. Khaled,A.R., Kim,K., Hofmeister,R., Muegge,K., & Durum,S.K. Withdrawal of IL-7 induces Bax translocation from cytosol to mitochondria through a rise in intracellular pH. *Proc Natl Acad Sci U S A* 96, 14476-14481 (1999).

74. Khaled,A.R. *et al.* Interleukin-3 withdrawal induces an early increase in mitochondrial membrane potential unrelated to the Bcl-2 family. Roles of intracellular pH, ADP transport, and F(0)F(1)-ATPase. *J Biol Chem* 276, 6453-6462 (2001).

75. Vander,H.M., Chandel,N.S., Schumacker,P.T., & Thompson,C.B. Bcl-xL prevents cell death following growth factor withdrawal by facilitating mitochondrial ATP/ADP exchange. *Mol Cell* 3, 159-167 (1999).

76. Nevins,J.R. The Rb/E2F pathway and cancer. *Hum. Mol. Genet.* 10, 699-703 (2001).

77. Pines,J. Four-dimensional control of the cell cycle. *Nat. Cell Biol.* 1, E73-E79 (1999).

78. Nilsson,I. & Hoffmann,I. Cell cycle regulation by the Cdc25 phosphatase family. *Prog. Cell Cycle Res.* 4:107-14., 107-114 (2000).

79. Mailand,N. *et al.* Rapid destruction of human Cdc25A in response to DNA damage. *Science* 288, 1425-1429 (2000).

80. Coulonval,K., Bockstaele,L., Paternot,S., & Roger,P.P. Phosphorylations of cyclin-dependent kinase 2 revisited using two-dimensional gel electrophoresis. *J. Biol. Chem.* 278, 52052-52060 (2003).

81. Mailand,N. *et al.* Regulation of G(2)/M events by Cdc25A through phosphorylation-dependent modulation of its stability. *EMBO J.* 21, 5911-5920 (2002).

82. Donzelli,M. *et al.* Hierarchical Order of Phosphorylation Events Commits Cdc25A to betaTrCP-Dependent Degradation. *Cell Cycle* 3, 469-471 (2004).

83. Vidal,A. & Koff,A. Cell-cycle inhibitors: three families united by a common cause. *Gene* 247, 1-15 (2000).

84. Goloudina,A. *et al.* Regulation of Human Cdc25A Stability by Serine 75 Phosphorylation Is Not Sufficient to Activate a S Phase Checkpoint. *Cell Cycle* 2, 473-478 (2003).

85. Dignam,J.D., Lebovitz,R.M., & Roeder,R.G. Accurate transcription initiation by RNA polymerase II in a soluble extract from isolated mammalian nuclei. *Nucleic Acids Res.* 11, 1475-1489 (1983).

86. Trede,N.S., Castigli,E., Geha,R.S., & Chatila,T. Microbial superantigens induce NF-kappa B in the human monocytic cell line THP-1. *J Immunol* 150, 5604-5613 (1993).

87. Khaled,A.R., Butfiloski,E.J., Villas,B., Sobel,E.S., & Schiffenbauer,J. Aberrant expression of the NF-kappaB and IkappaB proteins in B cells from viable motheaten mice. *Autoimmunity* 30, 115-128 (1999).

88. Khaled,A.R. *et al.* Trophic Factor Withdrawal: p38 Mitogen-Activated Protein Kinase Activates NHE1, Which Induces Intracellular Alkalinization. *Mol Cell Biol* 21, 7545-7557 (2001).

89. Rajnavolgyi,E. *et al.* IL-7 withdrawal induces a stress pathway activating p38 and Jun N-terminal kinases. *Cell Signal* 14, 761-769 (2002).

90. Lavoie,J.N., L'Allemain,G., Brunet,A., Muller,R., & Pouyssegur,J. Cyclin D1 expression is regulated positively by the p42/p44MAPK and negatively by the p38/HOGMAPK pathway. *J. Biol. Chem.* 271, 20608-20616 (1996).

91. Casanovas,O. *et al.* Osmotic stress regulates the stability of cyclin D1 in a p38SAPK2-dependent manner. *J. Biol. Chem.* 275, 35091-35097 (2000).

92. Sexl,V. *et al.* A rate limiting function of cdc25A for S phase entry inversely correlates with tyrosine dephosphorylation of Cdk2. *Oncogene* 18, 573-582 (1999).

93. Bulavin,D.V. *et al.* Initiation of a G2/M checkpoint after ultraviolet radiation requires p38 kinase. *Nature* 411, 102-107 (2001).

94. Bulavin,D.V., Amundson,S.A., & Fornace,A.J. p38 and Chk1 kinases: different conductors for the G(2)/M checkpoint symphony. *Curr. Opin. Genet. Dev.* 12, 92-97 (2002).

95. Busino,L., Chiesa,M., Draetta,G.F., & Donzelli,M. Cdc25A phosphatase: combinatorial phosphorylation, ubiquitylation and proteolysis. *Oncogene* 23, 2050-2056 (2004).

96. Falck,J., Mailand,N., Syljuasen,R.G., Bartek,J., & Lukas,J. The ATM-Chk2-Cdc25A checkpoint pathway guards against radioresistant DNA synthesis. *Nature* 410, 842-847 (2001).

97. Sorensen,C.S. *et al.* Chk1 regulates the S phase checkpoint by coupling the physiological turnover and ionizing radiation-induced accelerated proteolysis of Cdc25A. *Cancer Cell* 3, 247-258 (2003).

98. Shimuta,K. *et al.* Chk1 is activated transiently and targets Cdc25A for degradation at the Xenopus midblastula transition. *EMBO J.* 21, 3694-3703 (2002).

99. Hassepass,I., Voit,R., & Hoffmann,I. Phosphorylation at serine 75 is required for UV-mediated degradation of human Cdc25A phosphatase at the S-phase checkpoint. *J. Biol. Chem.* 278, 29824-29829 (2003).

100. Bartek,J. & Lukas,J. Chk1 and Chk2 kinases in checkpoint control and cancer. *Cancer Cell* 3, 421-429 (2003).

101. Khaled,A.R. & Durum,S.K. Death and Baxes: mechanisms of lymphotrophic cytokines. *Immunol. Rev.* 193, 48-57 (2003).

102. Olashaw,N. & Pledger,W.J. Paradigms of growth control: relation to Cdk activation. *Sci. STKE.* 2002, RE7 (2002).

103. Jinno,S. *et al.* Cdc25A is a novel phosphatase functioning early in the cell cycle. *EMBO J* 13, 1549-1556 (1994).

104. Blomberg,I. & Hoffmann,I. Ectopic expression of Cdc25A accelerates the G(1)/S transition and leads to premature activation of cyclin E- and cyclin A-dependent kinases. *Mol. Cell Biol.* 19, 6183-6194 (1999).

105. Plas,D.R., Talapatra,S., Edinger,A.L., Rathmell,J.C., & Thompson,C.B. Akt and Bcl-xL promote growth factor-independent survival through distinct effects on mitochondrial physiology. *J Biol Chem* 276, 12041-12048 (2001).

106. Janumyan,Y.M. *et al.* Bcl-xL/Bcl-2 coordinately regulates apoptosis, cell cycle arrest and cell cycle entry. *EMBO J.* 22, 5459-5470 (2003).

107. Cheng,N. *et al.* Bcl-2 inhibition of T-cell proliferation is related to prolonged T-cell survival. *Oncogene* 23, 3770-3780 (2004).

108. Khaled,A.R. & Durum,S.K. Lymphocide: cytokines and the control of lymphoid homeostasis. *Nat. Rev Immunol* 2, 817-830 (2002).

109. Grailer,J.J., Kodera,M., & Steeber,D.A. L-selectin: role in regulating homeostasis and cutaneous inflammation. *J. Dermatol. Sci.* 56, 141-147 (2009).

110. Link,A. *et al.* Fibroblastic reticular cells in lymph nodes regulate the homeostasis of naive T cells. *Nat. Immunol.* 8, 1255-1265 (2007).

111. Mueller,S.N. & Germain,R.N. Stromal cell contributions to the homeostasis and functionality of the immune system. *Nat. Rev. Immunol.* 9, 618-629 (2009).

112. Jiang,Q. *et al.* Cell biology of IL-7, a key lymphotrophin. *Cytokine Growth Factor Rev.* 16, 513-533 (2005).

113. Kovanen,P.E. & Leonard,W.J. Cytokines and immunodeficiency diseases: critical roles of the gamma(c)-dependent cytokines interleukins 2, 4, 7, 9, 15, and 21, and their signaling pathways. *Immunol. Rev.* 202, 67-83 (2004).

114. Surh,C.D., Boyman,O., Purton,J.F., & Sprent,J. Homeostasis of memory T cells. *Immunol. Rev.* 211, 154-163 (2006).

115. Chehtane,M. & Khaled,A.R. Interleukin-7 Mediates Glucose Utilization in Lymphocytes through Transcriptional Regulation of the Hexokinase II Gene. *Am. J. Physiol Cell Physiol*(2010).

116. Fauman,E.B. *et al.* Crystal structure of the catalytic domain of the human cell cycle control phosphatase, Cdc25A. *Cell* 93, 617-625 (1998).

117. Sancho,D., Gomez,M., & Sanchez-Madrid,F. CD69 is an immunoregulatory molecule induced following activation. *Trends Immunol.* 26, 136-140 (2005).

118. Kittipatarin,C., Tschammer,N., & Khaled,A.R. The interaction of LCK and the CD4 co-receptor alters the dose response of T-cells to interleukin-7. *Immunol. Lett.* 131, 170-181 (2010).

119. Li,W.Q., Guszczynski,T., Hixon,J.A., & Durum,S.K. Interleukin-7 regulates Bim proapoptotic activity in peripheral T-cell survival. *Mol. Cell Biol.* 30, 590-600 (2010).

120. Kerdiles,Y.M. *et al.* Foxo1 links homing and survival of naive T cells by regulating L-selectin, CCR7 and interleukin 7 receptor. *Nat. Immunol.* 10, 176-184 (2009).

121. Fabre,S. *et al.* FOXO1 regulates L-Selectin and a network of human T cell homing molecules downstream of phosphatidylinositol 3-kinase. *J. Immunol.* 181, 2980-2989 (2008).

122. Leisser,C. *et al.* Subcellular localisation of Cdc25A determines cell fate. *Cell Death. Differ.* 11, 80-89 (2004).

123. Huang,H., Regan,K.M., Lou,Z., Chen,J., & Tindall,D.J. CDK2-dependent phosphorylation of FOXO1 as an apoptotic response to DNA damage. *Science* 314, 294-297 (2006).

124. Bachmann,M.F., Wolint,P., Schwarz,K., & Oxenius,A. Recall proliferation potential of memory CD8+ T cells and antiviral protection. *J. Immunol.* 175, 4677-4685 (2005).

125. Boyman,O., Ramsey,C., Kim,D.M., Sprent,J., & Surh,C.D. IL-7/anti-IL-7 mAb complexes restore T cell development and induce homeostatic T Cell expansion without lymphopenia. *J. Immunol.* 180, 7265-7275 (2008).

126. Plum,J., De,S.M., Leclercq,G., Verhasselt,B., & Vandekerckhove,B. Interleukin-7 is a critical growth factor in early human T-cell development. *Blood* 88, 4239-4245 (1996).

127. Alves,N.L. *et al.* Characterization of the thymic IL-7 niche in vivo. *Proc. Natl. Acad. Sci. U. S. A* 106, 1512-1517 (2009).

128. Mazzucchelli,R.I. *et al.* Visualization and identification of IL-7 producing cells in reporter mice. *PLoS. One.* 4, e7637 (2009).

129. Clarke,D., Katoh,O., Gibbs,R.V., Griffiths,S.D., & Gordon,M.Y. Interaction of interleukin 7 (IL-7) with glycosaminoglycans and its biological relevance. *Cytokine* 7, 325-330 (1995).

130. Williams,I.R. *et al.* IL-7 overexpression in transgenic mouse keratinocytes causes a lymphoproliferative skin disease dominated by intermediate TCR cells: evidence for a hierarchy in IL-7 responsiveness among cutaneous T cells. *J. Immunol.* 159, 3044-3056 (1997).